REPORT

Tonkin+Taylor

Clifton to Tangoio Coastal Hazards Strategy 2120

Coastal Hazard Assessment

Prepared for
Hawke's Bay Councils (HBRC, NCC, and HDC)
Prepared by
Tonkin & Taylor Ltd
Date
May 2016
Job Number
20514.005.CHA.v8

Exceptional thinking together
www.tonkintaylor.co.nz

Distribution:

Hawke's Bay Councils (HBRC, NCC, and HDC)	PDF
Tonkin & Taylor (file)	1 copy
Hastings District Council	PDF
Napier City Council	PDF
Tonkin & Taylor Ltd (FILE)	1 copy

Table of contents

Executive summary

Purpose

Hawke's Bay Regional Council (HBRC), Hastings District Council (HDC) and Napier City Council (NCC) are working together to develop a strategy for managing, or mitigating, coastal hazard risks along the Hawke Bay shoreline from Tangoio to Clifton to make a more resilient community.

This report provides the results of a regional scale coastal hazard assessment that will be used as a basis for a coastal hazard risk assessment (reported separately). This coastal hazard erosion report builds on previous hazard studies and ongoing research and investigations in the coastal processes of this area. The report quantifies the possible extent of the following hazards:

- Coastal erosion (storm cut, trends, effects of sea level rise)
- Coastal inundation (storm surge, set-up, run-up, overtopping and sea level rise)
- Tsunami.

The report briefly describes the coastal processes and summarises key information required for the coastal hazard assessment based on the latest available information. However, the report does not seek to replicate information already contained in previous reports, particularly Komar and Harris (2014) and T+T (2012) and these should be read for more detailed descriptions of the physical processes affecting this area.

Coastal erosion hazard

The coastal erosion hazard assessment uses a probabilistic approach in determining the potential future shoreline position at 2065 and 2120 taking into account the following parameters: historic erosion trends, storm effects and backshore slope stability as well as the possible effects of sea level rise. The range of values for each of these parameters was determine from a range of sources, including LiDAR survey, aerial photographs, field investigations, beach profile data, numerical modelling and expert engineering judgement. A triangular probability distribution was assumed for each parameter and a Monte Carlo technique was used to assess the likelihood of the combined influence of each parameter. This approach differs from the previous erosion hazard assessment that was based on a deterministic approach of adding together the effects each parameter.

The approach used in this report is consistent with the Government's Envirolink "guide to good practice[1]"that recommends moving from deterministic predictions to probabilistic projections. The probabilistic approach recognises there will always be inherent uncertainties associated with projections and provides a more transparent way of capturing and presenting such uncertainty. This method results in a range of potential hazard zone extents, ranging from virtually certain to exceptionally unlikely.

Minimum set back values are developed to take into account limitations and uncertainties in our current understanding of processes that drive erosion hazard and in the data and modelling techniques. Utilising minimum values provides a targeted precautionary approach as advocated in the NZCPS without applying overly conservative factors of safety for sites with sufficient hazard zone widths.

Mapping of the erosion hazard extent was based on setbacks determined at each beach profile measured from present day vegetation lines or beach scarps. Due to the consideration of accretion trends as well as erosion trends the future erosion hazard extents can be less than the

[1] http: //www.envirolink.govt.nz/Envirolink-tools/

current erosion hazard zone. This is particularly evident between HB8 and HB12 where the maximum CEHZ is between -15 and -16 m, while for CEHZ21020 at these locations the hazard extent varies from -20 m to +23 m (i.e. at some locations the hazard zone is more seaward in the future than it is at the present day). Therefore, it is not recommended to select a particular line at a point in time to inform future planning, but a set of lines and likelihoods. For example it may be prudent to select the particular likelihood for present day CEHZ as well as a future likelihood event, so there is still a set-back distance to consider even in areas where, over time, accretion may reduce the hazard.

Coastal inundation hazard

The coastal inundation hazard extent was determined for both permanent and extreme inundation along the open coast for present day and for the years 2065 and 2120 for a 10%AEP, 1% AEP and 0.5%AEP event (i.e. a 10 year, 100 year and 200 year return period). Permanent inundation extents were based on the predicted rise in sea level added to present day tidal levels. Extreme inundation is caused by extreme events during which waves contribute to super-elevate water levels (astronomic tide + storm surge) through wave setup, wave run-up and wave overtopping. The combined effect of storm surge levels with the effect of onshore storms based was modelled at each beach profile using the X-Beach Gravel model. This provided information on both the extreme water level on the seaward side of the beach crest and the volume of seawater that can overtop the beach crest during storm events.

Mapping was based on the manual integration of the extreme water levels along the coast produced by X-Beach with the inundation extent resulting from overtopping from the catchment flood models of HBRC using engineering judgement to refine the inundation maps.

Tsunami inundation hazard

Tsunami hazard mapping was based on the work carried out by HBRC (http://www.hbemergency.govt.nz/hazards/portal) that included the potential effect of a 3 m, 5 m and 10 m amplitude tsunami. The tsunami amplitude was applied in deep water some 20 km from the Port of Napier and modelled to coincide with the high tide at Mean High Water Springs water level (Goodier, 2011). Based on the recent GNS report on tsunami (GNS, 2013), the 3, 5 and 10 m tsunami have been determined to conservatively represent approximately a 0.5%, 0.13% and a 0.025% AEP event (i.e. 200 year, 750 year and 4000 year return period).

Mapping information

Hazard maps have been prepared for erosion, sea inundation and tsunami. These maps have been provided to Council and are the basis for the baseline risk assessment reported separately.

Recommendations

The coastal hazard information is to be used for a baseline risk assessment. There are no recommendations on the preferred hazard information to use for any possible update of coastal hazard zones in regional or district plans. The selection of appropriate hazard maps should be based on the outcomes of the risk assessment and discussions on acceptable risk.

1 Introduction

1.1 Purpose

Hawke's Bay Regional Council (HBRC), Hastings District Council (HDC) and Napier City Council (NCC) have initiated the development of a strategy for managing or mitigating coastal hazard risks along the Hawke's Bay shoreline from Tangoio to Clifton to make a more resilient community.

A regional coastal hazard assessment was carried out in 2004 (T+T, 2004) that identified areas of potential erosion hazard and inundation levels inclusive of sea level rise to 2100. The information contained within this report and subsequent refinement reports carried out between 2004 and 2011 informed the Hawke's Bay Regional Coastal Environment Plan made operative on 8 November, 2014.

There are additional studies and investigations available to increase the level of information and data to support future revisions of the coastal hazard areas. This has included additional information on waves and coastal processes as well as updated information of shoreline change through HBRC's ongoing monitoring work, tsunami effects (GNS, 2013) and climate change (IPCC, 2013) with significantly greater levels of sea level rise to consider compared to the 2004 report.

1.2 Scope of works

The scope of this study has been to carry out a regional scale coastal hazard assessment to provide information on coastal processes and hazards operating within the study area. These include:

- The spatial extent of the study area is the open coast areas between Tangoio and Clifton
- Hazards to consider are:
  - Coastal erosion (storm cut, trends, effects of sea level rise)
  - Coastal inundation (storm surge, set-up, run-up, overtopping and sea level rise).

1.3 Report outline

Section 2 describes the physical environment of Hawke's Bay including geology, coastal profiles, water levels and wave information. Section 3 describes the methodology for the erosion hazard assessment that include the definition of the coastal behaviour cells and component derivation. Section 4 provides resulting erosion extents. Sections 5 and 6 present the inundation hazard assessment methodology and resulting inundation levels and information respectively. A summary and recommendation have been given in Section 7.

1.4 Datums and coordinates

All levels presented in this report are with respect to HBRC datum (RL). HBRC datum is 9.08 m above local Chart Datum (CD) and 10 m above Napier Vertical Datum 1962 (NVD-62). Coordinates have been provided in New Zealand Transverse Mercator.

1.5 Study limitations

Limitations and assumptions for this study, which may lead to less conservative results, include:

- Coastal erosion hazard assessment for the present day is based on a compilation of information sources, empirical and numerical modelling techniques. The most up-to-date information and data have been used at the time of assessment.
- Sea level rise projections are based on consideration of published information from IPCC (2015) and the MfE (2008) guidance document on coastal hazards and the Komar and Harris (2014) report.

- The extrapolation of trends and the effect of climate change have been assessed using equilibrium beach profile models which are standard and accepted methods.
- Historic sea level rise rates of 2 mm/yr. have been removed from future sea level rise projections on the basis that these rates are reflected in data for current trend analysis and this includes tectonic rates of change from GeoNet information.
- Inundation assessment has been undertaken assuming shoreline crest levels static.
- The probabilistic approach of assessing erosion hazard is a relatively new technique (Shand et al., 2015) but is consistent with the direction in Envirolink (Ramsay et al., 2012) guide to good practice for defining coastal hazard zones for setback lines. It has currently been applied for the Northland Region (NRC) and for Canterbury (ECAN).
- Modelling of long term trends used the recent (1995 to 2014) beach profile data set. This results in an assumption of status quo for extraction trends at Awatoto and Marine Parade and the continued nourishment at West shore.

2 Physical environment

This section provides an overview, with specific focus on information pertinent to the coastal hazard assessment. For a detailed summary of the physical setting and environment see Komar and Harris (2014).

2.1 Geology

The Hawke's Bay region has three major physiographic elements: inland mountain ranges; a central area of lowlands and river valleys; and coastal ranges of hills. Figure 2-1 (a) shows that the stretch of coast from Tangoio to Clifton is generally low lying estuarine deposits (white areas). South of Clifton the shoreline is backed by steep high cliffs (yellow areas). North of Bay View inland mountains approach the shore (brown). A rock outcrop (Bluff Hill; yellow) is located in Napier and separates the shoreline into two distinct stretches. This has been more clearly sketched by Komar and Harris (2014), see Figure 2-1 (b).

The coastal ranges are formed predominantly by sedimentary rocks of Cretaceous and Tertiary age and these include predominance of rock type ''papa''.

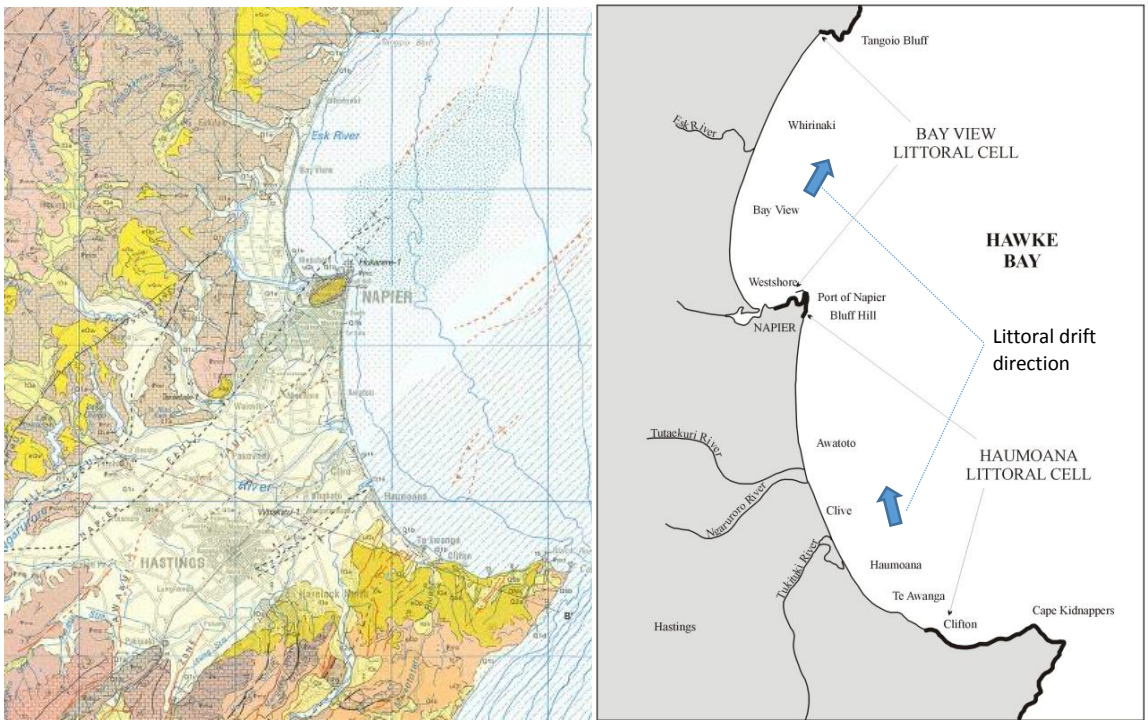

Figure 2-1: (A) Hawke's Bay geology (source: GNS), (B) Bay View and Haumoana Littoral Cells (Komar and Harris, 2014).

2.1.1 Seismic

The Hawke's Bay region lies in the most active seismic region of New Zealand (Hull, 1990). The Hawke's Bay region is dominated by the collision of the Australian plate and Pacific plate, with the latter giving way and sliding beneath the Australian plate (Komar and Harris, 2014). Figure 2-2 (A) shows the major faults around New Zealand. The collision of the two plates have formed and deformed the rocks along the coast and was the cause of the Hawke's Bay earthquake in 1931. This earthquake caused an uplift of about 2 m from Bay View to Tangoio, but caused a subsidence in the order of 1 m along the southern end of the Haumoana Littoral Cell (see Figure 2-2 – B).

Limited GPS measurements (2006-2009) by Beavan and Litchfield (2009) show that shoreline between Tangoio Bluff and Cape Kidnappers have been subsiding at a rate between about 0 and 1 mm/year, but with uncertainties having that same order of magnitude. This indicates active seismic activity along Hawke's Bay causing subsidence of the land.

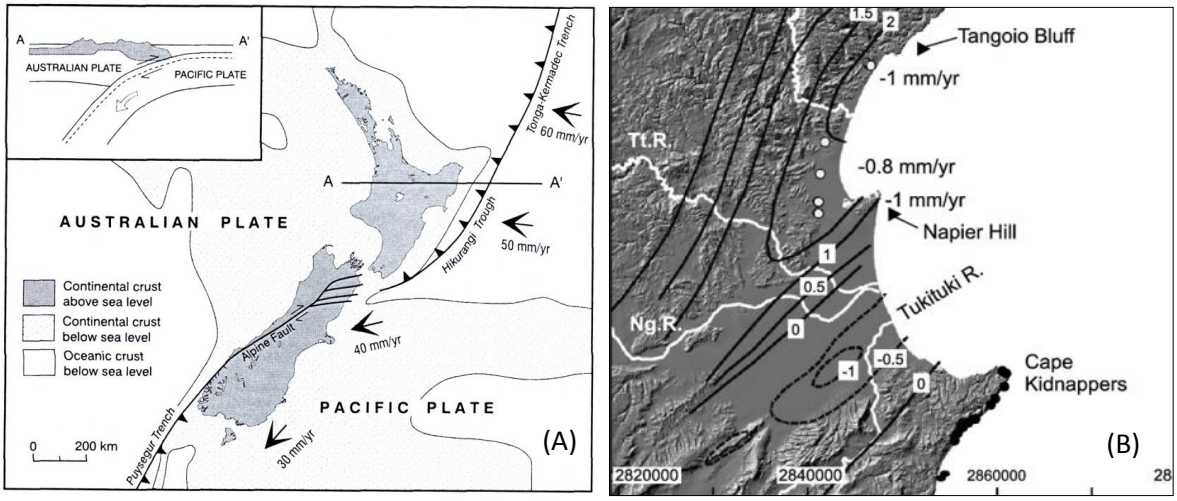

Figure 2-2: Tectonics and geomorphic features of New Zealand. (A) Plate subduction of the Pacific plate occurring at the Hikurangi Trough closest to Hawke's Bay (Source: Aitken, 1999). (B) Land changes resulting from the 1931 earthquake (Source: Hull, 1990).

2.2 Topography

LiDAR from April 2012 and July 2003 was provided by Hawke's Bay Regional Council. The coastal LiDAR dataset (2012) covers the coastal stretch from Tangoio to Clifton with a width between 100 and 300 m. The 2003 LiDAR dataset covers the area from Tangoio to Clifton and extends a minimum of 6 km inland. Figure 2-3 show the 2003 and 2012 LiDAR datasets coverage.

Digital Elevation Models (DEMs) were created from both the 2003 and 2012 LiDAR datasets to extract the position of the 11 m contours (approximately the Mean High Water Spring level). These are utilised in both the short-term and long-term shoreline fluctuation analyses (see Sections 3.2.2 and 3.2.4). Furthermore, the dune crest was digitised based on the 2012 DEM to extract dune crest elevations at 1 m spacing, which were used to assess the effect of sea level rise on erosion hazard (refer to Section 0).

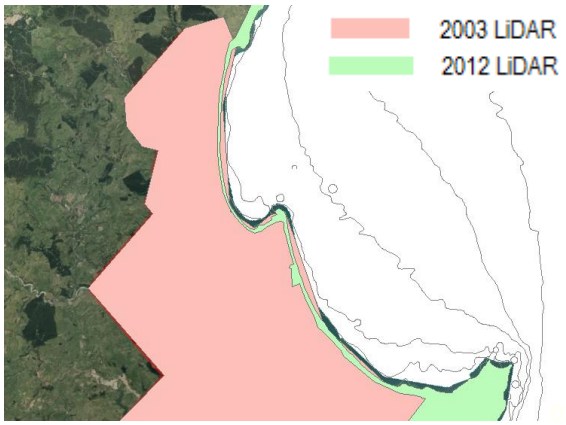

Figure 2-3: 2003 and 2012 LiDAR datasets coverage.

2.3 Historic aerial photographs

2011/2012 aerial photographs have been obtained from LINZ. These aerials are the most recent available. Historic aerial photographs were provided by Hawke's Bay Regional Council. The available aerial photographs used in this study are listed below:

- 2011/2012 (Tangoio – Clifton)
- March 1934 (Tangoio – Bay View)
- April 1943 (Bay View – Port of Napier)
- May 1949 (Port of Napier – Ngaruroro River)
- May 1950 (Ngaruroro River – Clifton).

Historical aerial photographs are georeferenced and have been used to digitise the shoreline/vegetation line. The historic and latest digitised shorelines were used in the long-term shoreline trend analysis (refer to Section 3.2.4). The latest shoreline/vegetation line has been adopted as the baseline from which the erosion hazard zones are determined (refer to Section 3).

2.4 Existing beach profiles

Beach profile information is available between Tangoio and Clifton. A series of 23 profiles (HB Series) along the shoreline provides representative information of change along a particular section of barrier beach and are regularly spaced (1-2 km increments).

Table 2-1 shows a summary of the HB Series data including first survey date and survey period. The beach profiles have been surveyed generally once a year until 2004 and were surveyed every month in 2004. After 2004 beach profiles have been surveyed multiple times a year. The majority of the beach profiles south of Napier have profile information from the seventies or eighties. However, profiles HB5 and HB6 were not surveyed until after construction of the first Ngaruroro groyne and profiles HB7, HB8 and HB11 have been surveyed since the thirties/forties (see Table 2-1). Beach profiles have been surveyed from 1991 north of Bay View except for Whirinaki (1974) and from the seventies between West Shore and Bay View (except for HB15). Appendix A shows a summary of the locations of all beach profiles along Hawke's Bay.

Several local additional profile datasets are available at West shore, Town Beach and East Clive. These beach profiles are typically spaced 50 – 100m and have been surveyed annually. We have reviewed the behaviour of the beach by assessing the trends of the Mean High Water Spring (MHWS) excursion distance for both the detailed data sets and the HB Series (refer to Section 3.2.2.1 for HB Series assessment). It was concluded that the HB series provided adequate representation of the trends and that additional beach profiles show similar trends. The additional data points were therefore not included in the assessment.

Beach profiles south of Clive River (HB1 – HB6) typically experience erosion which may be a consequence of land subsidence due to the 1931 Hawke's Bay earthquake. North of the river (HB8 – HB23) beach profiles are typically steepening (refer to Section 2.1.1 for description of land changes due to the Hawke's Bay earthquake).

Table 2-1: Summary of beach profile data for Hawke's Bay

Profile number	Location	First survey date	Last survey date	Survey period (years)	Number of surveys
HB1	Clifton	27/04/1972	22/12/2014	42	51
HB2	Te Awanga	23/01/1973	22/12/2014	41	72
HB3	Southern end of Haumoana	21/11/1974	22/12/2014	40	66
HB4	Haumoana	13/11/1974	22/12/2014	40	70
HB5	East Clive	4/10/1989	2/02/2015	25	91
HB6	Clive	4/10/1989	2/02/2015	25	91
HB7	Waitangi/Awatoto	1/01/1939	2/02/2015	76	102
HB8	Awatoto	1/01/1946	2/02/2015	70	94
HB9	Te Awa Avenue	19/12/1983	22/12/2014	31	65
HB10	Te Awa Avenue	19/12/1983	2/02/2015	31	99
HB11	Marine Parade	21/03/1930	22/12/2014	84	83
HB12	Northern end of Marine Parade	13/11/1974	2/02/2015	40	106
HB13	Southern end of West shore	27/08/1975	22/12/2014	39	101
HB14	West shore	20/09/1979	22/12/2014	35	74
HB15	Northern end of West shore	27/05/1948	23/12/2014	66	59
HB16	Southern end of Bay View	21/08/1974	23/12/2014	40	78
HB17	Bay View	20/12/1995	23/12/2014	19	43
HB18	Northern end of Bay View	5/12/1991	23/12/2014	23	48
HB19	Southern end of Whirinaki	5/12/1991	23/12/2014	23	47
HB20	Whirinaki	12/11/1974	23/12/2014	40	63
HB21	Northern end of Whirinaki	5/12/1991	23/12/2014	23	47
HB22	Tangoio	5/12/1991	23/12/2014	23	47
HB23	Tangoio	5/12/1991	30/12/2013	22	45

2.5 Sediments

Sediment size analysis of beach sediments from Tangoio to Clifton has been carried out by Smith (1968). Table 2-2 shows the mean grain size as measured by Smith (1968). Smith (1968) noted a trend in sorting from very poor in the south to moderate in the north. This is probably due to multiple sources that supply sediment to this system. The longshore pattern is overshadowed by a very distinct across shore formation, with considerable variation in the intertidal zone, well sorted to moderately well sorted at the backshore and moderately to very poorly sorted in the low tide. The rivers appear to be significant suppliers of sand, with high sand concentrations found in beach samples close to the river mouths.

Komar and Harris (2014) describe the beaches of the Bay View and Haumoana Littoral Cells as a mixture of gravel and sand derived from erosion of Mesozoic rock, a greywacke that originated in the deep ocean. Four major rivers transported large volumes of gravel to the beaches a century ago. Due to human interference but largely due to the tectonic uplift in 1931, three out of the four rivers were no longer able to transport gravel to the beaches.

The two largest present-day sediment sources are located at the southern side of Hawke's Bay; the Tukituki River and erosion of Cape Kidnappers. Gravel is transported northward due to the dominant northward alongshore transport, but is reduced in size due to gravel abrasion (Tonkin + Taylor, 2012; Komar and Harris, 2014). Bluff Hill separates the Bay View Littoral Cell from Haumoana Littoral Cell and since no sediment is carried along Bluff Hill (Komar, 2005, 2010), Bay View has a net zero longshore transport. Gravel extraction was carried out at Pacific Beach to nourish Westshore beach from 1993 to 2014 with some 13,800 m^3/yr transferred annually over this time period. Gravel extraction also takes place for commercial use at Awatoto, with an average annual extraction of 47,800 m^3/yr from 1973 to 2010. However, since 2006 the volumes extracted have been limited to 30,000m^3/yr. Over the period from 1995 to 2014, which is the basis of establishing recent long term trends for this study, the volumes extracted average around 40,100 m^3/yr. These sediment sources and sinks result in a negative net balance and have been described in more detail by Komar and Harris (2014) and T+T (2012). Sediment information has been utilised in the hydrodynamic modelling (refer to Sections 3.2.2.3 and 5.2.2.1).

Table 2-2: Mean sediment size measured by Smith (1968)

Location		Mean size		Location		Mean size	
No.	**HB series**	**phi**	**mm**	**No.**	**HB series**	**phi**	**mm**
1	HB23	-1.55	2.93	11	HB12	-1.72	3.29
2	HB22	-1.4	2.64	12	HB11	-1.13	2.19
3	HB21	-1.05	2.07	13	HB10	-0.83	1.78
4	HB20	-0.75	1.68	13	HB9	-0.83	1.78
5	HB19	-0.5	1.41	14	HB8	-1.03	2.04
6	HB18	-1.45	2.73	14	HB7	-1.03	2.04
7	HB17	-1.4	2.64	15	HB6	-1.32	2.50
7	HB16	-1.4	2.64	16	HB5	-2.06	4.17
8	HB15	-1.35	2.55	17	HB4	-1.52	2.87
8	HB14	-1.35	2.55	18	HB3	-2.18	4.53
9	HB13	1.4	0.38	19	HB2	-1.76	3.39
				19	HB1	-1.76	3.39

2.6 Water levels

Water levels play an important role in determining coastal erosion hazard both by controlling the amount of wave energy reaching the backshore causing erosion during storm events and by controlling the mean shoreline position on longer time scales.

Key components that determine water level are:

- Astronomical tides
- Barometric set-up and wind effects, generally referred to as storm surge
- Medium-term fluctuations, including seasonal effects, El Nino-Southern Oscillation (ENSO) and Inter-decadal Pacific Oscillation (IPO) effects commonly called mean sea level anomaly (MSLA)
- Long-term changes in sea level due to climate change.

All levels presented in this report are reduced to HBRC datum (mean sea level = 10 m Chart Datum), unless stated otherwise.

2.6.1 Astronomical tide

The astronomical tides are caused by the gravitational attraction of solar-system bodies, primarily the Sun and Earth's moon. These forces result in ocean long waves interacting with the continental shelf in a complex way to produce a rise and fall in sea levels (tides). In New Zealand the astronomical tides have the largest influence on sea level.

Tidal levels for primary and secondary ports of New Zealand are provided by Land Information New Zealand (LINZ) based on the average predicted values over the 18.6 year tidal cycle. These values, defined in chart datum, Napier Vertical Datum 1962 and HBRC datum (RL), for Napier are presented within Table 2-3. The spring tidal range is approximately 1.8 m and the mean sea level is around RL 10 m.

Table 2-3: Tidal levels at the port of Napier

	Chart datum (m)	Napier vertical datum 1962 (m)	HBRC datum (m)
Highest Astronomic Tide (HAT)	1.97	1.05	11.05
Mean High Water Spring (MHWS)	1.84	0.92	10.92
Mean High Water Neap (MHWN)	1.46	0.54	10.54
Mean Sea Level (MSL)	0.92	0	10
Mean Low Water Neap (MLWN)	0.40	-0.52	9.48
Mean Low Water Spring (MLWS)	0.06	-0.86	9.14
Chart Datum (CD)	0	-0.92	9.08

Source: LINZ (2012)

2.6.2 Storm surge

Storm surge results from the combination of barometric setup from low atmospheric pressure and wind stress from winds blowing along or onshore which elevates the water level above the predicted tide (Figure 2-4). Storm surge applies to the general elevation of the sea above the predicted tide across a region but excludes nearshore effects of storm waves such as wave setup and wave run-up at the shoreline.

A storm surge analysis for the New Zealand coast was done by de Lange (1996) based on measured surges. He found that the maximum expected elevations are in the range of 0.8 to 1 m with a return period of 100 years. A tidal constituent analysis was undertaken by Worley (2002) with 1 year of hourly data, who found 18 storm surges to reach at least 0.75 m above the predicted tides based on a 1-year record. This extreme-value analysis showed a tidal residual of about 0.9 m, similar to de Lange (1996).

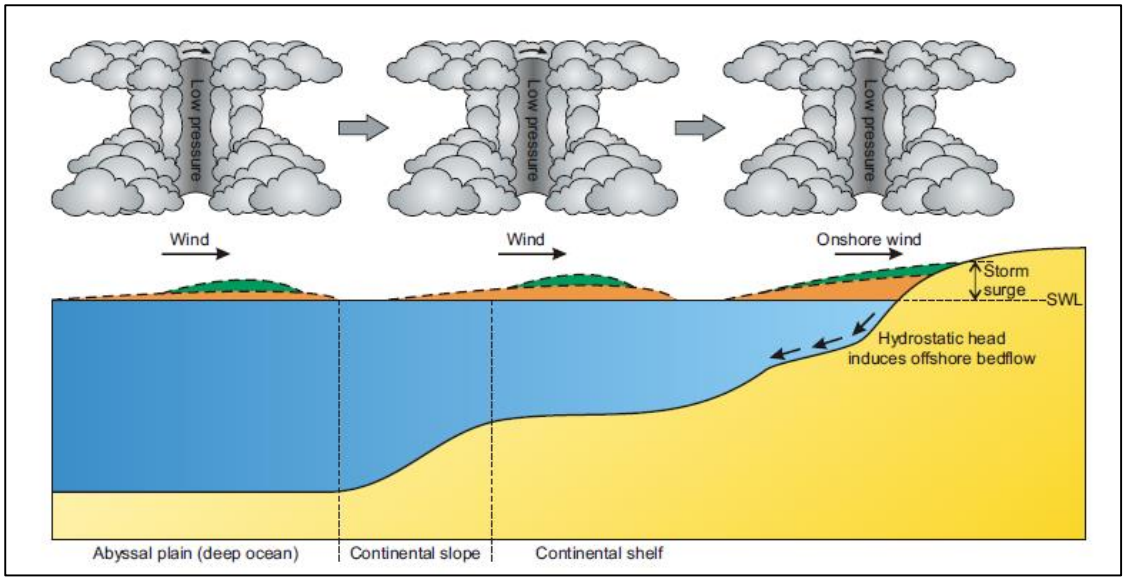

Figure 2-4: Processes causing storm surge.

2.6.3 Medium-term fluctuations

Atmospheric factors such as season, El Nino-Southern Oscillation (ENSO) and Inter-decadal Pacific Oscillation (IPO) can all affect the mean level of the sea at a specific time (refer to Figure 2-5). The combined effect of these fluctuations may be up to 0.25 m (Bell, 2012).

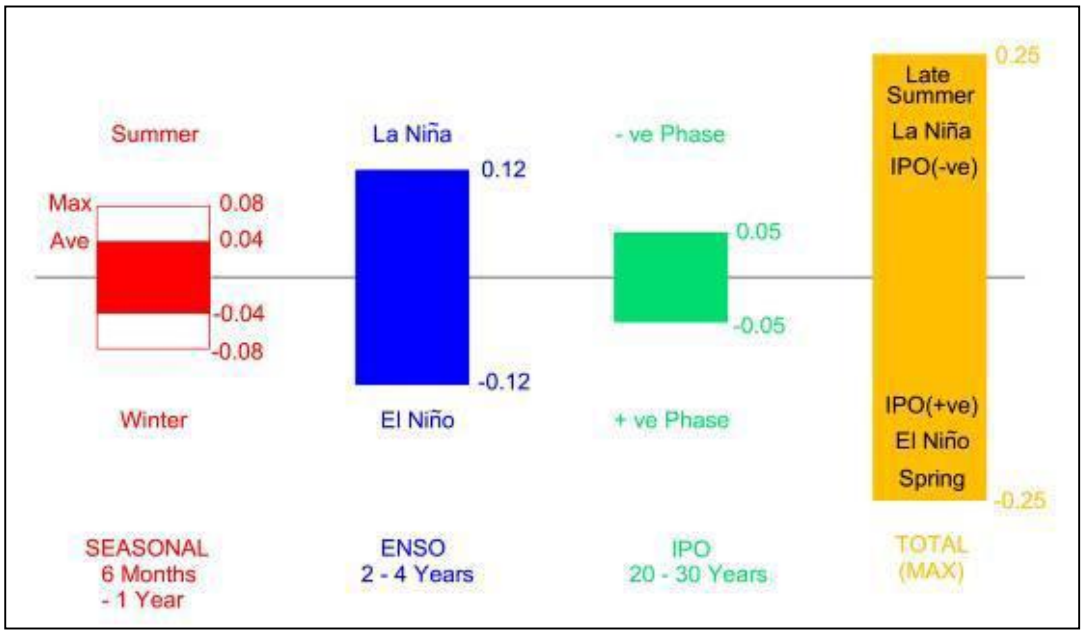

Figure 2-5: Components contributing to sea level variation over long-term periods (source: Bell, 2012).

2.6.4 Storm tide levels

The combined elevation of the predicted tide, storm surge and medium-term fluctuations is known as the storm tide. As discussed in Section 2.6.1, Worley (2002) undertook a joint probability analysis of the astronomical tides and tidal residuals resulting in a 100-year extreme water level of 2.7 m CD (11.78 m RL) based on 1 year of data.

Water level data at the Port of Napier is available measured by the port's tidal gauge. Water level records are available from 1989 to 2014 measured in CD, with a 4 year gap from 1995 to 1999 (see Figure 2-6). Based on this data we have undertaken annual maximum analysis of the 22-year dataset using a Weibull distribution and Gringorten plotting position formula. The Average Recurrence Interval (ARI) based on the annual maximum water level data is shown in Figure 2-6 and is tabulated in Table 2-4. It can be seen that the 1% ARI reaches an extreme water level of 2.4 m CD (11.48 m RL). We have adopted this value in our analysis as we consider the 22 year data set and the conventional curve fitting approach more reliable than the extreme-value analysis by Worley (2002) based on a 1-year dataset.

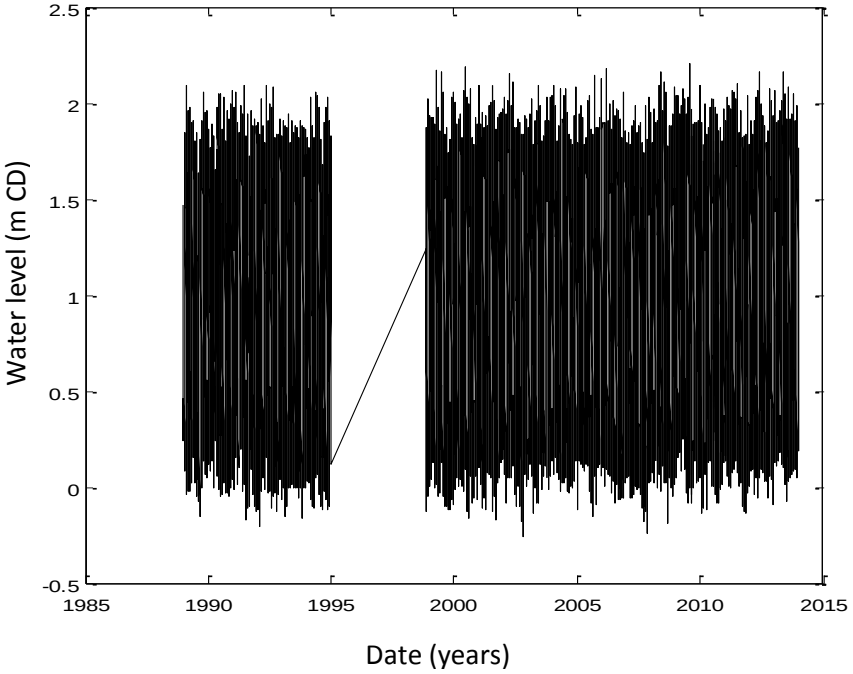

Figure 2-6: Water level measured by the tidal gauge at the Port of Napier from 1989 to 2014.

Table 2-4: Annual Recurrence Interval of annual maximum water level

Average Recurrence Interval (years)	**5**	**10**	**20**	**50**	**100**
Total Water Level (m CD)	2.21	2.27	2.32	2.38	2.40
Total Water Level (m RL)	11.29	11.35	11.40	11.46	11.48

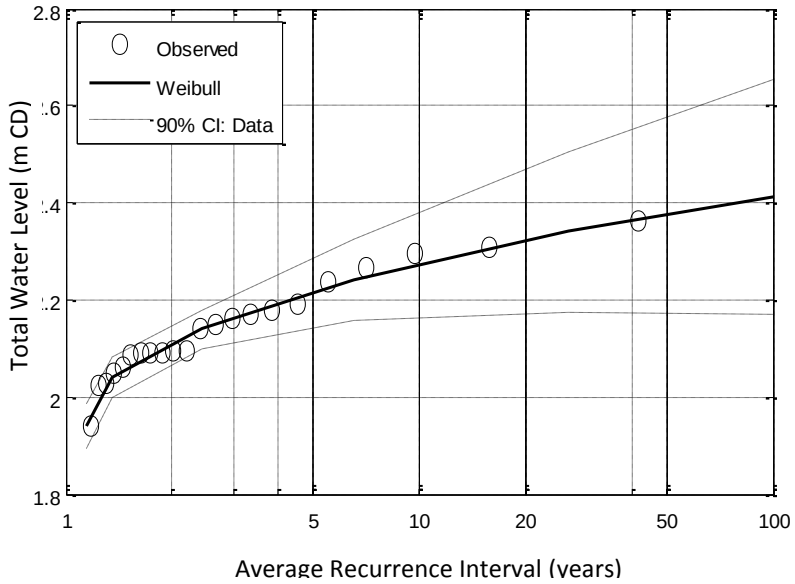

Figure 2-7: Average Recurrence Interval (ARI) of the annual maximum water level (in m CD) as recorded by the tidal gauge between 1989 and 2014.

2.6.5 Long-term sea levels

Historic sea level rise in New Zealand has averaged 1.7 ± 0.1 mm/year with Hawke Bay exhibiting a slightly higher rate of 2 mm/year (Komar and Harris, 2014). This includes tectonic rates of change based on GeoNet information. Climate change is predicted to accelerate this rate of sea level rise into the future. NZCPS (2010) requires that the identification of coastal hazards includes consideration of sea level rise over at least a 100 year planning period (i.e. 2120). Potential sea level rise over this time frame is likely to significantly alter the coastal erosion hazard.

The Ministry of Environment (MfE, 2008) guideline recommends a base value sea level rise of 0.5 m by 2090 (relative to the 1980-1999 average), with consideration of the consequences of sea level rise of at least 0.8 m by 2090 with an additional sea level rise of 10 mm per year beyond 2100. Bell (2013) recommends that for planning to 2115, these values are increased to 0.7 and 1.0 m respectively. Bell (2013) also recommends that when planning for new activities or developments, that higher potential rises of 1.5 to 2 m above the present mean sea level should be considered to cover the foreseeable climate-change effects beyond a 100 year period.

More site specific projections of future rates of sea level rise for Hawke's Bay have been derived by Komar and Harris (2014). The projections that they have derived for Hawke's Bay were based on a 'consensus' set of curves based on curves published by other climatologists (refer to Komar and Harris, 2014). The 'consensus' set of curves is an extension into the future of the regression line based on the Port's existing tidal gauge record. Figure 2-8 shows the derived set of curves by Komar and Harris (2014) and have been extrapolated to the year 2120 to capture the sea level rise relevant for this assessment. The 'consensus' set of curves yield the 'low', 'average' and 'high' sea level projections. The results indicate that the relative sea level could rise between 0.9 and 1.8 m (1.8 and 2.7 m CD in Figure 2-8) adopting a MSL = 0.95 m CD.

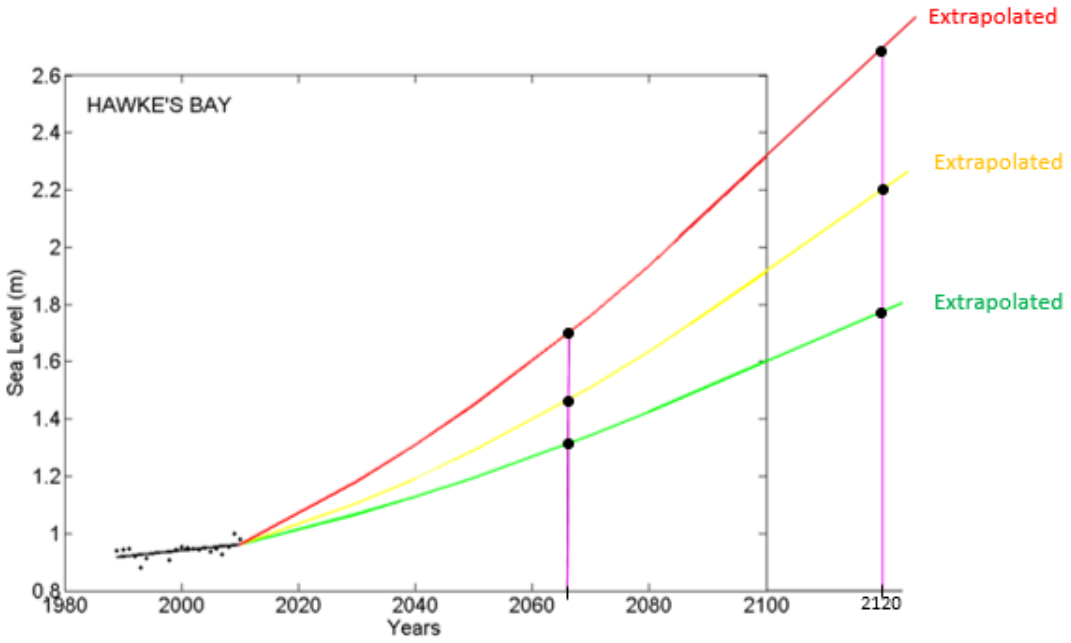

Figure 2-8: Projections of potential future sea level rise presented derived by Komar and Harris (2014) and extrapolated to the year 2120 in terms of Chart Datum.

2.7 Extreme nearshore waves

Wave hind cast data from MetOcean Ltd is available for the Hawke's Bay region. MetOcean used the SWAN model to do a 34-year hind cast of the wave climate, using various sources, and have provided wave output data at the 5 m and 10 m isobaths (MetOcean, 2011). The MetOcean wave output locations are shown in Appendix A. MetOcean have validated their wave hind cast modelling technique against wave buoy data from Port of Napier (MetOcean, 2008) and found a good agreement (within 14% of the satellite estimates).

An extreme value analysis was undertaken by MetOcean for the 10 m isobaths and by T+T for the 5 m isobath. Table 2-5 shows the return period value significant wave heights for the 5 m and 10 m water depth locations relevant for this study extrapolated from 22-year and 34-year hind cast respectively. This forms the basis for nearshore wave heights.

Other available wave data sources and their use in this study are:

- Port of Napier wave buoy data from 2000 to 2014. This data set was used to validate MetOcean wave data set (refer to Appendix D);
- Waves And Storm-surge Prediction (WASP) output at the 50 m isobath based on hind casts between 1970 and 2000 provided by NIWA (closest output point located 20 km offshore of Awatoto). This data set was used to define the storm shape (refer to Section 3.2.2.3).

We note that based on a wave height comparison between measured wave height data at the wave buoy and predicted wave height data at the wave buoy by MetOcean show an under prediction of waves larger than 3 m by MetOcean. The comparison is based on the maximum wave height for each year from 2002 to 2012. The under prediction by the MetOcean hind cast analysis is about 10% for waves larger than 3 m. Waves smaller than 2.5 m are slightly over predicted by MetOcean (< 10%). In shallower water (e.g. near the beach toe) the under prediction reduces to approximately 5% due to breaking of the largest waves.

A comparison of measured and modelled wave heights during Cyclone Pam (16 – 17 March 2015) confirmed the reasonableness of the modelled wave data (refer Figure 2-9), but with a slight under-estimation. The predicted significant wave height was just below 4 m while measured wave heights reached around 4.5 m. The predicted period was 12 seconds while the measured period reached 15 seconds (Goodier and Pearse, 2015).

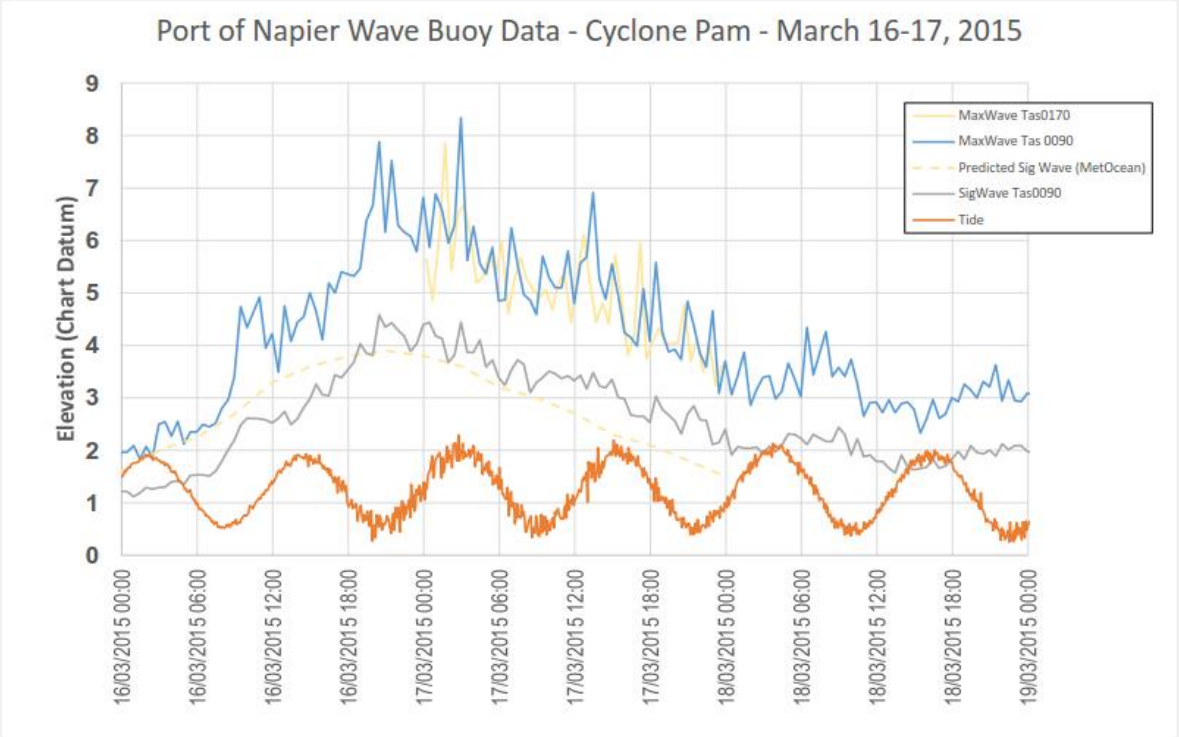

Figure 2-9 Comparison of measured and modelled wave and water level data at the Port of Napier buoy (source: Goodier and Pearse, 2015).

Table 2-5: Significant wave height (m) at 5 m and 10 m water depth

Site	Return period (years)					
	1	**5**	**10**	**25**	**50**	**100**
Bay View 5 m	2.6	3	3.15	3.25	3.4	3.48
Bay View 10 m[1]	2.62	3.05	3.20	3.38	3.50	3.61
West Shore 5 m	2	2.13	2.2	2.26	2.32	2.37
West Shore 10 m[1]	2.57	3.03	3.20	3.39	3.53	3.65
Napier 5 m	2.65	2.85	2.9	2.95	3.02	3.05
Napier 10 m[1]	2.82	3.28	3.45	3.65	3.79	3.91
Haumoana 5 m	2.2	2.35	2.4	2.46	2.53	2.58
Haumoana 10 m[1]	2.62	3.12	3.30	3.53	3.69	3.84
Te Awanga 5 m	2.02	2.04	2.05	2.07	2.09	2.1
Te Awanga 10 m[1]	2.76	3.25	3.43	3.66	3.81	3.95
Clifton 5 m	1.95	1.97	1.98	2	2.02	2.03
Clifton 10 m[1]	2.94	3.49	3.70	3.95	4.13	4.30

[1](Source: MetOcean, 2013)

3 Coastal erosion hazard zone (CEHZ) assessment methodology

The CEHZs were established from the cumulative effect of four main parameters (visualised in Figure 3-1):

$$CEHZ = ST + DS + (LT \times T) + SL \qquad \text{(Equation 1)}$$

Where:

ST = Short-term /horizontal coastline fluctuations including storm cut (m).

DS = Dune slope is characterized by the horizontal distance from the base of the eroded dune to the crest of a stable angle of repose (m).

LT = Long-term rate of horizontal coastline movement (m/yr.).

T = Timeframe (years). In this instance a period of 50 and around 100 years will be used for CEHZ2065 and CEHZ2120 respectively (i.e. 2065 and 2120).

SL = Horizontal coastline retreat due to possible accelerated sea level rise (m).

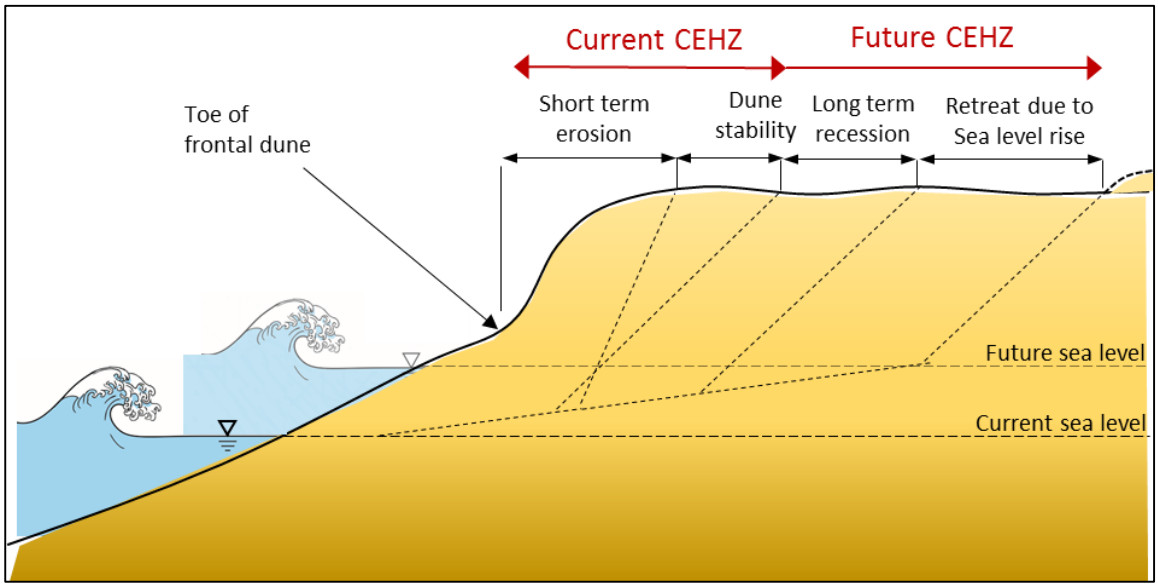

Figure 3-1: Definition sketch for CEHZ.

The CEHZ baseline to which values are referenced is the most recent dune toe/vegetation line derived from aerial photographs captured in 2011. In review of the position of the most recent dune toe/vegetation line with respect to the minimum and maximum envelope beach profile it was found that the most recent dune toe is near the minimum envelope profile for erosive beaches and near the maximum envelope profile for accretive beaches. So this method does not introduce a conservative approach.

The coastal erosion hazard zones are derived either by:

- Probabilistic projections utilising Equation 1, or
- Minimum set back values.

The Envirolink guide to good practice[2] recommends moving from deterministic predictions to probabilistic projections, and that the recognition and treatment of uncertainty is a key source of

[2] http: //www.envirolink.govt.nz/Envirolink-tools/

variance between CEHZ predictions by practitioners. We have adopted a probabilistic approach which is consistent with the Envirolink guide, and includes the following steps:

- Use probability distribution functions to contain the best estimate (mode), lower and upper bounds (e.g. triangle distribution as shown in Figure 3-2) of the four components based on either available data or heuristic reasoning based on experience. Quantification of the minimum, mode and maximum values used for the key components of the CEHZ formula are discussed in the following sections.
- Probability distributions constructed for each component are then randomly sampled and the extracted values used to define a potential CEHZ distance. This process is repeated 10,000 times using a Monte Carlo technique and an example of probability distributions of the four components are shown in Figure 3-3. These four distributions forecast the resultant CEHZ width (Figure 3-4) for a specific location.
- Utilise the probabilistic distributions to map the range of CEHZ distances for each time frame and assign a pragmatic probability or likelihood for each CEHZ (see example probabilities in both Figure 3-3 and Figure 3-4).

The probabilistic approach recognises there will always be inherent uncertainties associated with projections and provides a much more transparent way of capturing and presenting such uncertainty. We note that this method results in a range of potential hazard zone distances and that the selection of the appropriate probabilistic value will be based on discussions with Council. The probabilistic method also aligns with risk assessment approach where the results can be aligned with a range of likelihood scenarios if required.

Minimum set back values are developed to take into account limitations and uncertainties in our current understanding of processes that drive erosion hazard and in the data and modelling techniques. Utilising minimum values provides a targeted precautionary approach as advocated in the NZCPS without applying overly conservative factors of safety for sites with sufficient hazard zone widths.

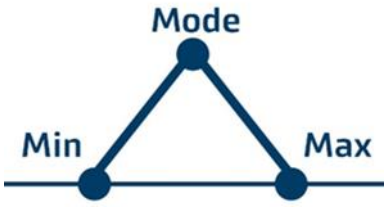

Figure 3-2: Triangular probability distribution function used for the four components of the CEHZ formulation

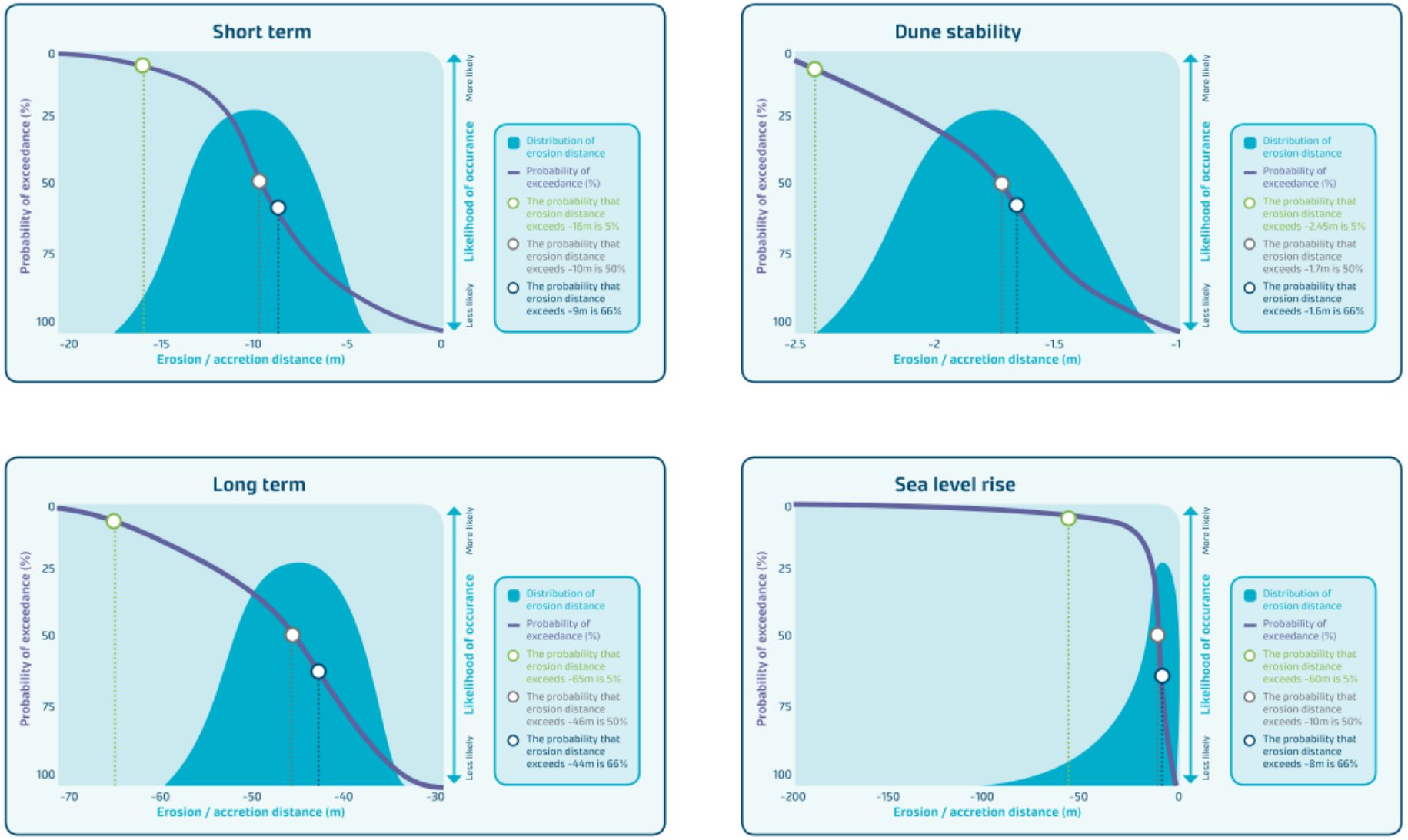

Figure 3-3: Example of cumulative distribution functions (lines) and probability density functions (distributions) of each parameter for 2120. The cumulative distribution function (line) shows the probability of exceedance versus the erosion/accretion distance. The probability density function (distribution) shows the likelihood of occurrence.

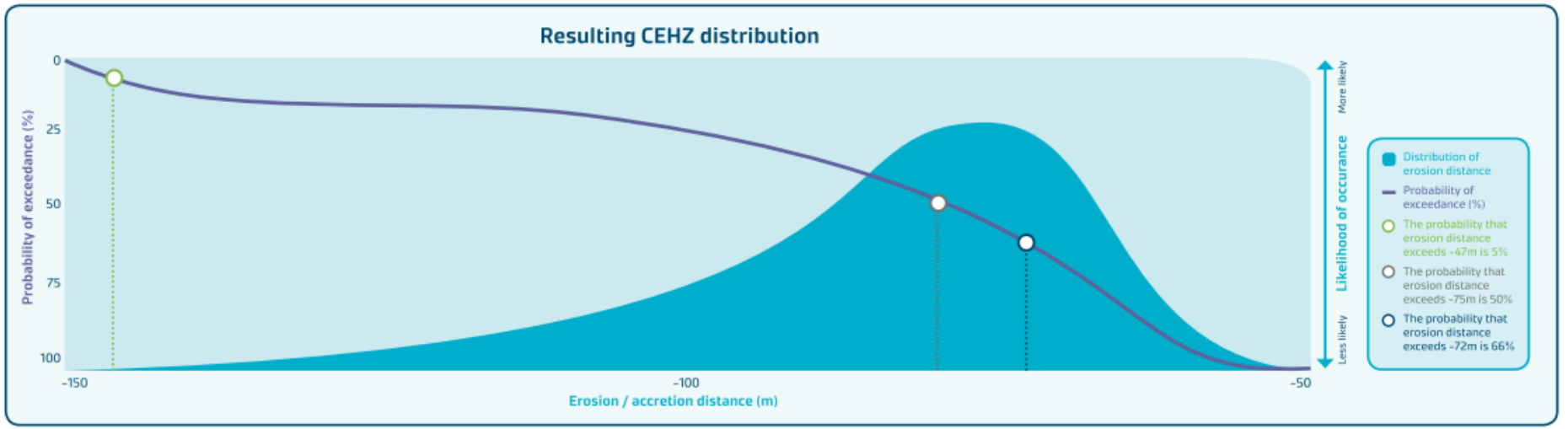

Figure 3-4: Example of resultant CEHZ distances for 2120. The cumulative distribution function (line) shows the probability of exceedance versus the erosion/accretion distance. The probability density function (distribution) shows the likelihood of occurrence.

3.1 Defining coastal behaviour cells

The open coast has been divided into coastal cells based on shoreline composition and behaviour which can influence in the resultant hazard. Factors which may influence the behaviour of a cell include:

- Cell morphology
- Profile geometry
- Backshore elevation
- Historic shoreline position.

Existing beach profiles of the HB series were used to define the coastal behaviour cells. The coast has been divided into 26 cells; 23 HB profiles plus 3 additional cells to represent the shoreline between the Port and Westshore. These cells represent the revetments extending from the Port to 350 m east of the Ahuriri estuary (HB12A) and just north of the Ahuriri estuary (HB13A), and the beach just east of the Ahuriri estuary (HB12B).

The coastal behaviour cells have been split up between the HB profiles based on the above described influencing factors. In this analysis a change in dune height, slope steepness, local wave climate and long-term shoreline trend were taken into account. Where no change in either of these influence factors was evident, coastal cells have been split in the middle of 2 adjacent HB profiles on the basis of a change in grain size (refer to Section 2.5). River areas as defined previously have been excluded from the coastal behaviour cells.

3.2 CEHZ component derivation

The CEHZ components identified in Section 3 and Equation 1 have been assessed for each behaviour cell and are described in the following sections below.

3.2.1 Planning timeframe (T)

Two planning time frames were applied to provide information on current hazards and information at sufficient time scales for planning and accommodating future development:

- 2065 Coastal Erosion Hazard Zone (50 years): CEHZ2065
- 2120 Coastal Erosion Hazard Zone (around 100 years): CEHZ2120.

Both the CEHZ2065 and CEHZ2120 implicitly include current hazards information.

3.2.2 Short-term (ST)

Short-term effects apply to coastlines where rebuilding follows periods of erosion. These effects include changes in horizontal shoreline position due to storm erosion caused by singular or clusters of storm events, or seasonal fluctuations in wave climate or sediment supply and demand. The short- term coastline movements can be assessed from statistical analysis of the MHWS excursion distance and numerical assessment of storm erosion potential.

3.2.2.1 Statistical methods

The horizontal position of shorelines derived from aerial photographs or contours derived from DEMs (typically MHWS) extracted from profile analysis can be used where available to assess short-term fluctuation.

The Beach Morphology Analysis Package (BMAP) has been used to calculate the change in horizontal shoreline position per surveyed beach profile. BMAP is an integrated set of computer analysis

routines compiled at the U.S. Army Engineer Waterways Experiment Station, Coastal Engineering Research Centre (CERC) for analysing beach profile morphology and its change (Larson and Kraus 1992).

Figure 3-5 shows an example of the available (91 surveyed) beach profiles for East Clive (HB6). The excursion of the RL 11 m contour, which is approximately high tide, has been assessed in BMAP to provide a plot of contour position over time (Figure 3-6). Refer to Appendix B for summary profile plots for each HB profile. Appendix C comprises contour excursion plot over time for each HB profile. The data has been de-trended to remove any long-term effects leaving residual excursion distances (Figure 3-7).

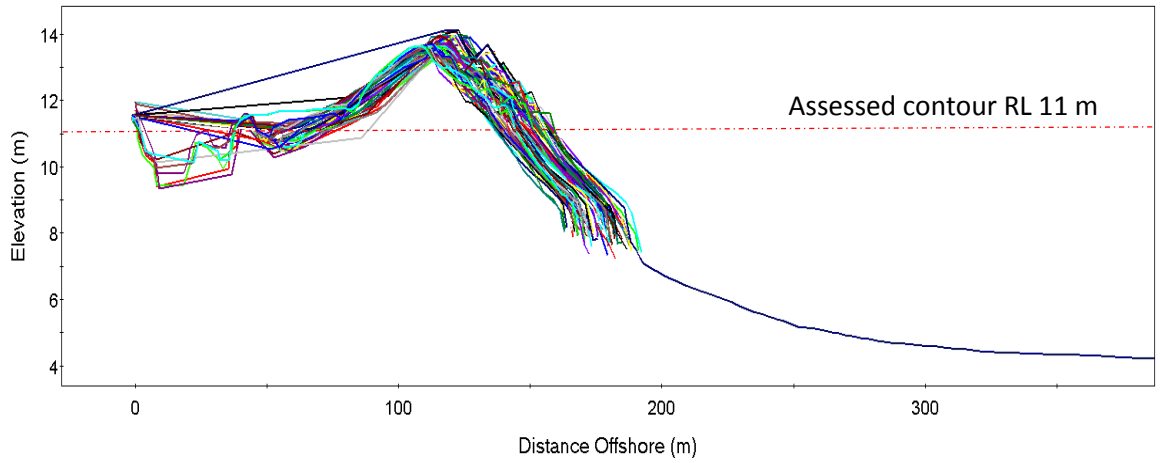

Figure 3-5: Example beach profiles for East Clive (HB6)

The standard deviation of residual describes the spread of the excursion distances. Previous work by Tonkin & Taylor (T+T, 2004; T+T 2006) found that the distribution of annual residual shoreline movement could be considered to be approximately normally distributed. The values at 1 standard deviation (SD), 2 x SD and 3 x SD from the mean will have corresponding annual probabilities of occurrence of 16%, 2.5%, and 0.5% respectively.

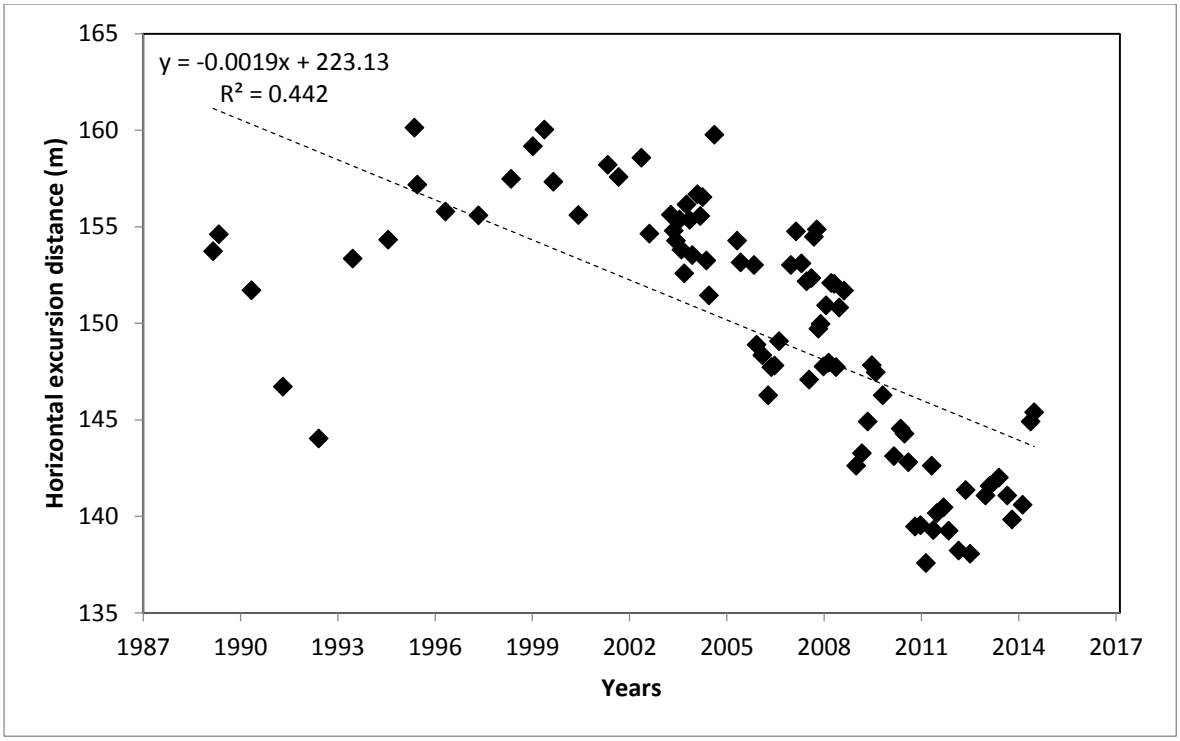

Figure 3-6: Example linear regression for East Clive (HB6)

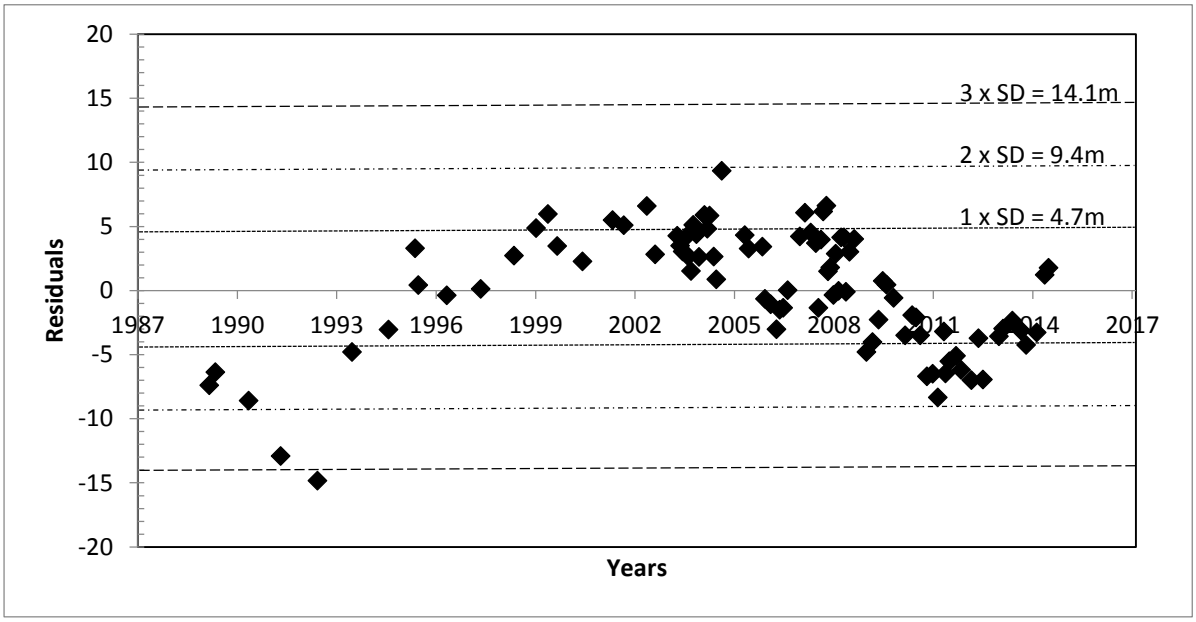

Figure 3-7: Example contour excursion residuals (de-trended) for East Clive (HB6)

With sufficient data, these may be interpreted as the bounding and modal parameters of the short-term fluctuation parameter. However, without frequent survey data, particularly immediately following storm events, it is likely that the maximum impact of storms is not well represented as some beach recovery will occur before the next regular survey or aerial photographic record.

Table 3-1 shows the average statistical measures of shoreline excursion. Two survey periods are shown in this table; the 1995-2014 period that is covered by all HB profiles, and the total survey periods which is variable. These results show that the standard deviation is generally situated between 2 m and 5 m for the 1995-2014 survey period. Exceptions are HB 4 – 7 which are

influenced by river deltas and construction of groynes, and HB 22 that is located in close proximity of the Te Ngarue River that discharges in the proximity of an offshore reef. River deltas are very dynamic, but can locally modify nearshore wave processes, affecting the longshore transport rate. Similarly offshore structures like reefs can do the same. Both these natural features can act like groyne structures which can reduce the alongshore transport of sediment until by-passing occurs. This is likely to affect the natural excursion of the 11 m contour. The standard deviation of the total surveyed period is generally similar to the 1995-2014 period, except for profiles that have been surveyed substantially longer or have been influence by human or natural interference (e.g. groynes or river deltas).

Table 3-1: Statistical measures of RL 11 m contour excursion

Profile	1995-2014			Total period (variable)		
	1 x SD	2 x SD	3 x SD	1 x SD	2 x SD	3 x SD
HB1	4.3	8.6	12.9	4.4	8.7	13.1
HB2	2.3	4.6	6.9	2.5	5.0	7.5
HB3	2.7	5.4	8.1	2.7	5.5	8.2
HB4	5.2	10.3	15.5	7.7	15.3	23.0
HB5	6.1	12.2	18.4	7.0	13.9	20.9
HB6	4.0	8.1	12.1	4.7	9.4	14.1
HB7	6.7	13.4	20.1	11.8	23.6	35.4
HB8	2.3	4.5	6.8	2.7	5.3	8.0
HB9	2.7	5.4	8.1	3.0	5.9	8.9
HB10	2.2	4.3	6.5	2.3	4.6	6.8
HB11	3.7	7.5	11.2	6.5	12.9	19.4
HB12	2.6	5.2	7.8	4.0	8.0	11.9
HB13	2.6	5.2	7.8	2.5	5.0	7.5
HB14	1.8	3.6	5.3	1.9	3.8	5.6
HB15	4.0	7.9	11.9	5.2	10.3	15.5
HB16	2.6	5.2	7.8	4.2	8.3	12.5
HB17	1.9	3.9	5.8	1.9	3.9	5.8
HB18	3.2	6.4	9.6	3.1	6.1	9.2
HB19	2.1	4.3	6.4	2.3	4.6	6.8
HB20	2.4	4.8	7.3	3.0	5.9	8.9
HB21	3.5	7.0	10.4	3.5	6.9	10.4
HB22	5.9	11.8	17.7	5.9	11.7	17.6
HB23	4.6	9.1	13.7	4.5	8.9	13.4

3.2.2.2 Numerical model assessment of storm erosion potential

Erosion of the upper beach is dependent on the energy able to reach the backshore, the duration of exposure to that energy and the erodibility of the upper beach material. The energy able to reach the backshore is dependent on water level and the offshore profile which controls wave breaking and energy dissipation. Both of these parameters change over the duration of a storm event.

The numerical process-based model X-Beach-Gravel (G) has been used to define storm cut volumes and horizontal movement of the dune toe. X-Beach-G is intended as a tool to assess the natural coastal response during time-varying storm conditions including dune erosion, over wash and breaching, by solving the depth averaged non-linear shallow water equations (McCall et al., 2014). These equations are forced by a time-dependent wave action balance that is solved on time-scale of wave groups. In this way the swash motion due to infragravity waves that are forced by the wave groups can be simulated. The X-Beach-G model covers in particular grain size, hydraulic conductivity (k), bottom aquifer (d_k) and ground water level (GWL) to accurately simulate the flow through the permeable gravel beach.

3.2.2.2.1 Model sensitivity

The sensitivity of the model has been tested for several cross-shore profiles by varying input parameters. The input parameters are the grain size, friction factor, hydraulic conductivity, ground water level (GWL) and Nielsen's phase lag. The grain size represents the median grain diameter (D_{50}) according to Smith, 1968 (see Section 2.5). The friction factor represents the non-dimensional sediment friction factor used to compute the initiation of motion of sediment and hence sediment transport, and should lie between 0.01 and 0.05 (Deltares, 2014). The hydraulic conductivity is a measure of the gravel's capacity to transmit water and lies between 0.001 and 1 m/s. The ground water level is the water level landward of the gravel barrier and lies between mean sea level and high water. The Nielson's phase lag represents the phase lag in degrees between the free stream velocity and the boundary layer velocity and should lie between 20 to 35 degrees (Deltares, 2014).

The above described parameters were tested over their given ranges and model results (11 m RL contour excursion/storm cut) were compared with the statistical method results (Table 3-1). It was found that both the hydraulic conductivity and Nielsen's phase lag parameters are sensitive:

- Low conductivity (0.001 m/s; minor flow through the gravel berm) led to a seaward excursion of the 11 m contour where a landward excursion was expected.
- High conductivity (1 m/s; large flow through gravel berm) led to an over prediction of the landward excursion/storm cut.
- A hydraulic conductivity of 0.01 m/s, measured on the east coast of Marlborough by Davidson and Wilson (2011), resulted in a similar landward excursion of the 11 m contour as was found using the statistical method (Section 3.2.2.1).
- Nielsen's phase lag of 35 degrees showed accretion where erosion was expected.
- Nielson's phase lag of 20 degrees showed an over prediction of the landward excursion/storm cut.
- A phase lag of 27.5 degrees was found to best represent the landward excursion of the 11 m contour.

The friction factor and grain size showed less variation of the 11 m contour over their ranges (> 5 m). The default friction factor (0.01) was therefore adopted. A ground water level at 10 m RL (MSL) and at 11.78 m RL (1% AEP water level) resulted in similar excursion of the 11 m contour. However, the overtopping rate increased for a lower GWL due to a larger head difference between sea water level and GWL. We have therefore adopted a GWL of 10 m RL.

By adopting the above described parameter values the X-Beach-G model simulates the 11 m contour storm cut in general in good agreement compared with the statistical model results (refer to Appendix E). It can therefore be concluded that a calibrated X-Beach-G model is able to perform well on mixed sand and gravel beaches.

3.2.2.3 Model input

Eleven cross-shore HB profiles, from the dune crest to approximately RL -10 m contour, representative for the entire shoreline between Clifton and Tangoio were used. These profiles are representative for the Hawke's Bay shoreline from Tangoio to Clifton (refer to Table 3-2).

Design storm nearshore time series including wave height, period and water level were applied at the outer profile boundary (see Figure 3-8). Design storms for 10 yr., 100 yr. and 2x100 yr. events are simulated with the latter allowing for potential clustering of storms. Such clustering may result in greater erosion as the first event lowers the beach height and relatively greater wave energy may reach the backshore in subsequent events. The shape of the design storm (see Figure 3-8) has been extracted from the WASP data set (refer to Section 2.7. Derivation of the design storms is shown in Appendix D.

Grain sizes according to Smith (1968) have been adopted for each HB profile (refer to Table 2-2). A sensitivity analysis has been undertaken to determine k, d_k and GWL. A hydraulic conductivity of 0.01 m/s and bottom aquifer and GWL at RL 10 m were found to best represent the Hawke's Bay gravel beaches.

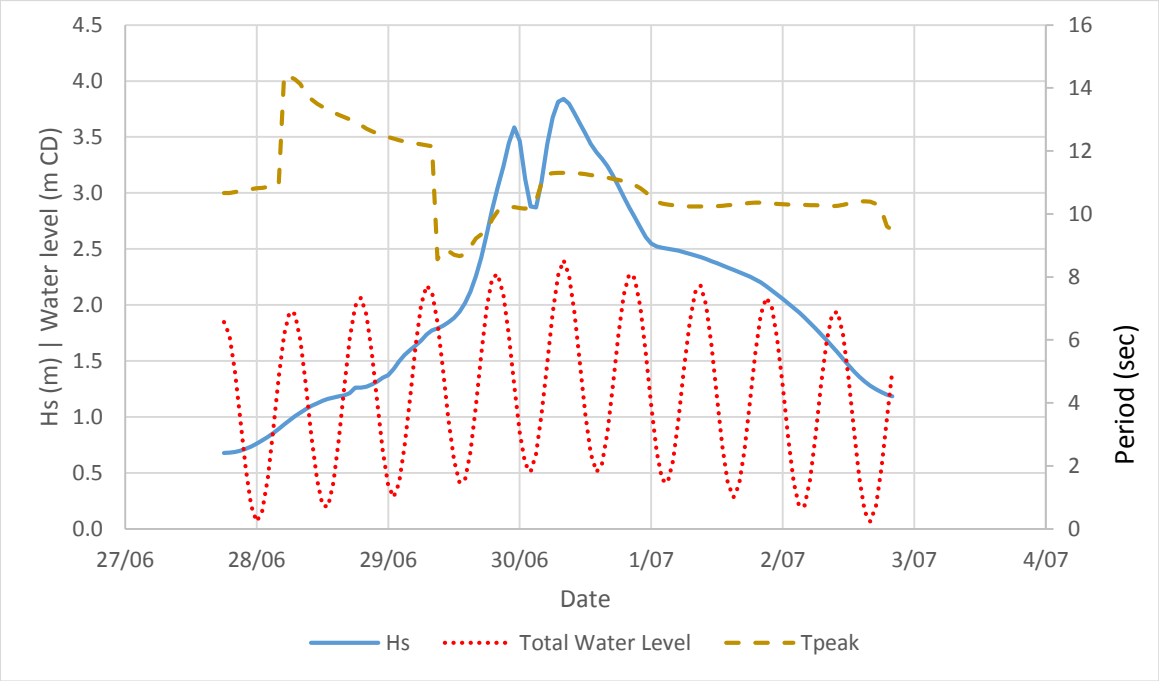

Figure 3-8: Example synthetic 100yr design storm input for East Clive (HB 6)

3.2.2.4 Model results

The initial and equilibrium profiles formed due to 10, 100 and 2x100 year storms for HB4 is shown in Figure 3-9. Changes in horizontal shoreline position provide information on short-term erosion distances. It can be seen that at profile HB 6 (see Figure 3-9) the storm cut near the 11 m contour (approx. MHWS) is in the same order for each storm (i.e. 8.5 m). The 12 m contour (approx. extreme water level) shows a larger storm cut due to the 2 x 100 yr. storm compared to the 10 yr. storm. Overtopping can be seen during the 10 yr. storm and the crest height remains approximately similar to the initial profile. The 2 x 100 yr. storm over washes the gravel beach and lowered the crest by approximately 0.8 m vertically. The eroded beach crest material is deposited landward of the lower crest (see Figure 3-9). The model appears to represent the physical process explained in more detail by Komar and Harris (2014) very well.

The model results are presented for both the 11 m contour (approx. MHWS) and 12 m contour (approx. extreme water level). The range of shoreline excursion distances calculated by X-Beach-G are shown in Table 3-2. The results show variable excursion distances, between 2 m and 18 m for each storm and both contours. Accretion at the 11 m contour was found for profiles HB13 and HB15. These profiles experienced erosion both above the 11 m contour and further down the profile. Eroded material from above the 11 m contour is deposited from the 11 m contour and down towards approximately the 8 m contour. Figure 3-10 shows accretion at the 11 m contour for profile HB 13 as a result of the 10 year and 100 year storms (0.5 m).

The landward shoreline excursion of 32 m at profile HB 13 as a result of a 2 x 100 year storm is visualised in Figure 3-10. As a result of erosion of the seaward barrier due to overwash, material is deposited further down the profile and the 11 m contour is shifted landward.

Table 3-2: Storm excursion distances (m) calculated by X-Beach-G

Profile	Contour	AEP storm		
		10%	**1%**	**2 x 1%**
HB1	11m	-5.5	-8	-9
	12m	-9	-15	-18
HB2	11m	-8.5	-9.5	-9.5
	12m	-8.5	-10	-11.5
HB4	11m	-4	-4.5	-5
	12m	-9	-11	-15
HB6	11m	-8.5	-8.5	-8.5
	12m	-11.5	-13.5	-17
HB12	11m	-14	-14	-12.5
	12m	-15.5	-16.5	-17
HB13	11m	accretion	accretion	-8.5
	12m	-4.5	-11	-32
HB15	11m	-1.5	accretion	accretion
	12m	-6.5	-7	-3
HB17	11m	-12	-12.5	-12.5
	12m	-12	-13	-13
HB19	11m	-14	-14	-15.5
	12m	-14	-15	-17
HB22	11m	-9	-9	-9
	12m	-12	-13	-14
HB23	11m	-6	-6	-2
	12m	-9	-10.5	-9

3.2.2.5 Adopted values

The assessment of the short-term fluctuation component (ST) was based on consideration of both statistical and numerical methods described above. It was considered that the HB beach profile dataset provides adequate information for statistical analysis to derive lower and modal bounds for the short-term component. The standard deviation of each coastal profile representative to the

corresponding cell was interpreted as the lower bound value for the short-term fluctuation component. Twice the standard deviation was adopted as model value. The 2 x 100 yr. storm results from the numerical X-Beach-G model at the 12 m contour were used to set the upper bounds. These values were adopted due to the potential over wash of several coastal profiles (e.g. see Figure 3-9). The statistical method does not take this into account and might underestimate the upper short-term fluctuation.

The short-term fluctuation component for HB12A, HB12B and HB13A were determined consistent with the method used by T+T (2006). An upper bound of 1.25 times the SD of HB13 and a lower of zero were adopted for HB12A and HB13A. An upper, modal and lower bound of 1, 2 and 3 x SD of HB13 was adopted for HB12B.

An overview of both methods results including adopted values are shown in appendix E. Table 3-3 shows the adopted values for each cell.

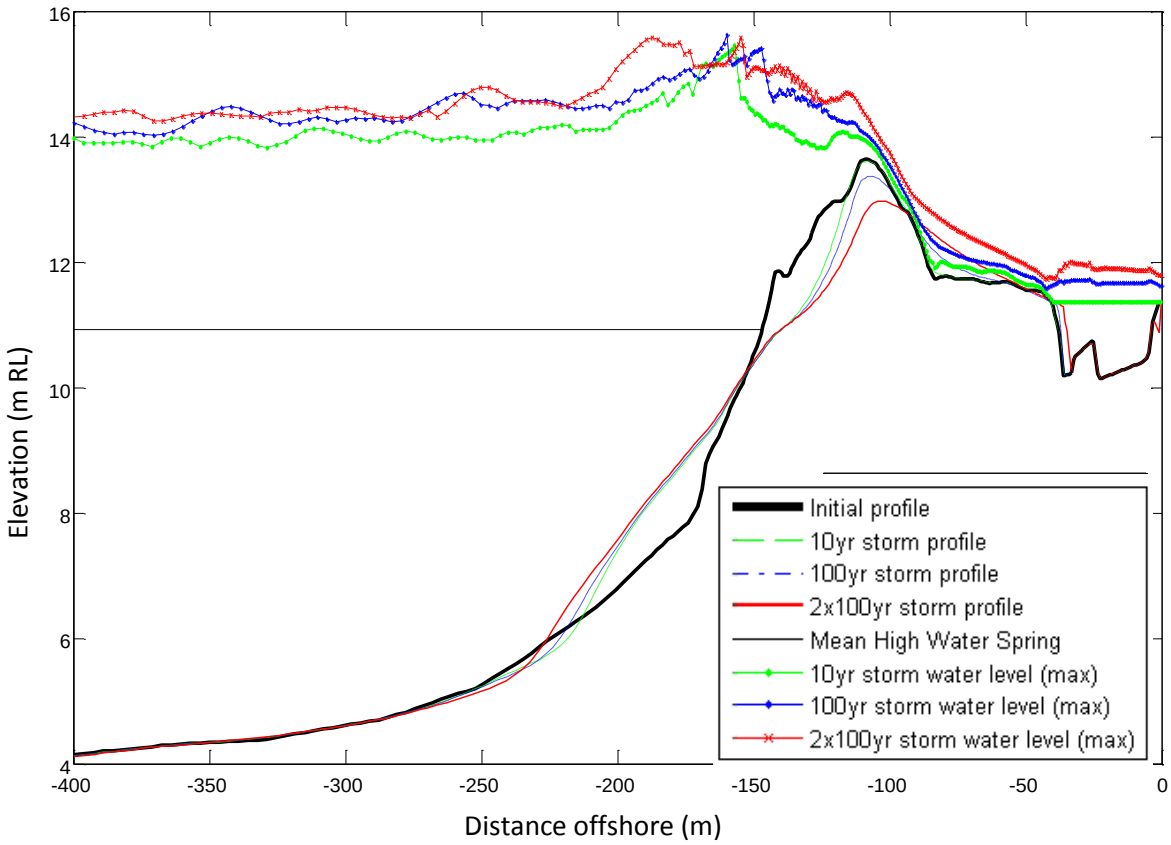

Figure 3-9: X-Beach-G results for East Clive (HB 6)

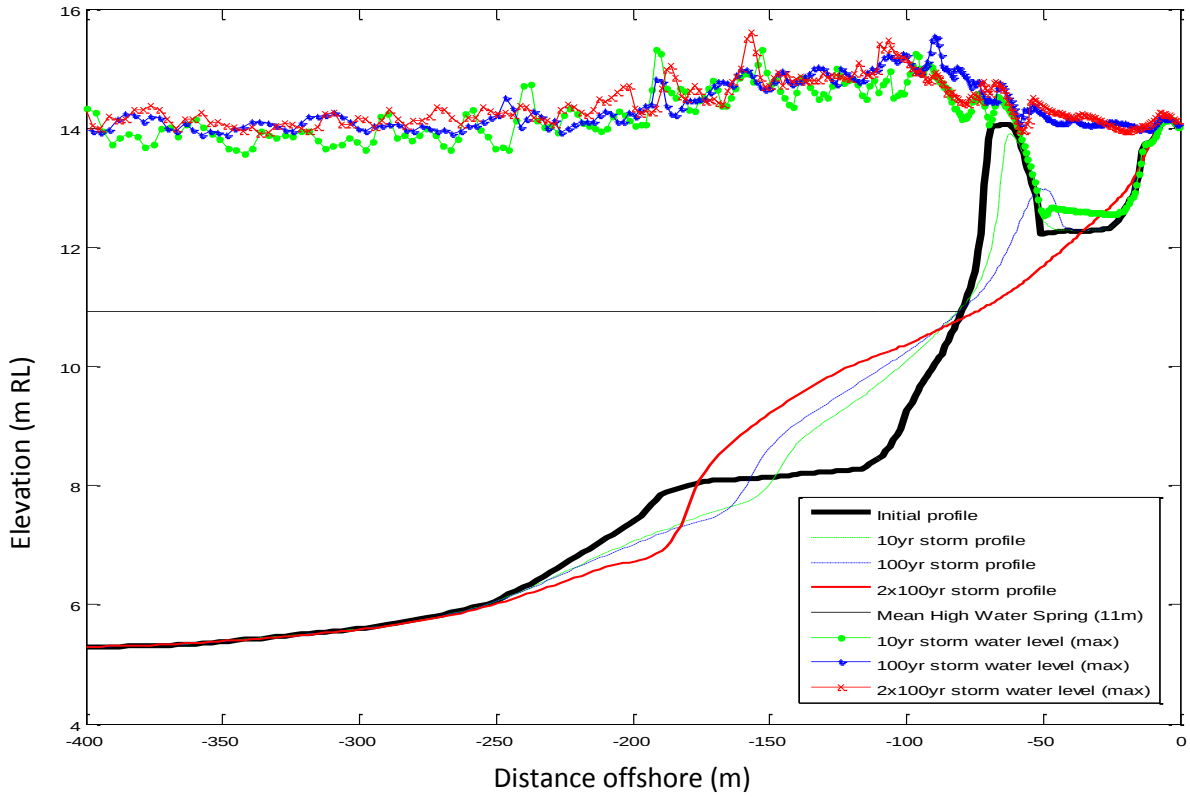

Figure 3-10: X-Beach-G results for Westshore (HB 13)

Table 3-3 Short-term erosion component values

Cell	Short-term component value bounds		
	Lower (m)	Mode (m)	Upper (m)
HB1	4.3	8.6	18.0
HB2	2.3	4.6	11.5
HB3	2.7	5.4	8.1
HB4	5.2	10.3	15.0
HB5	6.1	12.2	16.0
HB6	4.0	8.1	17.0
HB7	6.7	13.4	18.5
HB8	2.3	4.5	11.5
HB9	2.7	5.4	11.5
HB10	2.2	4.3	12.0
HB11	3.7	7.5	12.0
HB12	2.6	5.2	12.5
HB12A	0.0	1.6	3.2
HB12B	2.6	5.2	7.8
HB13A	0.0	1.6	3.2
HB13	2.6	5.2	32.0
HB14	1.8	3.6	5.4

Cell	Short-term component value bounds		
	Lower (m)	Mode (m)	Upper (m)
HB15	4.0	7.9	11.9
HB16	2.6	5.2	11.0
HB17	1.9	3.9	13.0
HB18	3.2	6.4	12.5
HB19	2.1	4.3	17.0
HB20	2.4	4.8	15.0
HB21	3.5	7.0	14.0
HB22	5.9	11.8	14.0
HB23	4.6	9.1	13.7

3.2.3 Dune stability (DS)

The dune stability factor delineates the area of potential risk landward of the erosion scarp by buildings and their foundations. The parameter assumes that storm erosion results in an over-steepened scarp which must adjust to a stable angle of repose for loose sand/gravel. The dune stability width is dependent on the height of the existing backshore and the angle of repose for loose sand/gravel. This has been obtained from an examination of historic reports, a review of the beach profile data and our assessment of the beach sediments obtained in this study. The dune stability factor is outlined below:

$$DS = \frac{H_{dune}}{2(\tan \alpha_{gravel})} \quad \text{(Equation 2)}$$

Where H_{dune} is the dune height from the 11 m contour to the crest and α_{gravel} is the stable angle of repose for sand/gravel (ranging from 32 to 35 degrees), consistent with T+T (2004). In reality, dune scarps will stand at steeper slopes due to the presence of binding vegetation and formation of talus slope at the toe. However, development immediately landward of the scarp and within the area defined by the formula may still be vulnerable. Parameter bounds are defined based on the variation in dune height along the coastal behaviour cell and potential range in stable angle of repose.

Table 3-4 Dune stability component values

	Dune stable angle value bounds (α_{gravel})		
Cell	**Lower (degrees)**	**Mode (degrees)**	**Upper (degrees)**
HB1 – HB 23	32	33.5	35

3.2.4 Long-term trends (LT)

The long-term rate of horizontal coastline movement includes both ongoing trends and long-term cyclical fluctuations. These may be due to changes in sea level, fluctuations in coastal sediment supply or associated with long-term climatic cycles such as IPO.

Rates of long-term shoreline change are derived from BMAP using linear regression analysis with the 95% confidence intervals providing bounding values for the parameter distribution (see Figure 3-11). The shoreline change rates between 1995 and 2014 have been generally used to have a consistent survey time-period for each HB profile. However, in reviewing both the longer survey period (see

Table 2-1) and the 1995-2014 survey period, we adopted the longer survey period in some cases where it better represented the long-term trend. This has been done to exclude non-natural effects on long-term trends by, for instance, the construction of groynes. Furthermore, both aerial photographs and the DEMs were used to review the adopted long term trends. The historic (1940s) and latest vegetation line (2012) were digitised based on the aerial photographs and compared with the long term trends. The DEMs (2003 and 2012) were used by extracting the 11 m contour and comparing their position. The review of both the aerial photographs and DEMs led in particular to adopting the longer survey periods for HB1 and HB2 as it better represented the long term trend. Table 2-1 shows profiles for which longer survey periods have adopted indicated with an asterisk.

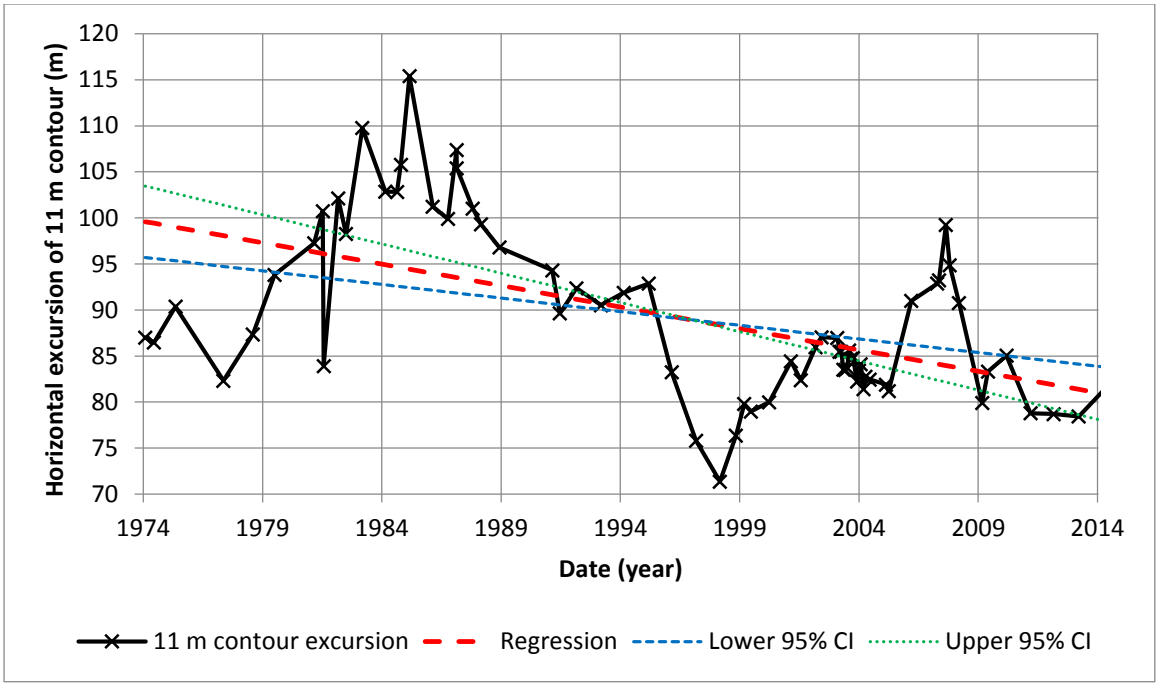

Figure 3-11: Regression of the 11 m contour including upper and lower 95% Confidence Intervals (CI) for HB4.

The lower and upper 95% confidence intervals have been adopted as upper and lower bound values for each cell. The average shoreline change rate was considered as the modal value. Table 3-5 shows the adopted long-term erosion component values for each cell. Figure 3-12shows an example of how minimum and maximum value bounds were selected.

A long-term rate of zero was adopted for HB12A and HB13B assuming that the seawalls are to be properly maintained or to be repaired following significant damage. HB12B is assumed to be influenced by both the adjacent breakwater and revetment on the east side, and we have therefore adopted a long-term of zero.

Table 3-5 Long-term erosion component values

Cell	Long-term component value bounds		
	Lower (m)	Mode (m)	Upper (m)
HB1*	-0.61	-0.49	-0.36
HB2*	-0.22	-0.15	-0.11
HB3	-0.77	-0.57	-0.38
HB4	-0.79	-0.18	0.42
HB5	-1.99	-1.72	-1.45

Cell	Long-term component value bounds		
	Lower (m)	Mode (m)	Upper (m)
HB6	-1.39	-1.24	-1.08
HB7	-0.86	-0.60	-0.34
HB8	0.43	0.54	0.66
HB9*	0.18	0.26	0.35
HB10	0.38	0.46	0.53
HB11*	0.62	0.75	0.88
HB12	-0.03	0.07	0.17
HB12A	0	0	0
HB12B	0	0	0
HB13A	0	0	0
HB13	-0.44	-0.37	-0.30
HB14	-0.16	-0.05	0.06
HB15*	-0.05	0.03	0.10
HB16	0.28	0.46	0.64
HB17	-0.06	0.08	0.22
HB18	-0.77	-0.54	-0.31
HB19	-0.57	-0.42	-0.27
HB20*	-0.43	-0.22	-0.02
HB21	-0.28	-0.02	0.23
HB22	-0.59	-0.17	0.26
HB23	-0.50	-0.17	0.16

* Longer survey period applied (refer to Table 2-1 for survey period)

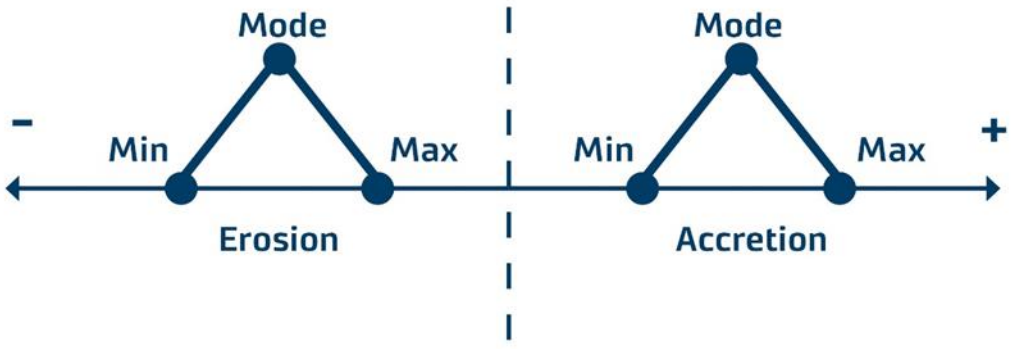

Figure 3-12: Example of triangle distributions and value bounds adopted for the long-term trends. The maximum value bounds represents the largest value of accretion or smallest (negative) value of erosion. The minimum value bounds represent the smallest value of accretion or largest (negative) value of erosion.

3.2.5 Effects of sea level rise (SL)

As discussed in Section 2.6.5 we have adopted a range of sea level rise values over the 100 year timeframe (i.e. 2120) based on Komar and Harris (2014). These projections represent the most probable increases based on the analysis by climatologists. This is considered prudent until evidence of emission stabilising justify use of a lower projection scenario. These projected sea levels range from 0.4 to 0.7 m by 2065 and 0.9 to 1.8 m by 2120 (refer to Section 2.6.5).

An average historic rate of sea level rise of 2 mm/year (Komar and Harris, 2014) has been deducted from these sea level rise values for use in this assessment on the basis that the existing long-term trends and processes already incorporate the response to historic increases of sea level. The rise in relative sea level for Hawke's Bay is somewhat greater than the average rate of 1.7 mm/year for New Zealand (e.g. Wellington and Lyttelton). However, a somewhat higher rate would be expected in view of the tectonic setting of Hawke's Bay (GeoNet; Komar and Harris, 2014).

The adjusted sea levels range from 0.3 to 0.6 m by 2065 and 0.6 to 1.5 m by 2120. The base year for the projections to 2120 is 2015. Table 3-6 presents sea level rise values used in this coastal hazard assessment.

Table 3-6 Sea level rise values utilised in assessment

Time frame	Lower (m)	Mode (m)	Upper (m)
Projected 2065	0.4	0.6	0.7
Adjusted 2065	0.3	0.5	0.6
Projected 2120	0.9	1.3	1.8
Adjusted 2120	0.6	1.0	1.5

Note: the adjusted values include a discount of 2 mm/year based on average historical trends.

3.2.5.1 Beach response

Geometric response models propose that as sea level is raised, the equilibrium profile is moved upward and landward conserving mass and original shape Figure 3-13. The most well-known of these geometric response models is that of Bruun (Bruun, 1962, 1988) which proposes that with increased sea level, material is eroded from the upper beach and deposited offshore to a maximum depth, termed closure depth. The increase in sea bed level is equivalent to the rise in sea level and results in landward recession of the shoreline. The model can be defined by the following equation:

$$SL = \frac{L_*}{B + h_*} S \qquad \text{(Equation 3)}$$

Where SL is the landward retreat, h_* defines the maximum depth of sediment exchange taken as the closure depth, L_* is the horizontal distance from the shoreline to the offshore position of h_*, B is the height of the berm/dune crest within the eroded backshore and S is the sea level rise.

The Bruun Rule is considered to provide an acceptable "order of magnitude" estimate of shoreline retreat distance due to a rise in sea level (Ramsey et al, 2012). However, it is governed by simple, two-dimensional conservation of mass principles and is limited in its application in the following aspects:

- The rule assumes that there is an offshore limit of sediment exchange or a 'closure depth' beyond which the seabed does not raise with sea level
- The rule assumes no offshore or onshore losses or gains

- The rule assumes an equilibrium beach profile where the beach may fluctuate under seasonal and storm influences but returns to a statistically average profile (i.e. the profile is not undergoing long-term steepening or flattening)
- The rule does not accommodate variations in sediment properties across the profile or profile control by hard structures such as substrate geology or adjacent headlands.

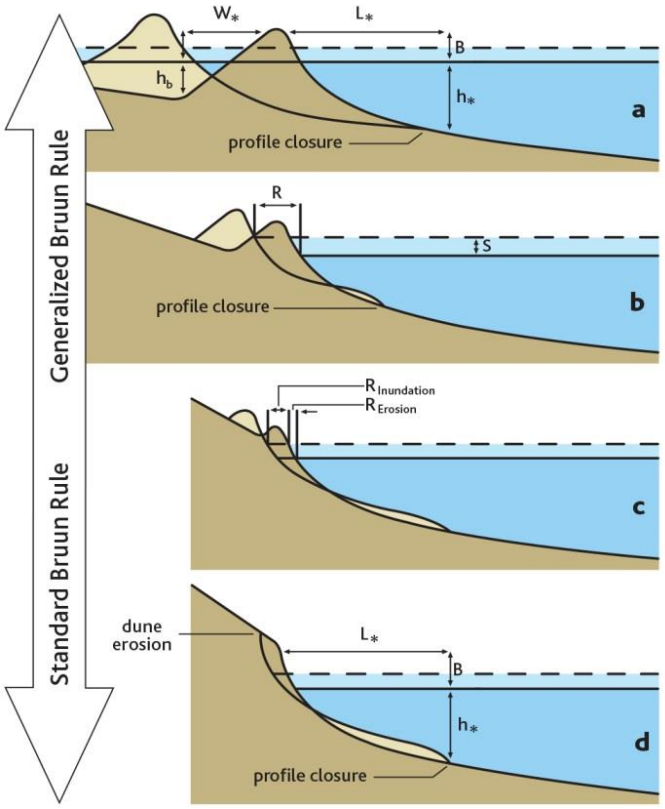

Figure 3-13 Schematic diagrams of the Bruun model modes of shoreline response (after Cowell and Kench, 2001)

Although the Bruun Rule has been the subject of intense debate since the early 1970's, the general consensus is that the rule still has an overall general validity (Komar et al., 1991; Diez, 2000). Furthermore, Komar and Harris (2014) describe that although the responses of sand beaches and gravel barrier ridges are fundamentally different, see Figure 3-13d (sand beach) and Figure 3-13a (gravel beach), the underlying geometry turns out to be essentially the same. In review of landward retreat based on the Standard Bruun Rule compared to the Generalised Bruun Rule (reviewing 7 low crested profiles) it was found that difference is minor (generally < 3 m). The Standard Bruun Rule was therefore utilised in this study.

Paterson (2000) identified that erosion has occurred along the shorelines where there was a relative increase in sea level due to the 1931 earthquake. However, his assessment of the Bruun rule utilising the slope of the gravel beach face to establish the effective beach slope suggested that the rule appeared to under predict the actual erosion indicating that other erosion forces, such as a net deficit in sediment supply may also be contributing to the erosion and/or the nearshore environment also attributed to the potential losses due to accelerated sea level rise. Paterson suggested that the closure depth is likely to be further off shore than the toe of the gravel beach.

While some have questioned the actual existence of a closure depth (Cooper and Pilkey, 2004), the Bruun Rule is not necessarily reliant on its physical existence. While long-term sediment exchange

may occur to very deep water depths (i.e. the 'pinch-out' point), this "ultimate limit" profile adjustment extent is only valid if either the profile response is instantaneous or if sea level changes and then stabilises with the profile 'catching up'. As sea level rise is expected to be ongoing and a lag in profile response is apparent, the outer limit of profile adjustment is likely to be left behind. The closure depth can therefore be more realistically defined as the point at which the profile adjustment can keep up with sea-level change and becomes a calibration parameter in lieu of an adequate depth dependent lag parameter.

To define SL component distributions, the Bruun rule estimates using the inner Hallermeier closure depth definition (d_i) have been adopted as upper bound values and results using the beach face slope (Komar, 1999) provide the lower (almost certain) bounds. An average of the beach slope and closure slope has been adopted as model value. The beach face is defined by average mean low water spring position and average beach crest height. The Hallermeier closure definition is defined as follows (Nicholls et al., 1998):

$$d_l = 2.28H_{s,t} - 68.5(H_{s,t}^2 / gT_s^2) \cong 2 \times H_{s,t} \qquad \text{(Equation 4)}$$

Where:

- d_l = the closure depth below *mean low water spring,*
- $H_{s,t}$ = non-breaking significant wave height exceeded for 12 hours in a defined time period (nominally one year), and
- T_s = the associated wave period.

The wave climate parameters were based on wave output from MetOcean (2013). A representative average cross-shore profile of each HB profile has been used to define both the beach face slope and closure depth. Appendix F presents a summary of the calculated closure depths, inner closure slopes and beach face slopes adopted for each profile.

3.2.6 Combination of parameters

For each coastal cell, the relevant component bounds influencing the CEHZ have been defined according to the methods described above as summarised in

Table 3-7 Theoretical erosion hazard parameter bounds

Parameter	Lower bound	Mode	Upper bound
ST (m)	1 x SD based on beach profile data	2 x SD based on beach profile data	Erosion resulting from a 2x1% AEP event from X-beach-G model study
DS (m)	H_{max} and α_{min}	H_{mean} and α_{mean}	H_{min} and α_{max}
LT (m/yr.)	-95% CI of smallest 1995-2014 trend in cell	Mean regression 1995-2014 trend	+95% CI of largest 1995-2014 trend in cell
SLR (m)	Lower 'consensus' SLR curve (Komar and Harris, 2014) minus historic trend	Middle 'consensus' SLR curve (Komar and Harris, 2014) minus historic trend	Upper 'consensus' SLR curve (Komar and Harris, 2014) minus historic trend
Closure slope	Slope across active beach face to typical swash excursion as based on Komar (2002)	Average of the active beach face and inner closure depth slope	Slope from dune crest to inner Hallermeier closure depth

Table 3-8 Input bound for each CEHZ components within each cell

Cells	Short-term (m)			Dune elevation (m)			Stable angle (deg)			Long-term (m/yr.)			Closure slope			SLR 2065 (m)			SLR 2120 (m)		
	Min	Mode	Max	Min	Mode	Max	Min	Mode	Max	Min	Mode	Max	Min	Mode	Max	Min	Mode	Max	Min	Mode	Max
HB1	4.3	8.6	18.0	1.5	2.5	3	32	33.5	35	-0.61	-0.49	-0.36	0.093	0.049	0.005	0.3	0.5	0.6	0.6	1.0	1.5
HB2	2.3	4.6	11.5	2	3	3.5	32	33.5	35	-0.22	-0.15	-0.11	0.096	0.053	0.010	0.3	0.5	0.6	0.6	1.0	1.5
HB3	2.7	5.4	8.1	2.25	2.75	3.25	32	33.5	35	-0.77	-0.57	-0.38	0.110	0.064	0.018	0.3	0.5	0.6	0.6	1.0	1.5
HB4	5.2	10.3	15.0	2.75	3	3.25	32	33.5	35	-0.79	-0.18	0.42	0.087	0.053	0.019	0.3	0.5	0.6	0.6	1.0	1.5
HB5	6.1	12.2	16.0	2.25	2.75	3.25	32	33.5	35	-1.99	-1.72	-1.45	0.081	0.050	0.019	0.3	0.5	0.6	0.6	1.0	1.5
HB6	4.0	8.1	17.0	2	2.5	3.25	32	33.5	35	-1.39	-1.24	-1.08	0.086	0.058	0.030	0.3	0.5	0.6	0.6	1.0	1.5
HB7	6.7	13.4	18.5	3	3.25	4	32	33.5	35	-0.86	-0.60	-0.34	0.090	0.068	0.046	0.3	0.5	0.6	0.6	1.0	1.5
HB8	2.3	4.5	11.5	3.5	4	4.5	32	33.5	35	0.43	0.54	0.66	0.096	0.071	0.046	0.3	0.5	0.6	0.6	1.0	1.5
HB9	2.7	5.4	11.5	3.25	4	4.25	32	33.5	35	0.18	0.26	0.35	0.095	0.070	0.045	0.3	0.5	0.6	0.6	1.0	1.5
HB10	2.2	4.3	12.0	3.25	3.75	4	32	33.5	35	0.38	0.46	0.53	0.095	0.066	0.038	0.3	0.5	0.6	0.6	1.0	1.5
HB11	3.7	7.5	12.0	4	4.25	4.5	32	33.5	35	0.62	0.75	0.88	0.090	0.067	0.043	0.3	0.5	0.6	0.6	1.0	1.5
HB12	2.6	5.2	12.5	4	4.5	5.25	32	33.5	35	-0.03	0.07	0.17	0.091	0.067	0.044	0.3	0.5	0.6	0.6	1.0	1.5
HB12A	0.0	1.6	3.2	3.25	3.5	3.75	32	33.5	35	0	0	0	0.119	0.069	0.019	0.3	0.5	0.6	0.6	1.0	1.5
HB12B	2.6	5.2	7.8	3.25	3.5	3.75	32	33.5	35	0	0	0	0.060	0.040	0.019	0.3	0.5	0.6	0.6	1.0	1.5
HB13A	0.0	1.6	3.2	2	2.5	3	32	33.5	35	0	0	0	0.070	0.039	0.008	0.3	0.5	0.6	0.6	1.0	1.5
HB13	2.6	5.2	32.0	2.5	3	3.5	32	33.5	35	-0.44	-0.37	-0.30	0.070	0.039	0.008	0.3	0.5	0.6	0.6	1.0	1.5
HB14	1.8	3.6	5.4	4.25	4.5	5	32	33.5	35	-0.16	-0.05	0.06	0.100	0.063	0.026	0.3	0.5	0.6	0.6	1.0	1.5
HB15	4.0	7.9	11.9	4.5	4.75	5	32	33.5	35	-0.05	0.03	0.10	0.103	0.070	0.038	0.3	0.5	0.6	0.6	1.0	1.5
HB16	2.6	5.2	11.0	6	6.5	7	32	33.5	35	0.28	0.46	0.64	0.070	0.060	0.050	0.3	0.5	0.6	0.6	1.0	1.5
HB17	1.9	3.9	13.0	6	6.5	7	32	33.5	35	-0.06	0.08	0.22	0.100	0.079	0.057	0.3	0.5	0.6	0.6	1.0	1.5
HB18	3.2	6.4	12.5	6.5	7	7.5	32	33.5	35	-0.77	-0.54	-0.31	0.094	0.082	0.069	0.3	0.5	0.6	0.6	1.0	1.5
HB19	2.1	4.3	17.0	7.75	8	8.25	32	33.5	35	-0.57	-0.42	-0.27	0.100	0.089	0.078	0.3	0.5	0.6	0.6	1.0	1.5

Cells	Short-term (m)			Dune elevation (m)			Stable angle (deg)			Long-term (m)			Closure slope			SLR 2065 (m)			SLR 2120 (m)		
	Min	Mode	Max	Min	Mode	Max	Min	Mode	Max	Min	Mode	Max	Min	Mode	Max	Min	Mode	Max	Min	Mode	Max
HB20	2.4	4.8	15.0	8	8.25	8.75	32	33.5	35	-0.43	-0.22	-0.02	0.100	0.094	0.088	0.3	0.5	0.6	0.6	1.0	1.5
HB21	3.5	7.0	14.0	7.25	7.75	8.5	32	33.5	35	-0.28	-0.02	0.23	0.107	0.083	0.059	0.3	0.5	0.6	0.6	1.0	1.5
HB22	5.9	11.8	14.0	7	7.5	7.75	32	33.5	35	-0.59	-0.17	0.26	0.106	0.074	0.043	0.3	0.5	0.6	0.6	1.0	1.5
HB23	4.6	9.1	13.7	5.5	6.5	7.25	32	33.5	35	-0.50	-0.17	0.16	0.100	0.069	0.039	0.3	0.5	0.6	0.6	1.0	1.5

Probability distributions constructed for each parameter have been randomly sampled and the extracted values used to define a potential CEHZ distance. This process has been repeated 10,000 times using a Monte Carlo technique and the probability distribution of the resultant CEHZ width is forecast.

A risk-based approach to managing coastal hazard is advocated by the NZCPS (2010) with the likelihood and consequence of hazard occurrence requiring consideration. For example, the NZCPS (2010) suggests consideration of areas both 'likely' to be affected by hazard and areas 'potentially' affected by hazard. While the term 'likely' may be related to a likelihood over a defined timeframe based on guidance provided by MfE (2008), i.e. a probability greater than 66% as shown in Table 3-9, the term potential is less well defined, but could be considered 'conceivable' (i.e. 1-10%). This assessment therefore aims to derive a range of hazard zones corresponding to differing likelihoods which may be applied to risk assessment.

Table 3-9 Likelihood of scenario occurring within the selected planning horizon

Designation	Frequency	Description	IPCC definition
			Virtually certain (> 99% chance that a result is true)
A	Almost certain	Is expected to happen, perhaps more than once	Very likely (90–99%)
B	Likely	Will probably happen	Likely (66–90%)
C	Possible	Might occur; 50/50 chance	Medium (33–66%)
D	Unlikely	Unlikely to occur, but possible	Unlikely (10–33%)
E	Rare	Highly unlikely, but conceivable	Very unlikely (1–10%)
			Exceptionally unlikely (< 1%)

3.2.7 Mapping the CEHZ

Coastal erosion hazard zone distances are mapped as offsets to the existing baseline of the 2011/2012 dune toe/vegetation line. Where the hazard values differ between adjacent coastal cells, the mapped CEHZ is either merged over a distance of at least 10 x the difference between values providing smoother transitions or along contours or material discontinuities where these are present.

3.2.8 Uncertainties and limitations

Uncertainty may be introduced to the assessment by:

- An incomplete understanding of the components influencing the coastal erosion hazard zone
- An imprecise description of the natural processes affecting, and the subsequent quantification of, each individual parameter
- Errors introduced in the collection and processing of data
- Variance in the processes occurring within individual coastal cells.

Of these uncertainties, the alongshore variance of individual coastal cells may be reduced by splitting the coast into continually smaller cells. However, data such as beach profiles are often available only at discrete intervals, meaning increasing cell resolution may not necessarily increase data resolution and subsequent accuracy. We believe we have refined the cells as far as practical based on factors which could significantly affect results. Residual uncertainty may be allowed for by selecting a lower probability CEHZ value.

The first two uncertainty items listed above are being continually developed within coastal research fields. However, there is generally a lag time between scientific developments, and their use in practical assessment as they are refined, tested and made generically applicable. This assessment has used relatively new techniques by incorporating probabilistic assessment of components.

Similarly, numerical models are beginning to better resolve the physical processes responsible for coastal erosion such as the X-Beach-G model used for this study. However, complex coupled models are computationally expensive and heavily reliant on quality, long-term data. Without such data, complex model results are largely meaningless. We have attempted to balance the use of numerical modelling where useful (wave and beach response) with analytical and empirical assessment to ensure results are robust and sensible.

Uncertainty in individual parameter is incorporated into the present assessment within the individual parameter bounds. Greater uncertainty utilises wider parameter bounds while less uncertainty utilises narrower bounds. For instance, sea level rise has a great uncertainty and hence broad parameter bounds, where the stable angle of repose of gravel has narrow bounds due to its grain size dependence. Both the dune elevation and long-term parameters are dependent of the quality of the data and generally have narrow bounds. The short-term and closure slope parameters both are derived from calculations and have wider bounds. This allows independent uncertainty terms to be combined within the probabilistic framework rather than utilising a single factor or adding uncertainty to each term as has been done previously.

Uncertainties in individual components will reduce as better and longer local data is acquired, particularly around rates of short- and long-term shoreline movement and shoreline response to sea level rise. Data collection programmes such as beach profiling are essential to reducing this uncertainty and should be continued. Our approach can also allow for uncertainties and data limitations by the user defined selection of the P value output. We recommend that conservative, lower probability CEHZ values are selected for implementation.

3.2.9 Anthropogenic effects

The human influences on coastal erosion hazard assessment include:

- Construction of land protection works (groynes, seawalls/revetments, etc.)
- Mining and removal of beach gravel, or nourishment.

3.2.9.1 Groynes and seawalls

Several groynes have been constructed in the past that locally influence the location of the coastal hazard zones:

- Hastings sewer outfall/groyne (1979)
- Ngaruroro groyne 1 (1988)
- Ngaruroro groyne 2 (1993)
- Tukituki groyne (1999).

The Hastings sewer outlet is located approximately 500 m north of HB 5. The Ngaruroro groynes are located between the Hastings sewer outfall and the Ngaruroro River. The Tukituki groyne is located just north of HB 4 on the south side of the Tukituki River mouth. We note there is also a small groyne is also present at the southern side of the Port of Napier, which is at the northern boundary of the Haumoana Littoral Cell and does not materially affect the coastal hazard zone location as it is within the Port area.

Several revetments are present between HB 1 and Clifton, and a seawall has been on the seaward side of Clifton Road. At the southern side of the Bay View Littoral Cell several revetments were constructed.

While properly designed coastal protection works can reduce erosion rates for the land area the structure is designed to protect, the shoreline position is generally returned to its long-term equilibrium position rapidly once the structure fails or is removed. We have therefore evaluated the hazard extent excluding the effects of the majority of these structures apart from the shoreline from Ahuriri Lagoon to the Port. This identifies the potential land area that could be affected, or the area that is benefitting with the structure. Informed decision around the future maintenance or re-consenting of structures can then be made.

3.2.9.2 Extraction

Beach gravel and sand have been extracted from both Pacific Beach in Napier (1993 to 2014) and along the shores to the north of the Ngaruroro River at Awatoto (1973 to present). The extracted gravel and sand is serving as the source of sediment for nourishment of the beach at West shore (HB13). The estimated extracted annual rates according to Komar and Harris (2014) are:

- Awatoto extraction: 47,800 m^3/year (HB8)
- Pacific beach extraction: 13,800 m^3/year (HB12)

Gravel volumes extracted at Awatoto have been limited to 30,000 m^3/yr since 2006 and this reduction in volume has resulted in an average extraction rate of 41,100 m^3/yr since 1995. Yearly gravel extracted volumes at both Awatoto and Pacific Beach until 2010 can be found in T+T (2012). Extraction at Pacific Beach ceased in 2014, so no further extraction at this location will occur.

As the long term trend has been based on measured shoreline information at the 23 beach profile location, historic extraction has been taken into account in determining the upper, modal and lower bound values for the long-term trend component. As we have adopted the long-term trend from the 1995 – 2014 survey period for both HB8 and HB12, the larger extractions that historically occurred at Awatoto have not been taken into account, although ongoing extraction at Pacific Beach is conservatively included. With reduced extraction at Awatoto and Pacific Beach it is anticipated that the observed accretion trends observed at HB8 to 12 will continue, so the erosion hazard extents at these locations may be slightly conservative.

At HB13 the average long term trend from 1995 to 2014 was 0.37m/yr (refer Table 3-8). The influence of the present nourishment can be examined by comparing shoreline trends from 1974 to 1993, prior to beach nourishment which gives an annual erosion rate of 0.69 m/yr. Therefore without ongoing nourishment of this area to “hold the line” the erosion rate under present day conditions could double. However, as evidenced both by existing long term trends at HB 13 and the potential future effect of climate change, the gravel volumes placed at Westshore would need to be progressively increased to maintain the ‘hold the line’ approach currently in place.

4 Coastal erosion hazard assessment results

Components have been assessed for each coastal cell based on the data and methodologies described in preceding sections. Table 4-1, Table 4-2 and Table 4-3 show the CEHZ results for the present day, 2065 and 2120 timeframe respectively. Appendix G shows graphs of the CEHZ results for the three timeframes. The 2065 plot includes the CHZ1 extent as included in the HBRC coastal plan. The 2120 plot includes the CHZ2 extent.

4.1 Discussion of results

Due to the consideration of accretion trends as well as erosion trends the future erosion hazard extents can be less than the current erosion hazard zone. This is particularly evident between HB8 and HB12 where the maximum CEHZ is between -15 and -16 m, while for CEHZ21020 at these locations the hazard extent varies from -20 m to +23 m (i.e. at some locations the hazard zone is more seaward in the future than it is at the present day). Therefore, it is not recommended to select a particular line at a point in time to inform future planning, but a set of lines and likelihoods. For example it may be prudent to select the particular likelihood for present day CEHZ as well as a future likelihood event, so there is still a set-back distance to consider even in areas where, over time, accretion may reduce the hazard.

It can be seen from graphs presented in Appendix G that CEHZs are largest between the Ngaruroro River and Tukituki River (HB5 – HB6) for both the 2065 and 2120 time frames. This is evident by the construction of the groynes and outfall structures (refer to Section 3.2.9.1). Slightly smaller CEHZs are evident south of the Tukituki River (HB1 – HB4) with the largest maximum CEHZ at Clifton (HB1). The combination of a large maximum short term and long term component, and low maximum dune elevation incorporating a maximum sea level rise of 1.5 m resulted in the large maximum CEHZ.

The large CEHZs, in particular for the 2120 time frame, south of the Ngaruroro River (HB1 – HB6) are potentially a consequence of land subduction post the 1931 earthquake which resulted in a cut off of gravel supply. CEHZs north of the Ngaruroro River and south of Napier (HB8 – HB11) are significantly smaller and show accretion for the 2120 time frame. Gravel extraction in the vicinity of HB12 induces CEHZs that are slightly larger compared to HB8 – HB11 due to the more negative long-term component.

The CEHZs at HB12A, HB12B and HB13A have narrow bounds due to reduced wave climate in the lee of the Port of Napier and construction of revetments along these sections.

North of the Port tectonic uplifting from the 1931 earthquake has generally resulted in higher dune crest elevations with respect to dunes south of Napier, except for at HB13. Larger CEHZ for all timeframes at HB13, due to the low beach crest elevation, is therefore evident. A gradually increasing dune elevation and long term trend from HB14 to HB17 induces gradually decreasing CEHZ widths, with possible accretion evident at HB16 for the 2120 time frame. It is noted that the uplift recorded during the 1931 earthquake was against the trend of earlier earthquakes that generally resulted in subsidence.

CEHZs at HB18 and HB19 are larger compared to HB14 – HB17, induced by larger negative long-term trends possibly influenced by the Esk River. Further north (HB20 – HB23), CEHZs comprise a maximum width of up to 100 m for the 2120 time frame.

Table 4-1: Probability of CEHZ exceedance results for the present day

Location	Min	99%	95%	90%	80%	70%	66%	60%	50%	40%	33%	30%	20%	10%	5%	1%	Max
HB1	-6	-7	-8	-8	-9	-10	-10	-11	-12	-13	-13	-14	-15	-16	-17	-19	-20
HB2	-4	-5	-5	-6	-6	-7	-7	-7	-8	-9	-9	-9	-10	-11	-12	-13	-14
HB3	-5	-5	-6	-6	-6	-7	-7	-7	-7	-8	-8	-8	-8	-9	-9	-10	-10
HB4	-7	-8	-9	-10	-11	-11	-12	-12	-12	-13	-13	-14	-14	-15	-16	-17	-17
HB5	-8	-9	-10	-11	-12	-12	-13	-13	-14	-14	-15	-15	-15	-16	-17	-18	-18
HB6	-6	-7	-8	-8	-9	-10	-10	-11	-11	-12	-13	-13	-14	-15	-17	-18	-19
HB7	-9	-10	-11	-12	-13	-14	-14	-15	-16	-16	-17	-17	-18	-19	-19	-20	-21
HB8	-5	-6	-6	-7	-7	-8	-8	-8	-9	-9	-10	-10	-11	-12	-13	-14	-15
HB9	-5	-6	-7	-7	-8	-8	-8	-9	-9	-10	-10	-10	-11	-12	-13	-14	-14
HB10	-5	-5	-6	-6	-7	-8	-8	-8	-9	-9	-10	-10	-11	-12	-13	-14	-15
HB11	-7	-8	-8	-9	-9	-10	-10	-10	-11	-11	-12	-12	-12	-13	-14	-15	-15
HB12	-6	-7	-7	-8	-8	-9	-9	-9	-10	-11	-11	-11	-12	-13	-14	-15	-16
HB12A	-3	-3	-3	-3	-4	-4	-4	-4	-4	-4	-5	-5	-5	-5	-5	-6	-6
HB12B	-5	-6	-6	-6	-7	-7	-7	-8	-8	-8	-8	-8	-9	-9	-10	-10	-11
HB13A	-2	-2	-2	-3	-3	-3	-3	-3	-3	-4	-4	-4	-4	-4	-5	-5	-5
HB13	-5	-6	-7	-8	-9	-11	-11	-12	-14	-16	-18	-19	-22	-25	-28	-31	-34
HB14	-5	-6	-6	-6	-6	-7	-7	-7	-7	-7	-7	-7	-8	-8	-8	-9	-9
HB15	-7	-8	-9	-9	-10	-11	-11	-11	-11	-12	-12	-12	-13	-14	-14	-15	-15
HB16	-7	-8	-9	-9	-10	-10	-10	-11	-11	-12	-12	-12	-13	-14	-14	-15	-16
HB17	-7	-7	-8	-8	-9	-9	-10	-10	-11	-12	-12	-12	-13	-15	-16	-17	-18
HB18	-8	-9	-10	-10	-11	-11	-12	-12	-12	-13	-13	-14	-14	-15	-16	-17	-18
HB19	-8	-9	-9	-10	-11	-12	-12	-12	-13	-14	-15	-15	-17	-19	-20	-22	-23
HB20	-9	-9	-10	-10	-11	-12	-12	-13	-13	-14	-15	-15	-16	-18	-19	-20	-22

Location	Min	99%	95%	90%	80%	70%	66%	60%	50%	40%	33%	30%	20%	10%	5%	1%	Max
HB21	-9	-10	-11	-11	-12	-13	-13	-13	-14	-15	-15	-15	-16	-17	-18	-19	-20
HB22	-11	-12	-13	-14	-15	-15	-15	-16	-16	-17	-17	-17	-18	-18	-19	-19	-20
HB23	-9	-10	-11	-11	-12	-13	-13	-14	-14	-140	-1	-15	-16	-17	-17	-18	-19

Table 4-2: Probability of CEHZ exceedance results for 2065 timeframe

Location	Min	99%	95%	90%	80%	70%	66%	60%	50%	40%	33%	30%	20%	10%	5%	1%	Max
HB1	-33	-36	-39	-40	-42	-44	-44	-45	-47	-48	-49	-50	-52	-57	-62	-80	-134
HB2	-15	-18	-20	-21	-22	-23	-24	-24	-25	-26	-27	-28	-30	-33	-37	-46	-64
HB3	-29	-34	-36	-38	-40	-41	-42	-43	-44	-45	-46	-47	-49	-51	-53	-58	-71
HB4	3	-4	-10	-14	-20	-24	-25	-28	-31	-35	-37	-38	-43	-48	-53	-59	-72
HB5	-89	-95	-99	-101	-104	-106	-106	-108	-109	-111	-112	-113	-115	-118	-121	-126	-134
HB6	-67	-71	-74	-76	-78	-79	-80	-80	-82	-83	-84	-84	-86	-88	-90	-93	-100
HB7	-34	-39	-43	-44	-47	-49	-50	-51	-52	-54	-55	-56	-58	-60	-62	-66	-70
HB8	22	19	17	16	14	13	13	12	11	11	10	10	8	7	6	3	0
HB9	6	3	2	1	-1	-1	-2	-2	-3	-4	-4	-5	-6	-7	-8	-10	-14
HB10	16	13	12	11	9	8	8	8	7	6	5	5	4	3	1	-1	-5
HB11	31	27	25	24	22	21	21	20	19	18	18	18	16	15	14	11	7
HB12	-4	-7	-9	-10	-11	-12	-12	-13	-14	-15	-15	-16	-17	-18	-19	-22	-28
HB12A	-6	-7	-8	-9	-9	-10	-10	-11	-11	-12	-12	-13	-14	-16	-18	-22	-30
HB12B	-11	-14	-15	-16	-17	-18	-18	-19	-20	-20	-21	-21	-23	-25	-27	-31	-39
HB13A	-7	-9	-11	-11	-13	-14	-14	-15	-16	-17	-18	-18	-21	-26	-31	-43	-67
HB13	-28	-33	-35	-37	-40	-42	-43	-44	-47	-49	-51	-52	-55	-60	-65	-76	-102
HB14	-8	-10	-12	-13	-14	-15	-16	-16	-17	-18	-19	-19	-20	-22	-23	-27	-32
HB15	-8	-11	-13	-14	-15	-16	-16	-16	-17	-18	-18	-19	-20	-21	-22	-24	-29

Location	Min	99%	95%	90%	80%	70%	66%	60%	50%	40%	33%	30%	20%	10%	5%	1%	Max
HB16	16	13	11	10	8	6	6	5	4	3	2	2	0	-2	-3	-6	-10
HB17	-2	-5	-7	-8	-10	-11	-12	-12	-13	-14	-15	-15	-17	-19	-20	-22	-27
HB18	-30	-34	-37	-39	-41	-43	-43	-44	-45	-47	-48	-48	-50	-52	-54	-57	-61
HB19	-27	-30	-33	-34	-36	-38	-38	-39	-40	-41	-42	-43	-44	-46	-48	-51	-55
HB20	-15	-19	-22	-23	-26	-27	-28	-28	-30	-31	-32	-33	-34	-36	-38	-41	-46
HB21	-5	-9	-12	-13	-16	-18	-18	-19	-21	-22	-24	-24	-26	-29	-31	-34	-38
HB22	-6	-12	-16	-19	-23	-26	-27	-28	-31	-33	-35	-36	-39	-43	-46	-50	-58
HB23	-8	-14	-18	-20	-23	-26	-26	-28	-29	-31	-33	-33	-36	-39	-41	-45	-50

Table 4-3: Probability of CEHZ exceedance results for 2120 timeframe

Location	Min	99%	95%	90%	80%	70%	66%	60%	50%	40%	33%	30%	20%	10%	5%	1%	Max
HB1	-55	-64	-68	-71	-75	-77	-78	-80	-83	-86	-88	-89	-94	-105	-117	-160	-303
HB2	-26	-31	-34	-36	-38	-40	-41	-42	-44	-46	-48	-49	-53	-61	-70	-92	-145
HB3	-54	-61	-66	-69	-74	-77	-78	-79	-82	-85	-87	-88	-92	-97	-102	-114	-144
HB4	18	4	-8	-17	-28	-37	-40	-45	-51	-59	-63	-66	-75	-87	-95	-109	-142
HB5	-170	-179	-186	-190	-196	-200	-202	-204	-207	-211	-213	-215	-219	-225	-230	-241	-261
HB6	-128	-135	-140	-143	-146	-149	-150	-151	-154	-156	-158	-158	-161	-165	-169	-176	-186
HB7	-55	-66	-72	-76	-81	-85	-86	-88	-91	-94	-96	-97	-101	-106	-110	-116	-130
HB8	50	44	41	38	36	34	33	32	30	29	28	27	25	22	20	15	8
HB9	17	13	10	9	6	5	4	3	2	1	0	-1	-3	-5	-7	-11	-20
HB10	37	32	30	28	26	24	23	23	21	20	19	18	16	14	11	6	-5
HB11	70	63	59	57	54	52	51	50	48	46	45	44	42	39	37	33	23
HB12	-1	-6	-10	-12	-14	-16	-16	-17	-19	-20	-21	-22	-24	-27	-29	-33	-39
HB12A	-9	-11	-13	-14	-15	-17	-17	-18	-19	-21	-22	-22	-25	-30	-35	-45	-69

Location	Min	99%	95%	90%	80%	70%	66%	60%	50%	40%	33%	30%	20%	10%	5%	1%	Max
HB12B	-18	-22	-24	-26	-28	-30	-31	-32	-34	-36	-37	-38	-41	-46	-51	-61	-77
HB13A	-13	-16	-19	-21	-23	-25	-26	-27	-30	-33	-35	-36	-41	-52	-64	-90	-157
HB13	-51	-58	-63	-66	-70	-74	-75	-77	-80	-84	-86	-88	-93	-103	-114	-141	-213
HB14	-9	-15	-18	-20	-23	-25	-26	-27	-29	-31	-32	-33	-35	-39	-43	-51	-65
HB15	-9	-13	-16	-17	-19	-21	-22	-23	-24	-25	-26	-27	-29	-31	-34	-39	-48
HB16	43	36	31	29	25	22	21	20	18	15	14	13	10	7	4	-1	-10
HB17	3	-2	-6	-8	-11	-13	-14	-15	-17	-19	-20	-21	-23	-26	-28	-32	-40
HB18	-52	-59	-63	-66	-71	-74	-75	-77	-79	-82	-84	-85	-88	-93	-96	-101	-110
HB19	-45	-52	-56	-58	-61	-64	-64	-66	-68	-70	-71	-72	-74	-77	-80	-84	-93
HB20	-22	-27	-32	-35	-39	-42	-43	-45	-47	-49	-51	-52	-55	-59	-62	-67	-76
HB21	1	-6	-11	-15	-19	-23	-24	-26	-29	-32	-34	-35	-39	-44	-47	-53	-61
HB22	-1	-10	-18	-23	-31	-37	-39	-43	-47	-52	-55	-57	-63	-71	-77	-86	-99
HB23	-7	-16	-23	-27	-34	-39	-40	-43	-46	-50	-53	-54	-59	-66	-70	-77	-88

5 Coastal inundation hazard assessment methodology

The coastal inundation hazard is determined based on permanent and extreme inundation along the open coast for present day and for the years 2065 and 2120. Permanent inundation is defined as the result of a rise in sea level on the astronomic tidal processes, whereas extreme inundation is a result of storm effects in addition to the astronomic tide level changes.

5.1 Permanent inundation

Permanent inundation extents are assessed based on Highest Astronomic Tide (HAT) + sea level rise. It is assumed that the HAT level at the Port (refer to Section 2.6.1) is the same along the entire shoreline. This is a reasonable assumption based on the Port being centrally placed within the Hawke Bay, the bathymetry being reasonably consistent and the distance to the extents of the study area from the port being less than 22 km. A rise in level of 0.5 m and 1.0 m has been adopted for the 2065 and 2120 timeframe respectively. These values are recommended by the Ministry of Environment (2008) in particular for longer planning and decision timeframes and have therefore been adopted instead of the more conservative values derived by Komar and Harris (2014).

5.2 Extreme inundation

Extreme inundation is caused by extreme events during which waves contribute to super-elevate water levels (astronomic tide + storm surge) through wave setup and wave run-up. Wave setup occurs as energy is dissipated during the wave breaking process and results in elevated water level at the coast which contributes to coastal flooding. Wave run-up occurs when the waveform is not dissipated completely within the surf zone and reaches the shoreline with excess momentum. Run-up bores may be hazardous near the coastal edge but their momentum is quickly dissipated and their intermittent nature means they do not generally contribute significantly to coastal flooding.

5.2.1 Extreme inundation hazard

Extreme inundation extents are determined taking into account storm surge, set-up and run-up. Similar to the CEHZ assessment, the numerical model X-Beach-G is used which takes into account storm surge (water level time series input), wave setup and run-up (generated by X-Beach-G based on wave time series input). The model input as described in Section 3.2.2.3 is used to simulate the 10% AEP, 1% AEP and 2 x 1% AEP extreme inundation levels at the HB profile-based cells for the present day time frame.

X-Beach-G presents a time series of the absolute vertical position of the water line (Z) and the wave run-up elevation above the tide and surge level (R). The 2% exceedance values of Z and R are determined through an empirical cumulative distribution function of all waterline elevation maxima that exceed the mean waterline elevation (Deltares, 2014). A comparison between modelled and measured hydrodynamics by McCall et al. (2014) showed that that X-Beach-G is capable of reproducing wave run-up well. An example of $_{R2\%}$ and $Z_{2\%}$ X-Beach-G output is shown in Figure 5-1. Both the $R_{2\%}$ and $Z_{2\%}$ are used to determine the extreme inundation extents.

To validate the X-Beach-G model results we have compared these results with extreme inundation levels utilising the method by Komar and Harris (2014), see Section 6.2.3.

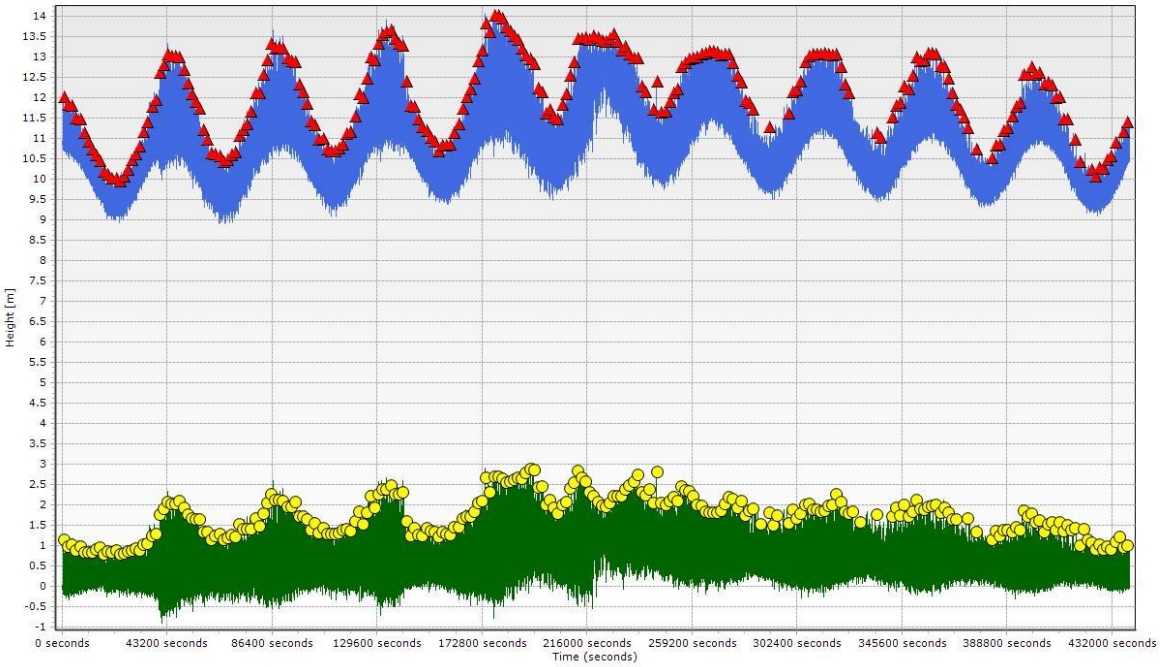

Figure 5-1: Example run-up output X-Beach-G at HB1. This plot shows the absolute water level (blue) and wave run-up level (green) over the simulation domain (432000 sec = 120 hr). $Z_{2\%}$ is shown as red triangles, $R_{2\%}$ is shown as yellow circles.

5.2.2 Overtopping flow

If run-up levels exceed the crest overtopping occurs. The numerical process-based model X-Beach-G has been used to predict the overtopping flow for each coastal cell. Overtopping is represented in X-Beach-G as cross-shore directed discharge along the cross-shore profile for each time step. This includes both the discharge/overtopping landward of the dune crest as well as the discharge/flow through the gravel barrier.

5.2.2.1 X-Beach-G input

The boundary water levels along the shoreline are used as input into X-Beach-G and are represented by the storm tide levels for present day, 2065 and 2120 (10% AEP, 1% AEP and 0.5% AEP). The 10% AEP, 1% AEP and 0.5% AEP storm surge levels for 2015 are shown in Table 5-1 together with the Highest Astronomic Tide (HAT) level for the Port. A rise in level of 0.5 m and 1.0 m have been added to the 2065 and 2120 timeframe respectively (see Table 5-1) as recommended by MfE (2008). It is assumed that the water levels are the same along the entire shoreline.

Table 5-1: Storm surge level along Hawke's Bay shoreline

	Year		
Water level	**2015**	**2065**	**2120**
Highest Astronomic Tide	11.1	11.6	12.1
10% AEP (m RL)	11.4	11.9	12.4
1% AEP (m RL)	11.5	12.0	12.5
0.5% AEP (m RL)	11.54	12.04	12.54

The wave climate at the 5 m contour (refer to Section 2.7) was used as input for the 10% AEP, 1% AEP and 0.5% AEP design storm time series. This was done to reduce wave refraction processes affecting overtopping at the more sheltered locations due to an overestimation of the wave height. It is likely that this process does not affect the majority of the shorelines where waves are more shore normal. Furthermore, nearshore depth-limited significant wave heights slightly increase with increased rise in sea level and this has been incorporated in the model simulations. However, an increase in wave energy with increased future sea level as suggested by Komar and Harris (2014) has not been included.

The MetOcean 5 m contour wave output locations are representative for the majority of the shoreline except for coastal cells HB12A, HB12B and HB13A. This is due to the significant change in shoreline orientation with respect to cell HB12A, HB12B and HB13 and wave refraction processes are likely to reduce the wave height. A UNIBEST-LT simulation was done to calculate the significant wave height near the toe of the beach, because the toe is roughly parallel to shoreline. Profile HB12A and profile W40 (West shore dataset) for HB13A were used as representative profiles. A synthetic profile for HB12B was created based on the 2012 LiDAR and surrounding existing profiles (e.g. HB12B and West shore dataset). The wave climate at the 10 m contour (MetOcean, 2011) was used as input. An elaborate description of the UNIBEST-LT model can be found in T+T (2006).

Figure 5-2 shows an example of the UNIBEST-LT output at HB13A (W40). The significant wave height is reduced to approximately 0.7 m at the toe of the beach at -50 m offshore. The reduced significant wave heights as calculated by UNIBEST-LT were used as input for the design storm time series to calculate overtopping. Increased depth-limited significant wave heights with increased sea levels has been taken into account in the UNIBEST-LT modelling.

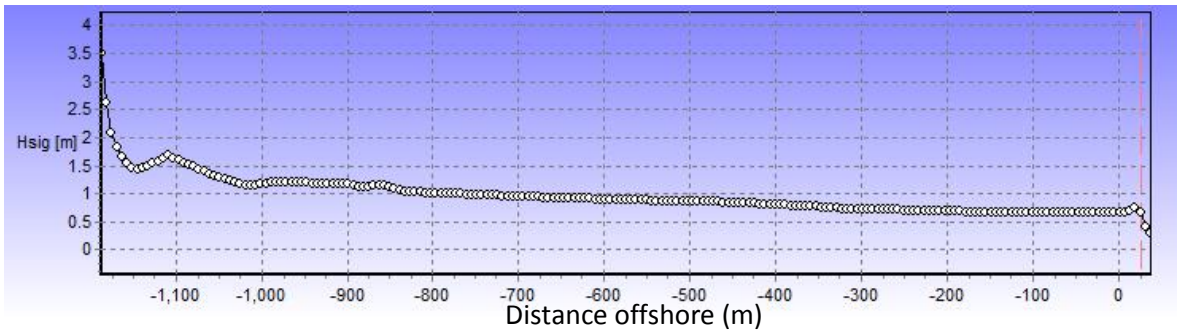

Figure 5-2: Example UNIBEST-LT output: Significant wave height over HB13A profile (cross-shore).

Research by McCall et al. (2014) concluded that X-Beach-G can be used to estimate the initial wave overtopping, but may be over conservative over time due to changes to the beach berm. To minimise this effect but to maintain a sufficient duration we have used a time series discharge distribution of 4 hours (starting 2 hours before the storm peak).

Simulations of the 10% AEP, 1% AEP and 0.5% AEP were done for the present day, 2065 and 2120. For overtopping with future sea level rise scenarios, it is assumed that the same beach profile will be present so the only change in variable is the additional sea level. However, due to the dynamic nature of the modelling, the increased sea level also affects nearshore wave height, run-up and overtopping.

5.3 Defining coastal behaviour cells

The open coast has been divided into coastal cells based on profile geometry and backshore elevation which can influence in the resultant hazard. Factors which may influence the behaviour of a cell include:

- Profile geometry
- Backshore elevation.

Similar to the CEHZ assessment (Section 0) existing beach profiles of the HB series were used to define the coastal behaviour cells and were divided into 26 cells; 23 HB profiles plus 3 additional cells. Note that for the extreme inundation simulations only the HB profiles were used and that for the overtopping flow simulations all 26 cells were used. Appendix H shows the alongshore cell division based on the dune crest elevation.

5.4 Uncertainty

A key uncertainty is the matching of crest height with ongoing sea level rise. Theoretically the crest of the gravel beach should increase to match the sea level rise as waves push gravel material to the crest. Observation of beach profiles at the southern end of Hawke Bay suggest this does not happen in areas of net sediment deficit. At the northern end of Hawke Bay the 1931 earthquake caused an uplift (~2 m) larger than the potential rise in sea level (1.5 m) and since the dune crest is well above the sea level (> 5 m) the crest level is unlikely to increase with ongoing sea level rise. There is also a likelihood of the gravel barrier becoming narrower due to this process, increasing risk of breach failure. Assuming crest levels remain at present day levels along the entire shoreline may provide a conservative approach with sea level rise, but is considered appropriate due to uncertainty of gravel barrier response and increased risk of episodic breaching.

The rise in sea level is a key uncertainty as inundation levels are largely dependent on this value. By adopting the values recommended by MfE (2008) we comply with national guidelines.

6 Coastal inundation hazard assessment results

6.1 Permanent inundation levels

Permanent inundation levels determined as described in Section 5.1 are presented in Table 6-1 for present day, 2065 and 2120 timeframes for a range on common datums, rounded to 1 decimal place. Ground levels lower than the HAT level are likely to experience frequent inundation from the sea.

Table 6-1: Permanent inundation levels

	Chart datum (m)	Napier vertical datum 1962 (m)	HBRC datum (m)
Present day Highest Astronomic Tide (HAT)[1]	2.0	1.1	11.1
HAT 2065	2.5	1.6	11.6
HAT 2120	3.0	2.1	12.1

[1] Predicted by LINZ (2012)

6.2 Extreme inundation levels

6.2.1 Current extreme inundation levels

Extreme water levels for the 10%, 1% and 2 x 1% AEP events based on X-Beach-G model results ($Z_{2\%}$) are shown in Table 6-2. Where run-up levels exceed the crest elevation overtopping occurs. This is shown in the table as shaded cells. It can be seen that specifically the southern profiles (HB1 – HB7) are subjected to overtopping (Beach crests at profile HB5 and HB6 are overtopped). This is due to the lower crest height along the southern shoreline of Hawke's Bay as a result of land subsidence. With the exception of HB7, the profiles north of the Ngaruroro River have a higher crest level and generally do therefore not experience overtopping apart from during the 2 x 1% AEP storms situation at HB8, HB12, HB13 and HB14. Further north the crest levels are significantly higher (2-5m) as a result of 1931 earthquake induced land uplift.

The current extreme water levels range from 2.6 m to 3.3 m above HAT from HB1 to HB7 based on the XBeach-G results. For HB8 – HB12 current extreme water levels range from 3.6 m to 4.4 m, for HB14 – HB23 it ranges from 3.3 m to 4.3 m and at HB13 the water is 3 m above HAT.

Table 6-2: Current extreme water levels (X-Beach-G results)

Extreme water levels (m RL)							
Profile	**10% AEP**	**1% AEP**	**2x1% AEP**	**Profile**	**10% AEP**	**1% AEP**	**2x1% AEP**
HB1	14.0	14.0	14.0	HB13	14.1[1]	14.1[1]	14.1
HB2	13.9	13.9	14.0	HB14	14.8	15.4	15.5
HB3	13.9	14.0	14.1	HB15	14.7	15.1	15.1
HB4	13.7	14.2	14.2	HB16	14.6	14.4	14.6
HB5	14.3[1]	14.3[1]	14.3[1]	HB17	14.7	15.3	15.3
HB6	13.7[1]	13.7[1]	13.7[1]	HB18	15.1	15.3	15.3
HB7	14.3	14.4	14.4	HB19	15.0	15.2	15.2
HB8	15.1	15.2	15.2	HB20	14.6	15.2	15.2

Extreme water levels (m RL)							
Profile	**10% AEP**	**1% AEP**	**2x1% AEP**	**Profile**	**10% AEP**	**1% AEP**	**2x1% AEP**
HB9	15.2	15.2	15.2	HB21	15.1	15.1	15.3
HB10	14.7	15.0	15.1	HB22	14.7	15.4	15.4
HB11	15.2	15.5	15.5	HB23	14.6	15.1	15.3
HB12	15.0	15.5	15.5				

Extreme water levels that induce overtopping are shaded.

[1] Beach subjected to overtopping, where flood exclusion bank is not subjected to overtopping.

Results of inundation were also compared to the observed inundation and overtopping that occurred during Cyclone Pam (Goodier and Pearse, 2015). Inundation to around 13.5 m to 14 m was observed around the surf club at Westshore. This compares to 14.1 m inundation at HB13 modelled by X-Beach. Overtopping occurred onto the road at certain locations, with debris levels of around 15.5 m from the Esplanade to Charles Street and at around 15 to 15.25 m north of Airport Gap. This compares to extreme water levels of between 14.7 m and 15.1 m at HB14 and HB15.

Along Marine Parade the debris line reached around 15.5 m to 15.75 m compared to 15.2 to 15.5 m modelled at HB 11 and HB12. The observed debris line reduced to around 14.25 m to 14.5 m north of Tutaekuri River while modelling showed extreme water levels of around 14.7 m to 15.2m. At Haumoana and Te Awanga debris levels reached around 13.25 m. X-Beach indicated extreme water levels of 13 to 14 m for present day extreme events. These comparisons show that X-Beach provides a reasonable estimate of extreme water levels and the extent of wave run-up extents on the open coast.

6.2.2 Future extreme inundation levels

Future extreme water levels for 2065 and 2120 are shown in Table 6-3 and Table 6-4 respectively. These levels are based on the current extreme inundation levels and include a rise in sea level of respectively 0.5 m and 1.0 m for 2065 and 2120. These levels are somewhat conservative, but indicate that inundation is expected to be more frequent in 2065 and 2120 at specifically the southern profiles HB1 – HB7. The extreme inundation levels range from 3.1 to 4.9 m above HAT in 2065 and from 3.6 to 5.4 m above HAT in 2120.

Table 6-3: Extreme water levels for 2065

Extreme water levels (m RL)							
Profile	**10% AEP**	**1% AEP**	**2x1% AEP**	**Profile**	**10% AEP**	**1% AEP**	**2x1% AEP**
HB1	14.5	14.5	14.5	HB13	14.6	14.6	14.6
HB2	14.4	14.4	14.5	HB14	15.3	15.9	16.0
HB3	14.4	14.5	14.6	HB15	15.2	15.6	15.6
HB4	14.2	14.7	14.7	HB16	15.1	14.9	15.1
HB5	14.8	14.8	14.8	HB17	15.2	15.8	15.8
HB6	14.2	14.2	14.2	HB18	15.6	15.8	15.8
HB7	14.8	14.9	14.9	HB19	15.5	15.7	15.7
HB8	15.6	15.7	15.7	HB20	15.1	15.7	15.7
HB9	15.7	15.7	15.7	HB21	15.6	15.6	15.8
HB10	15.2	15.5	15.6	HB22	15.2	15.9	15.9

Extreme water levels (m RL)							
Profile	**10% AEP**	**1% AEP**	**2x1% AEP**	**Profile**	**10% AEP**	**1% AEP**	**2x1% AEP**
HB11	15.7	16	16	HB23	15.1	15.6	15.8
HB12	15.5	16	16				

Table 6-4: Extreme water levels for 2120

Extreme water levels (m RL)							
Profile	**10% AEP**	**1% AEP**	**2x1% AEP**	**Profile**	**10% AEP**	**1% AEP**	**2x1% AEP**
HB1	15	15	15	HB13	15.1	15.1	15.
HB2	14.9	14.9	15	HB14	15.8	16.4	16.5
HB3	14.9	15	15.1	HB15	15.7	16.1	16.1
HB4	14.7	15.2	15.2	HB16	15.6	15.4	15.6
HB5	15.3	15.3	15.3	HB17	15.7	16.3	16.3
HB6	14.7	14.7	14.7	HB18	16.1	16.3	16.3
HB7	15.3	15.4	15.4	HB19	16	16.2	16.2
HB8	16.1	16.2	16.2	HB20	15.6	16.2	16.2
HB9	16.2	16.2	16.2	HB21	16.1	16.1	16.3
HB10	15.7	16	16.1	HB22	15.7	16.4	16.4
HB11	16.2	16.5	16.5	HB23	15.6	16.1	16.3
HB12	16	16.5	16.5				

6.2.3 Comparison wave run-up levels

Komar and Harris (2014) developed a method to calculate the extreme water/inundation levels for the Hawke's Bay. Their methodology includes calculation of the Total Water Level (TWL) and Extreme Scenario TWL (EWL) for the present day and 2100 timeframe. The TWL is determined by the summation of MSL and run-up ($R_{2\%}$). The EWL is determined by the summation of the storm tide water level (HAT + storm surge) and run-up. For the 2100 timeframe a rise in mean sea level of 1.1 m is added and a larger run-up level included due to the increased water depth. Komar and Harris (2014) utilise the Stockdon et al. (2006) formula to calculate run-up.

The TWL and EWL were calculated for present day and 2100 timeframe using the methodology by Komar and Harris (2014) and compared these levels with the X-Beach-G results. Wave data from MetOcean (2013) and water level data as used as input into the X-Beach-G model was used. The 10% AEP wave data and water level were used for the present day and the 1% AEP wave data and water level for the 2100 timeframe.

Figure 6-1 and Figure 6-2 show the TWL and EWL for the present day and 2120 timeframe calculated according to Komar and Harris (2014) and by the X-Beach-G model at HB1 and HB14 respectively. The X-Beach-G output is the maximum level of the water level as shown in Figure 3-10. When the TWL and EWL calculated by X-Beach-G exceed the crest elevation (refer to Figure 3-9) it indicates that overtopping processes need to be considered (see Table 6-2). It is evident that the X-Beach-G water levels (dashed lines) are more conservative than the water level as calculated according to Komar and Harris (solid lines) for all the HB1, 2120 case where levels are similar. The EWLs (HB14) calculated by X-Beach-G are on average 5% larger than the EWLs as calculated according Komar and Harris (2014) and is less than 10% for each profile.

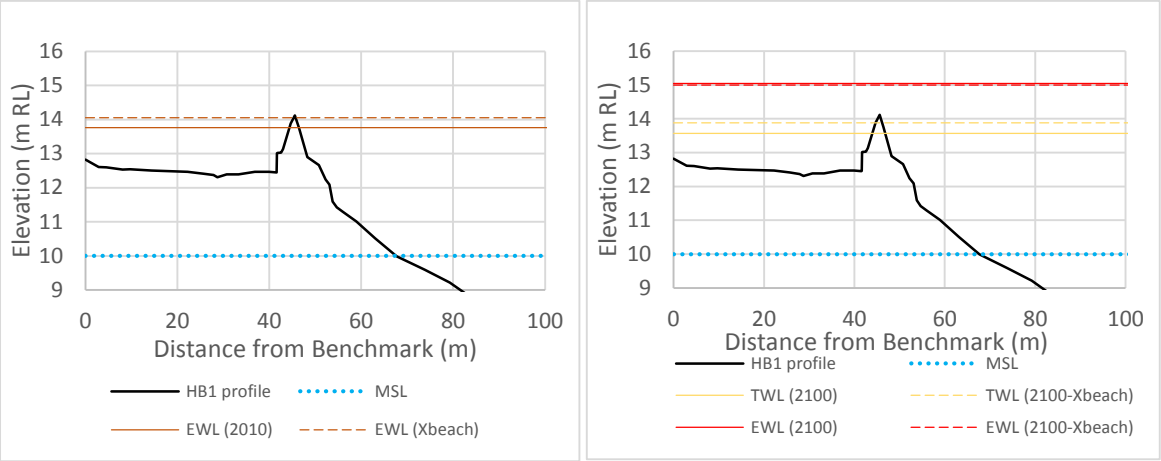

Figure 6-1: Extreme Water Level (EWL) and Total Water Level (TWL) results using the method by Komar and Harris (2014), and X-Beach-G results for the present day (left) and 2120 timeframe (right) at HB1.

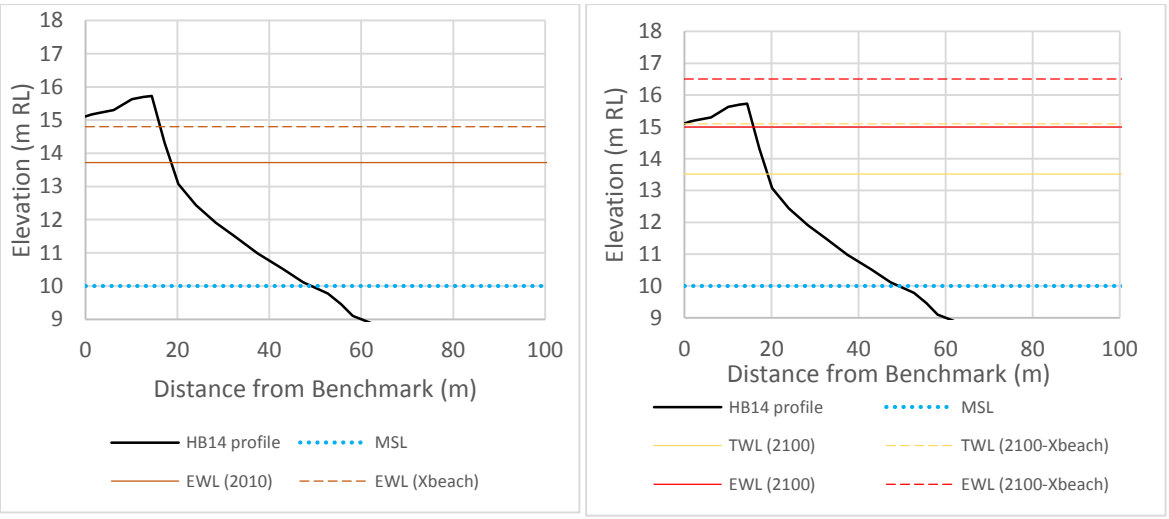

Figure 6-2: Extreme Water Level (EWL) and Total Water Level (TWL) results using the method by Komar and Harris (2014), and X-Beach-G results for the present day (left) and 2120 timeframe (right) at HB14.

6.2.4 Overtopping flow information

Table 6-6 shows the overtopping flow information for profile HB1 to HB14. Profile HB15 – HB23 did not experience overtopping in any of the future scenarios modelled. Table 6-6 provides the total overtopped volume for the storm duration (m^3/m shoreline), the total duration used for the overtopping modelling and the mean cross-shore discharge for the present day, 2065 and 2120 time periods. Note that these values can be different from what has been indicated in Table 6-2 (shaded where subjected to overtopping) due to the limited simulation duration to calculate overtopping flow (duration of 4 hrs versus 120 hrs) and the total discharge is very sensitive to the elevation of the bank.

The overtopping flow information has typically been extracted just landward of the dune crest for each profile, except for at profiles HB5, HB6 and HB13. At HB5 and HB6 overtopping flow information has been extracted just landward of the flood exclusion bank for the present day time frame. However, for 2065 erosion has encroached through the flood exclusion bank at HB5. Therefore overtopping flow is extracted at the beach crest as the flood exclusion bank is considered

to have failed its coastal protection function (refer to Section 4 for erosion hazard extent) unless additional work is done to either strengthen and enlarge the structure or relocate it landward. These options can be assessed in future studies, but by considering the flood impact, the extent of flooding if action is not taken is demonstrated. At 2120 erosion occurs at both HB5 and HB6, so overtopping flow is extracted at the beach crest for both areas. Overtopping flow information for HB13 is extracted at the landward back barrier crest for the present day, 2065 and 2120 time frames.

6.2.4.1 Discussion of results

It can be seen from Table 6-6 that overtopping is predicted at HB1 to HB4 but at no other location for the present time frame. It is possible that due to the relatively narrow gravel berm and low laying back land at these profiles enhanced seepage through the gravel berm occurs. Furthermore, overtopping is evident at HB12B for the present day time frame likely due to its unfavourable shoreline orientation with respect to the incident waves refracting around the Port of Napier. Direct inundation, rather than overtopping discharge will dominate where the extreme water levels presented in Table 6-2 to Table 6-4 extend to, or over the crest.

Overtopping is shown to be occur along the southern end of Hawke Bay at profiles HB1 – HB8, except at HB6 (flood exclusion bank still intact), for the 2065 time frame. This is likely to be a consequence of land subsidence south of the Ngaruroro River (HB1 – HB6) caused by the 1931 earthquake, which also slightly affects HB7 and HB8 where low overtopping flows are found. At profiles HB12B, increased overtopping with respect to present day time frame, and HB13A, low lying area, overtopping flow is evident for the 2065 time frame. HB14, at which the dune crest height is relatively low compared to the dune crest height between Tangoio and West Shore (excluding HB13), overtopping occurs during a 0.5% AEP event.

For the 2120 time frame overtopping occurs at profiles HB1 – HB8 and HB12B – HB13A for all considered AEP events, with the largest overtopping flow volumes at HB1, HB4 and HB6. Profiles HB9 and HB12 are subjected to overtopping during the 0.5% AEP event for the 2120 time frame. Although the crest height at HB12 is typically higher (~0.5 m) compared to at HB10 and HB11 (refer to Appendix H), there is a shallower nearshore elevation and slightly gentler beach slopes at profile HB10 and HB11 compared to HB12 which limit waves to reach the beach crest. The deeper nearshore and steeper beach face results in more overtopping at HB12 than at HB10 and HB11. Furthermore, overtopping occurs at profile HB13 and HB14 for both the 1% and 0.5% AEP events for the 2120 time frame.

These results indicate that specifically the shoreline south of the Ngaruroro River is prone to inundation/overtopping for the future scenarios. Additional, the low lying area in the vicinity of West Shore (HB12B – HB14) is likely to be subjected to overtopping in the future. The remaining part of the shoreline that experienced uplift during the 1931 earthquake (HB8 – HB12 and HB15 – HB23) generally is less likely to be subjected to overtopping for the future time frames (2065 and 2120).

6.3 Mapping

Coastal inundation maps have been prepared using storm surge and run-up information included in Table 6-2 to Table 6-4 to provide sea inundation levels seaward of the coast for the present day, 2065 and 2120 sea level rise projections combined with the resulting inundation from overtopping presented in Table 6-6.

The coastal inundation layers contain overtopping model output data received by HBRC, and extreme water level inundation (storm surge + wave run up) from a connected bathtub model

developed by T+T. The bathtub model was applied on the full 2003 LiDAR DEM extent and applied seaward of the overtopping model connection where applicable. Where no overtopping was modelled, the current beach crest was applied as landward boundary.

The original overtopping model output is a raster dataset with 20x20 meter cell size. To allow the raster dataset to be merged with the bathtub model vector dataset, the following process was (using ArcMap/ArcCatalogue 10.3).

- Reclassification of raster value in 0.25 meter increments (mapping shows the lower end of the range for each cell)
- Raster to polygon conversion
- Manual removal of unconnected cells in built up areas.

After processing, the vectorised overtopping dataset was merged with the bathtub inundation dataset, and further manual edits applied with expert judgement to determine the final extent and depths within the inundation layers. The final dataset has been dissolved based on inundation level.

For both the present day and future sea level rise situation the existing dune crest has been used to delineate the boundary between the sea inundation and sea induced overtopping interface. This is a simplification of the possible future shoreline position as the shoreline may be more landward than the present shoreline as a result of shoreline erosion. However, due to the range of possible shoreline positions and no confirmed shoreline likelihood yet agreed, this mapping approach for inundation was seen as reasonable.

Table 6-5 Example of extreme levels exceeding crest heights along the coast indicating inundation extents for the 1%AEP extreme water level case

Profile	Elevation along dune crest from LiDAR (m RL)			1%AEP present day	1%AEP + 0.5 m	1%AEP+1 m
	Min	Mode	Max			
HB1	12.5	13.5	14.0	14.0	14.5	15.0
HB2	13.0	14.0	14.5	13.9	14.4	14.9
HB3	13.3	13.8	14.3	14.0	14.5	15.0
HB4	13.8	14.0	14.3	14.2	14.7	15.2
HB5	13.3	13.8	14.3	14.3	14.8	15.3
HB6	13.0	13.5	14.3	13.7	14.2	14.7
HB7	14.0	14.3	15.0	14.4	14.9	15.4
HB8	14.5	15.0	15.5	15.2	15.7	16.2
HB9	14.3	15.0	15.3	15.2	15.7	16.2
HB10	14.3	14.8	15.0	15.0	15.5	16.0
HB11	15.0	15.3	15.5	15.5	16.0	16.5
HB12	15.0	15.5	16.3	15.5	16.0	16.5
HB12A	14.3	14.5	14.8	14.1	14.6	15.1
HB12B	14.3	14.5	14.8	14.1	14.6	15.1
HB13A	13.0	13.5	14.0	14.1	14.6	15.1
HB13	13.5	14.0	14.5	14.1	14.6	15.1

Profile	Elevation along dune crest from LiDAR (m RL)			1%AEP present day	1%AEP + 0.5 m	1%AEP+1 m
	Min	Mode	Max			
HB14	15.3	15.5	16.0	15.4	15.9	16.4
HB15	15.5	15.8	16.0	15.1	15.6	16.1
HB16	17.0	17.5	18.0	14.4	14.9	15.4
HB17	17.0	17.5	18.0	15.3	15.8	16.3
HB18	17.5	18.0	18.5	15.3	15.8	16.3
HB19	18.8	19.0	19.3	15.2	15.7	16.2
HB20	19.0	19.3	19.8	15.2	15.7	16.2
HB21	18.3	18.8	19.5	15.1	15.6	16.1
HB22	18.0	18.5	18.8	15.4	15.9	16.4

Table 6-6: Overtopping flow information

Profile	AEP	Current			2065			2120		
		Total volume (m^3/m)	Duration (s)	Mean cross shore discharge ($m^3/s/m$)	Total volume (m^3/m)	Duration (s)	Mean cross shore discharge ($m^3/s/m$)	Total volume (m^3/m)	Duration (s)	Mean cross shore discharge ($m^3/s/m$)
HB1	10%	0.8	14400	0.000054	409.0	14400	0.028400	1,232.6	14400	0.0855950
	1%	33.1	14400	0.002300	576.2	14400	0.040011	1,523.5	14400	0.1058000
	0.50%	53.4	14400	0.003706	689.2	14400	0.047858	1,717.6	14400	0.1192800
HB2	10%	1.1	14400	0.000077	10.9	14400	0.000757	86.4	14400	0.0060000
	1%	3.2	14400	0.000220	102.2	14400	0.007100	106.0	14400	0.0073600
	0.50%	18.3	14400	0.001270	113.8	14400	0.007905	150.4	14400	0.0104470
HB3	10%	1.0	14400	0.000070	52.4	14400	0.003637	62.1	14400	0.0043100
	1%	3.4	14400	0.000238	59.8	14400	0.004153	77.6	14400	0.0053900
	0.50%	15.5	14400	0.001078	61.2	14400	0.004253	87.8	14400	0.0060954
HB4	10%	8.4	14400	0.000580	36.6	14400	0.002539	244.8	14400	0.0170000
	1%	14.5	14400	0.001006	18.5	14400	0.001284	1,254.5	14400	0.0871180
	0.50%	40.7	14400	0.002828	46.9	14400	0.003260	3,024.4	14400	0.2100300
HB5	10%	0.0	0	0	28.8	14400	0.002000	316.8	14400	0.0220000
	1%	0.0	0	0	86.4	14400	0.006000	676.8	14400	0.0470000
	0.50%	0.0	0	0	115.2	14400	0.008000	1,944.0	14400	0.1350000
HB6	10%	0.0	0	0	0.0	0	0.000000	316.8	14400	0.0220000
	1%	0.0	0	0	0.0	0	0.000000	676.8	14400	0.0470000
	0.50%	0.0	0	0	0.0	0	0.000000	1,944.0	14400	0.1350000

Profile	AEP	Current			2065			2120		
		Total volume (m^3/m)	Duration (s)	Mean cross shore discharge ($m^3/s/m$)	Total volume (m^3/m)	Duration (s)	Mean cross shore discharge ($m^3/s/m$)	Total volume (m^3/m)	Duration (s)	Mean cross shore discharge ($m^3/s/m$)
HB7	10%	0	0	0	1.4	14400	0.000096	14.4	14400	0.000997
	1%	0	0	0	32.8	14400	0.002276	43.6	14400	0.003031
	0.50%	0	0	0	49.8	14400	0.003456	122.3	14400	0.008490
HB8	10%	0	0	0	0.6	14400	0.000042	37.5	14400	0.002607
	1%	0	0	0	33.7	14400	0.002339	67.9	14400	0.004714
	0.50%	0	0	0	77.3	14400	0.005365	125.4	14400	0.008707
HB9	10%	0	0	0	-	0	0.000000	-	0	0.000000
	1%	0	0	0	-	0	0.000000	-	0	0.000000
	0.50%	0	0	0	-	0	0.000000	-	0	0.000079
HB10	10%	0	0	0	-	0	0.000000	-	0	0.000000
	1%	0	0	0	-	0	0.000000	-	0	0.000000
	0.50%	0	0	0	-	0	0.000000	-	0	0.000000
HB11	10%	0	0	0	-	0	0.000000	-	0	0.000000
	1%	0	0	0	-	0	0.000000	-	0	0.000000
	0.50%	0	0	0	-	0	0.000000	-	0	0.000000
HB12	10%	0	0	0	-	0	0.000000	-	0	0.000000
	1%	0	0	0	-	0	0.000000	-	0	0.000000
	0.50%	0	0	0	-	0	0.000000	25.4	14400	0.001763
HB12A	10%	0	0	0	-	0	0.000000	-	0	0.000000
	1%	0	0	0	-	0	0.000000	-	0	0.000000

Profile	AEP	Current			2065			2120		
		Total volume (m^3/m)	Duration (s)	Mean cross shore discharge ($m^3/s/m$)	Total volume (m^3/m)	Duration (s)	Mean cross shore discharge ($m^3/s/m$)	Total volume (m^3/m)	Duration (s)	Mean cross shore discharge ($m^3/s/m$)
	0.50%	0	0	0	-	0	0.000000	-	0	0.000000
HB12B	10%	-	0	0	-	0	0	24.2	14400	0.00168
	1%	-	0	0	19.6	14400	0.0013619	49.6	14400	0.0034439
	0.50%	-	0	0	56.8	14400	0.0039443	77.8	14400	0.005405
HB13A	10%	-	0	0	-	0	0	24.2	14400	0.00168
	1%	-	0	0	77.8	14400	0.0054048	113.0	14400	0.0078438
	0.50%	-	0	0	91.9	14400	0.006381	158.1	14400	0.01098
HB13	10%	-	0	0	0.1	14400	7.54E-06	17.1	14400	0.0011865
	1%	-	0	0	15.8	14400	0.0010986	136.2	14400	0.0094598
	0.50%	-	0	0	77.7	14400	0.0053983	142.4	14400	0.0098864
HB14	10%	-	0	0	-	0	0	1.0	14400	0.0000698
	1%	-	0	0	0.1	14400	7.71E-06	33.6	14400	0.0023366
	0.50%	-	0	0	27.5	14400	0.0019075	69.3	14400	0.0048141

7 Tsunami

7.1 Hazard assessment

Tsunami hazard mapping has been based on the work carried out by HBRC (http://www.hbemergency.govt.nz/hazards/portal) that included the potential effect of a 3 m, 5 m and 10 m tsunami. These tsunami amplitudes were applied in deep water some 20 km from the Port of Napier and modelled at to coincide with the high tide at Mean High Water Springs water level (Goodier, 2011). At the shoreline the maximum wave amplitudes for these three events were 5.8 m, 8 m and 12.3 m respectively, although the height of the wave varied along the coastline for each of these events (refer Table 7-1).

Table 7-1 Range of tsunami height at the coast along the Hawke Bay coastline

	3 m offshore	5 m offshore	10 m offshore
Maximum	5.8	8.0	12.3
Average	3.9	6.4	9.1
Minimum	2.8	5.3	6.3

This information was compared to the GNS tsunami update report (Powers, 2013) that updated their 2005 study, taking into account the knowledge and understanding of the 2011 Tohoku tsunami in Japan. The GNS report included tsunami hazard curves for Napier based on the maximum tsunami height along some 20 km of coast (refer Figure 7-1). The possible sources for these tsunami include local and far field sources. The 3, 5 and 10 m tsunami have been determined to represent approximately a 0.5%, 0.13% and a 0.025% AEP event (i.e. 200 year, 750 year and 4000 year return period) based on the 50 percentile curve generated by GNS.

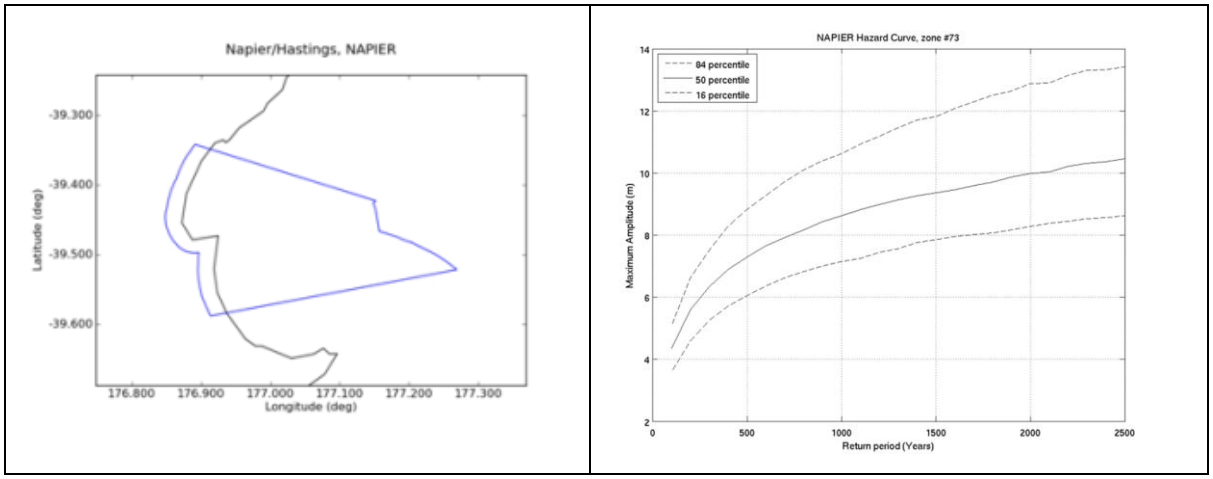

Figure 7-1: Area map and tsunami hazard curve for Napier (Source: Powers, 2013)

Only the effect of present day sea level has been considered for the 0.5%, 0.13% and 0.025% tsunami occurring at Mean High Water Springs (MHWS). Not including consideration of sea level rise with tsunami is considered appropriate due to:

- the lower probability of the tsunami event compared to erosion and inundation
- the further reduction in likelihood possible with it coinciding at high tide (around 11 m HBRC datum) rather than Mean Sea Level (10 m HBRC datum).

7.2 Tsunami hazard mapping

The extent of the tsunami has been carried out by HBRC using a Mike 21-HD hydrodynamic model with a 20 m rectangular grid with a series of five waves applied for each event, with the third wave being the largest.

8 Summary and recommendations

8.1 Purpose

Hawke's Bay Regional Council (HBRC), Hastings District Council (HDC) and Napier City Council (NCC) are working together to develop a strategy for managing, or mitigating, coastal hazard risks along the Hawke Bay shoreline from Tangoio to Clifton to make a more resilient community.

This report provides the results of a regional scale coastal hazard assessment that will be used as a basis for a coastal hazard risk assessment (reported separately). This coastal hazard erosion report builds on previous hazard studies and ongoing research and investigations in the coastal processes of this area. The report quantifies the possible extent of the following hazards:

- Coastal erosion (storm cut, trends, effects of sea level rise)
- Coastal inundation (storm surge, set-up, run-up, overtopping and sea level rise).

The report briefly describes the coastal processes and summarises key information required for the coastal hazard assessment based on the latest available information. However, the report does not seek to replicate information already contained in previous reports, particularly Komar and Harris (2014) and T+T (2012) and these should be read for more detailed descriptions of the physical processes affecting this area.

8.2 Coastal erosion hazard

The coastal erosion hazard assessment uses a probabilistic approach in determining the potential future shoreline position at 2065 and 2120 taking into account the following parameters: historic erosion trends, storm effects and backshore slope stability as well as the possible effects of sea level rise. The range of values for each of these parameters was determine from a range of sources, including LiDAR survey, aerial photographs, field investigations, beach profile data, numerical modelling and expert engineering judgement. A triangular probability distribution was assumed for each parameter and a Monte Carlo technique was used to assess the likelihood of the combined influence of each parameter. This approach differs from the previous erosion hazard assessment that was based on a deterministic approach of adding together the effects each parameter.

The approach used in this report is consistent with the Government's Envirolink "guide to good practice[3]"that recommends moving from deterministic predictions to probabilistic projections. The probabilistic approach recognises there will always be inherent uncertainties associated with projections and provides a more transparent way of capturing and presenting such uncertainty. This method results in a range of potential hazard zone extents, ranging from virtually certain to exceptionally unlikely.

Minimum set back values are developed to take into account limitations and uncertainties in our current understanding of processes that drive erosion hazard and in the data and modelling techniques. Utilising minimum values provides a targeted precautionary approach as advocated in the NZCPS without applying overly conservative factors of safety for sites with sufficient hazard zone widths.

Mapping of the erosion hazard extent was based on setbacks determined at each beach profile measured from present day vegetation lines or beach scarps. Due to the consideration of accretion trends as well as erosion trends the future erosion hazard extents can be less than the current erosion hazard zone. This is particularly evident between HB8 and HB12 where the maximum CEHZ is between -15 and -16 m, while for CEHZ21020 at these locations the hazard extent varies from -20

[3] http: //www.envirolink.govt.nz/Envirolink-tools/

m to +23 m (i.e. at some locations the hazard zone is more seaward in the future than it is at the present day). Therefore, it is not recommended to select a particular line at a point in time to inform future planning, but a set of lines and likelihoods. For example it may be prudent to select the particular likelihood for present day CEHZ as well as a future likelihood event, so there is still a set-back distance to consider even in areas where, over time, accretion may reduce the hazard.

8.3 Coastal inundation hazard

The coastal inundation hazard extent was determined for both permanent and extreme inundation along the open coast for present day and for the years 2065 and 2120 for a 10%AEP, 1% AEP and 0.5%AEP event (i.e. a 10 year, 100 year and 200 year return period). Permanent inundation extents were based on the predicted rise in sea level added to present day tidal levels. Extreme inundation is caused by extreme events during which waves contribute to super-elevate water levels (astronomic tide + storm surge) through wave setup, wave run-up and wave overtopping. The combined effect of storm surge levels with the effect of onshore storms based was modelled at each beach profile using the X-Beach Gravel model. This provided information on both the extreme water level on the seaward side of the beach crest and the volume of seawater that can overtop the beach crest during storm events.

Mapping was based on the manual integration of the extreme water levels along the coast produced by X-Beach with the inundation extent resulting from overtopping from the catchment flood models of HBRC using engineering judgement to refine the inundation maps.

8.4 Tsunami inundation hazard

Tsunami hazard mapping was based on the work carried out by HBRC (http://www.hbemergency.govt.nz/hazards/portal) that included the potential effect of a 3 m, 5 m and 10 m amplitude tsunami. The tsunami amplitude was applied in deep water some 20 km from the Port of Napier and modelled to coincide with the high tide at Mean High Water Springs water level (Goodier, 2011). Based on the recent GNS report on tsunami (GNS, 2013), the 3, 5 and 10 m tsunami have been determined to represent a 0.5%, 0.13% and a 0.025% AEP event (i.e. 200 year, 750 year and 4000 year return period) based on the 50 percentile curve.

8.5 Mapping information

Hazard maps have been prepared for erosion, sea inundation and tsunami. These maps have been provided to Council and are the basis for the baseline risk assessment reported separately.

8.6 Recommendations

The coastal hazard information is to be used for a baseline risk assessment. There is no recommendations on the preferred hazard information to use for any possible update of coastal hazard zones in regional or district plans. The selection of appropriate hazard maps should be based on the outcomes of the risk assessment and discussions on acceptable risk.

9 Applicability

This report has been prepared for the benefit of Hawke's Bay Councils (HBRC, NCC, and HDC) with respect to the particular brief given to us and it may not be relied upon in other contexts or for any other purpose without our prior review and agreement.

Tonkin & Taylor Ltd

Environmental and Engineering Consultants

Report prepared by:	Authorised for Tonkin & Taylor Ltd by:
.....	.....
Patrick Knook	Richard Reinen-Hamill
Richard Reinen-Hamill	Director

RRH
t:\auckland\projects\20514\20514.0050\workingmaterial\report cha\20151015.rrh.draft report.v8.docx

10 Glossary

AEP	annual exceedance probability (for coastal inundation event)
ARI	average recurrence interval
BMAP	beach morphology analysis package
CD	chart datum (0 = 9.08m RL datum)
CEHZ	coastal erosion hazard zone
CEHZ 2065	c. 50 years coastal erosion hazard zone
CEHZ 2120	c.100 year coastal erosion hazard zone
CERC	Coastal Engineering Research Center (USA)
CIHZ	coastal inundation hazard zone
DEM	digital elevation model
DS	dune stability
ENSO	El Nino southern oscillation
GWL	ground water level
HAT	highest astronomic tide
IPCC	Intergovernmental Panel on Climate Change
IPO	interdecadal Pacific oscillation
LT	long-term trend
MfE	Ministry for the Environment
MHWS	mean high water spring
MLWS	mean low water spring
MSL	mean sea level
MSLA	mean sea level anomaly
NZCPS	New Zealand Coastal Policy Statement 2010
PCE	Parliamentary Commissioner for the Environment
RL	HBRC datum (Reduced Level: 10m = 0.92m CD)
SLR	sea level rise
TAG	Technical Advisory Group = senior staff reps. from each participant Council
WASP	waves and storm surge prediction
X-Beach-G	X beach-gravel (model)

11 References

Aitken, J.J. (1999). Rocked and Ruptured: Geological Faults in New Zealand. Reed Books, Auckland, 88 pp.

Beaven R.J. and Litchfield, N.J. (2012). Vertical land movement around the New Zealand coastline: implications for sea-level ri9se, GNS Science Report 2012/29. 41p.

Bell, R.G. (2013). Submission on the Proposed Northland Regional Policy Statement of Evidence, 26 May 2013. 22p.

Bell, R. (2012). Sea Levels for New Zealand: Give us a Number Please! *Presentation at Sea level Rise: meeting the Challenge Conference*, Wellington May 10-11, 2012.

Bruun P. (1962). Sea-level rise as a cause of shore erosion. J. Waterways Harbors Div 88:117–130.

Bruun, P. (1988). The Bruun Rule of erosion by sea level rise: a discussion on large-scale two- and three-dimensional usages. JCR, 4, 627–648.

Cooper, J.A.G. and Pilkey O.H. (2004). Sea-level rise and shoreline retreat: time to abandon the Bruun Rule. Global and Planetary Change 43, 157-171.

Davidson, P., Wilson, S. (2011). Groundwaters of Marlborough. Chapter 9: Aquifer Hydraulic Properties.

Deltares (2014). XBeach-G. Graphical user interface for setting up, running and analysing XBeach-G calculations.

Diez, J.J. (2000). A Review of Some Concepts Involved in the Sea-Level Rise Problem. Journal of Coastal Research, Vol 16, No. 4: 1179-1187.

Goodier, C. (2011). Hawke's Bay: Tsunami inundation model, preliminary results, Tangoio to Cape Kidnappers. HBRC plan number 4256, May 2011

Goodier, C. and L. Pearse (2015) Storm report: Cyclone Pam, March 15-18, 2015. HBRC response to Cyclone Pam, HBRC Report No. 4728, Plan No. AM15/03

GNS (2013). Review of Tsunami Hazard in New Zealand (2013 update). GNS Science Consultancy Report 2013/131.

Hull, A.G. (1990). Tectonics of the 1931 Hawke's Bay Earthquake. New Zealand Journal of Geology and Geophysics, 29:75-82

IPCC (2013). Working Group I contribution to the IPCC 5th Assessment Report "Climate Change 2013: The Physical Science Basis". DRAFT report by Intergovernmental Panel on Climate Change. June, 2013

IPCC (2015). ''Climate Change 2014: Synthesis Report''. Report by Intergovernmental Panel on Climate Change.

Komar, P.D., and others (1991). The response of beaches to sea-level changes: A review of predictive models: Journal of Coastal Research, v. 7, n. 3, p. 895-921. [Scientific Committee on Ocean Research Working Group 89]

Komar, P.D., McDougal, W.G., Marra, J.J. and Ruggiero, P. (1999). The Rational Analysis of Setback Distances: Application to the Oregon Coast. Shore and Beach Vol. 67 (1) 41-49.

Komar, P. D. (2005) .Hawke's Bay, New Zealand: Environmental Change, Shoreline Erosion, and Management Issues: Report for the Hawke's Bay Regional Council.

Komar, P.D. (2010) Shoreline evolution and management of Hawke's Bay, New Zealand: Tectonics, coastal processes and human impacts: Journal of Coastal Research, v. 26, n. 1, p. 143-156.

Komar,P.D., Harris, E. (2014). Hawke's Bay, New Zealand. Global climate change and barrier-beach responses. Report to the Hawke's Bay Regional Council.

de Lange, W.P. (1996). Storm surges on the New Zealand coast: Tephra, v. 15, no. 1, p. 24-31.

Larson, M and Kraus, N C (1989). "SBEACH: Numerical Model for Simulating Storm-Induced Beach Change, Report 1: Theory and Model Foundation". *Technical Report CERC-89-9*, US Army Engineer Waterways Experiment Station, Coastal Engineering Research Center, Vicksburg USA.

McCall, R., Masselink, G., Poate, T.G., Roelvink, J.A., Almeida, L.P., Davidson, M., Russell, P.E. (2014). Modelling storm hydrodynamics on gravel beaches with XBeach-G. Coastal Engineering 91 (2014) 231-250.

MetOcean (2008). Whakarire Ave Breakwater Design Studies and Surf Effects Modelling. Prepared for Beac Ltd, April 2008.

MetOcean (2011). Hawkes Bay Wave Climate: MetOcean Solutions Ltd., New Plymouth, New Zealand, 42 pp.

MetOcean (2013). Hawkes Bay Wave Climate: MetOcean Solutions Ltd., New Plymouth, New Zealand.

MfE (2008). Coastal Hazards and Climate Change. A guidance manual for local government in New Zealand. 2nd edition. Revised by Ramsay, D. and Bell, R. (NIWA). Prepared for Ministry for the Environment. Viii+127 p.

Nicholls, R.J., Laron, M., Capobianco, M. and Birkemeier, W.A. (1998). Depth of Closure: Improving Understanding and Prediction. ICCE 1998.

NZCPS (2010). New Zealand Coastal Policy Statement.

Paterson, M.C.H. (2000). The effect of earthquake induced relative sea level change on gravel beach geomorphology, Hawke's Bay, New Zealand. Master's Thesis, School of Earth Science, Victoria University, Wellington.

Power, W. (2013) Review of tsunami hazard in New Zealand (2013 Update). GNS Science Consultancy Report, August 2013.

Ramsey, D., Gibberd, B., Dahm, J., Bell, R. (2012). Defining coastal hazard zones for setback lines: A guide to good practice. NIWA Ltd. 91 p.

Shand, R.D. (2012). Kapiti Coast erosion hazard assessment. 2012 Update report prepared for the Kapiti Coast District Council by Coastal Systems Ltd. Client report No. 2012-8 CRep, August 2012.

Shand, T.D., Shand, Reinen-Hamill, R.A., Kench, P., Ivamy, M, Knook, P. and Howse, B. (2015) Methods for Probabilistic Coastal Erosion Hazard Assessment. Proceedings of the Australasian Coasts and Ports Conference, Auckland Sept 15-18 2015.

Smith, R.K. (1968). South Hawke Bay Beaches: Sediments and Morphology. Unpublished Master's thesis, Department of Geography, University of Canterbury, Christchurch.

Tonkin and Taylor (2004). Hawkes Bay Regional Coastal Hazard Assessment. Report prepared for Hawkes Bay Regional Council.

Tonkin & Taylor (2006). Regional assessment of areas susceptible to coastal erosion. Technical report prepared for Auckland Regional Council.

Tonkin & Taylor (2012). Haumoana Coastal Erosion Study. Concept design and assessment of groyne field protection. Report prepared for Hastings District Council and Hawke's Bay Regional Council.

Worley (2002). Port of Napier: Design Criteria Report for Outer Breakwater Extension: 20 December 2002 report to the Port of Napier, Worley Infrastructure Pty Ltd, Perth, Australia.

Appendix A: Location plan

Path: P:\20514\20514.0050\WorkingMaterial\GIS\MapDocuments\AppendixA_LocationPlan.mxd Date: 23/06/2015 Time: 4:15:55 p.m.

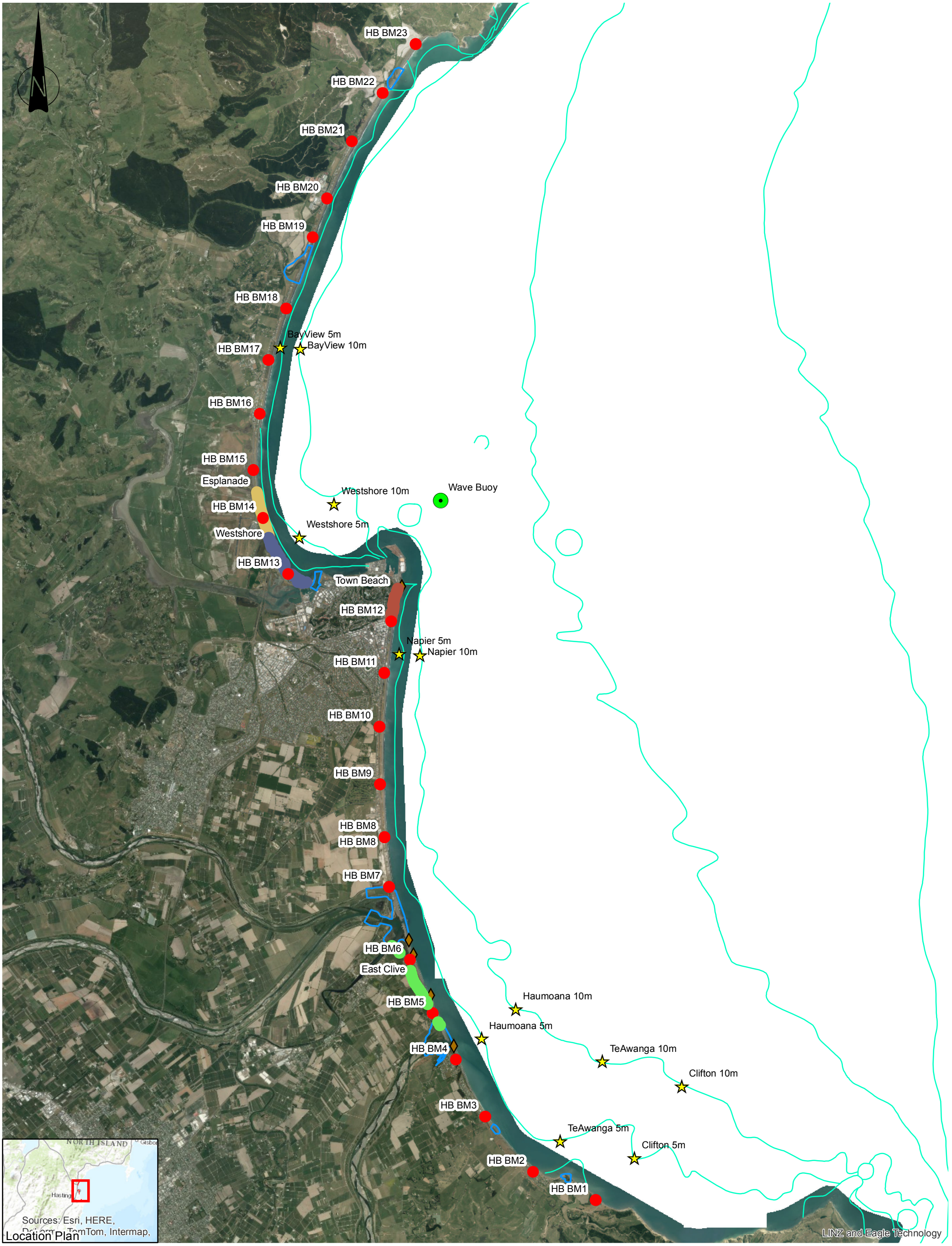

Notes: Aerial photograph: 2011/2012 (LINZ)

A3 SCALE 1:100,000

0 1 2 3 4 5 (km)

Tonkin & Taylor
Environmental and Engineering Consultants

www.tonkin.co.nz

DRAWN	PPK	Jun.15
CHECKED		
APPROVED		
ARCFILE	AppendixA_LocationPlan.mxd	
SCALE (AT A3 SIZE)	1:100,000	
PROJECT No.	20514.005	

Hawke's Bay Councils (HBRC, NCC, HDC)
Coastal Hazard Assessment
Location Plan

FIGURE No. Figure 1.

Rev. 0

Appendix B: Beach profiles

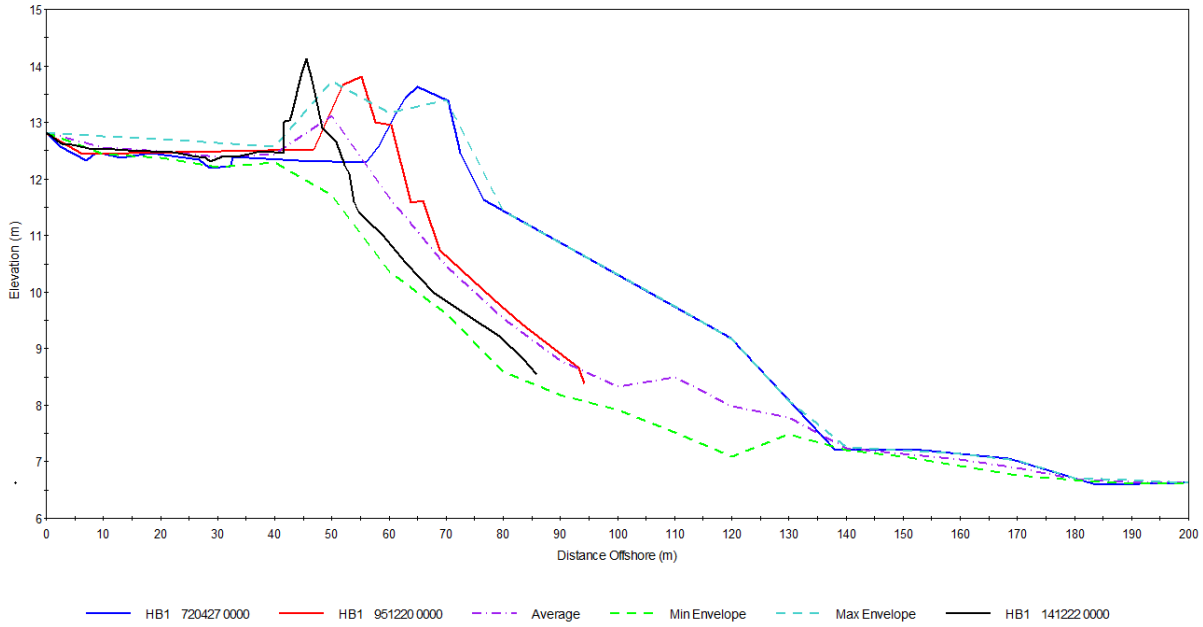

Figure B1: Beach profile plots for HB1

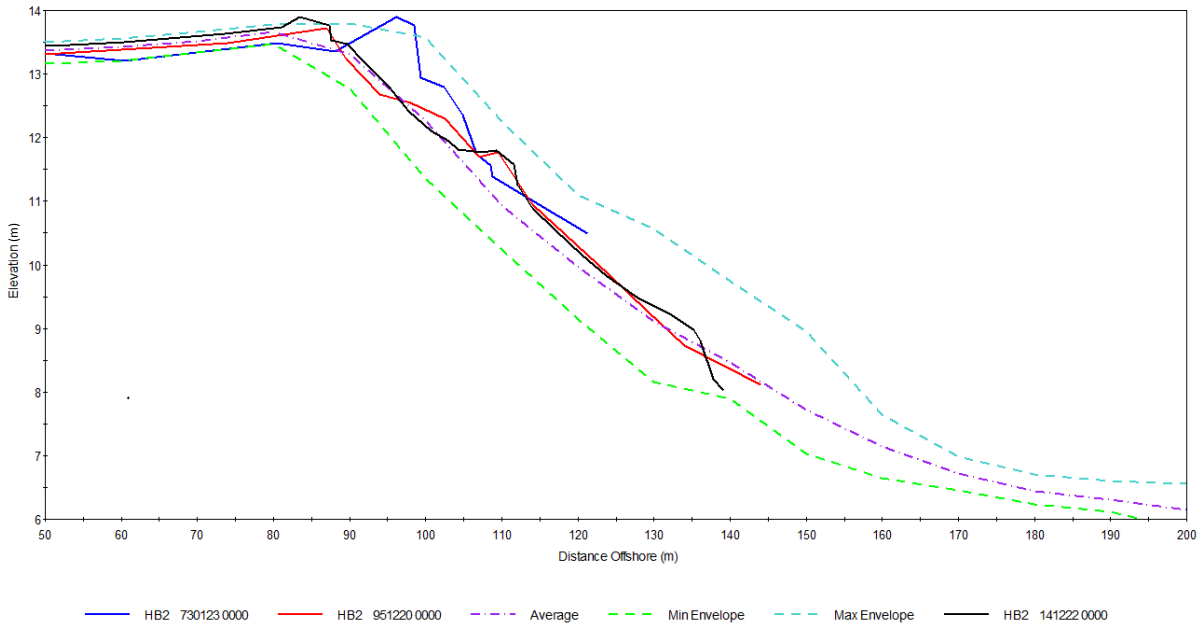

Figure B2: Beach profile plots for HB2

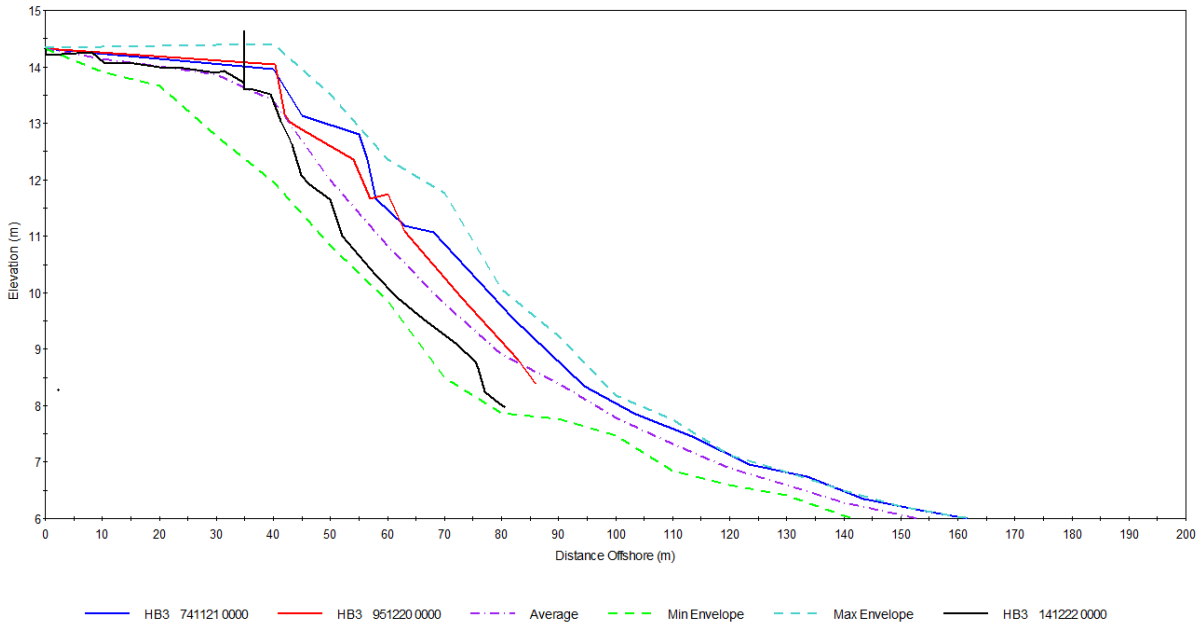

Figure B3: Beach profile plots for HB3

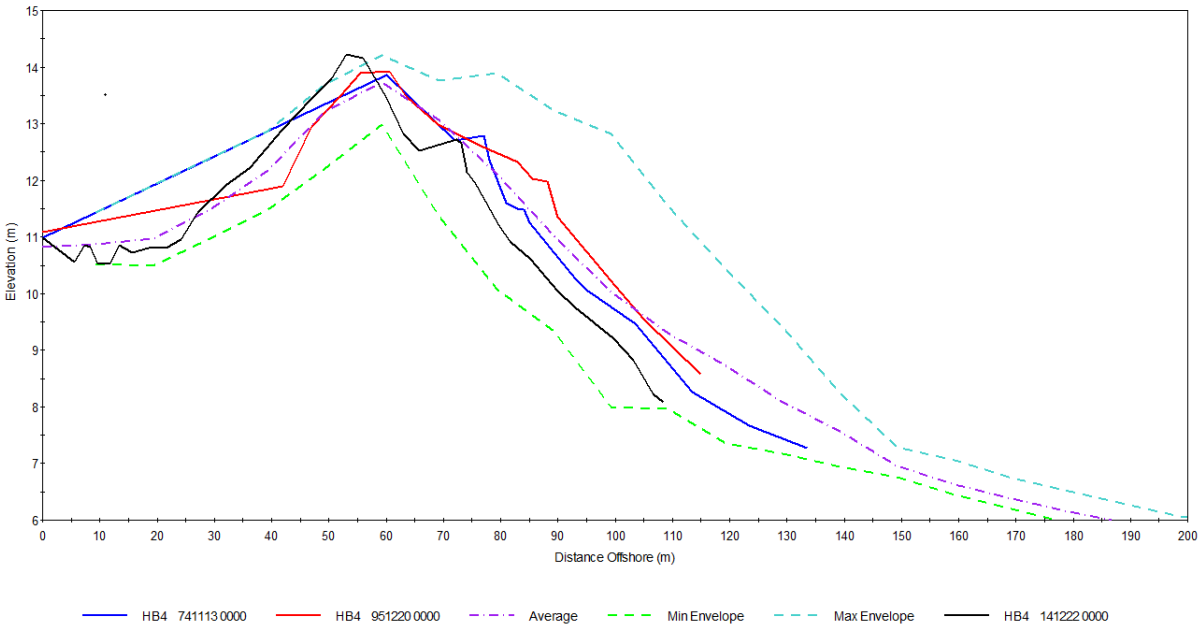

Figure B4: Beach profile plots for HB4

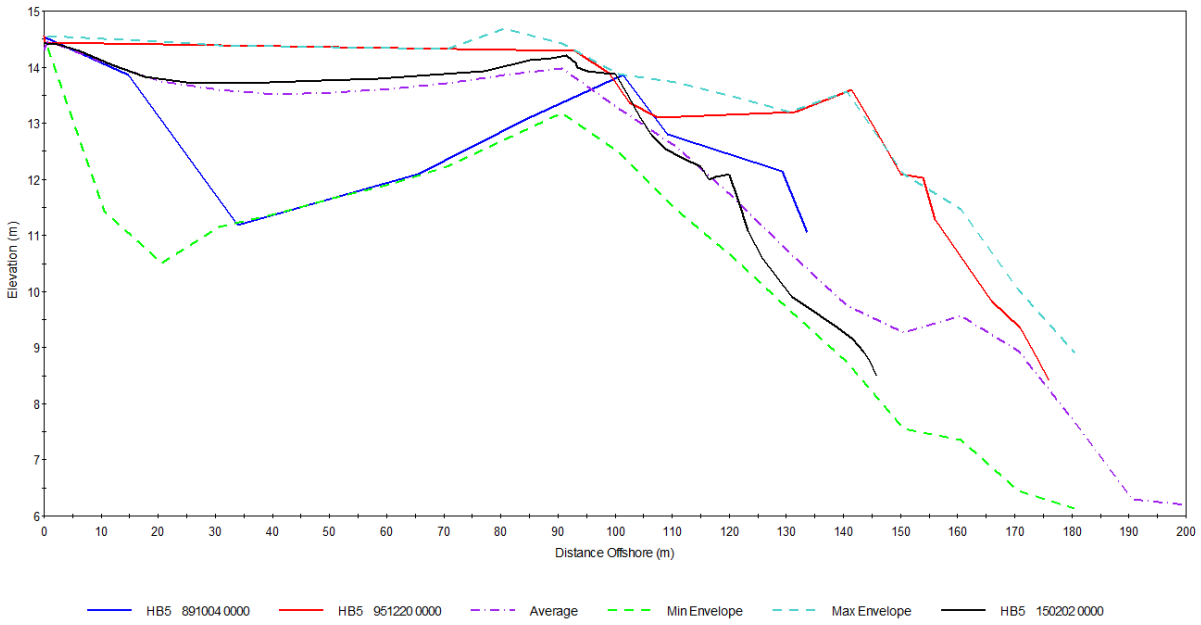

Figure B5: Beach profile plots for HB5

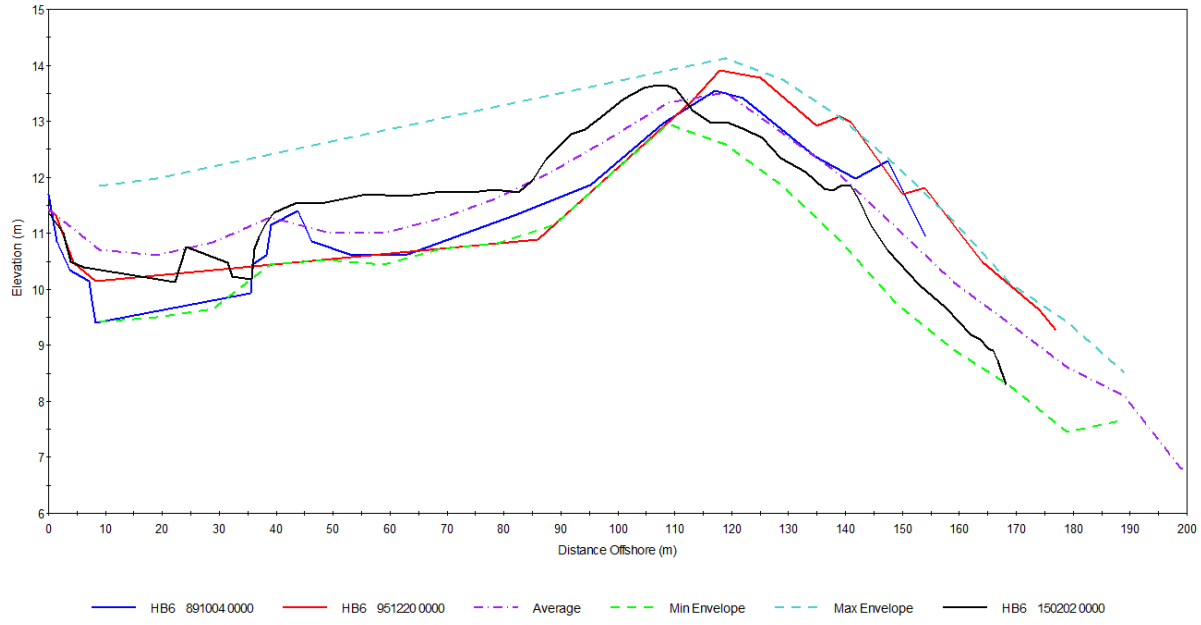

Figure B6: Beach profile plots for HB6

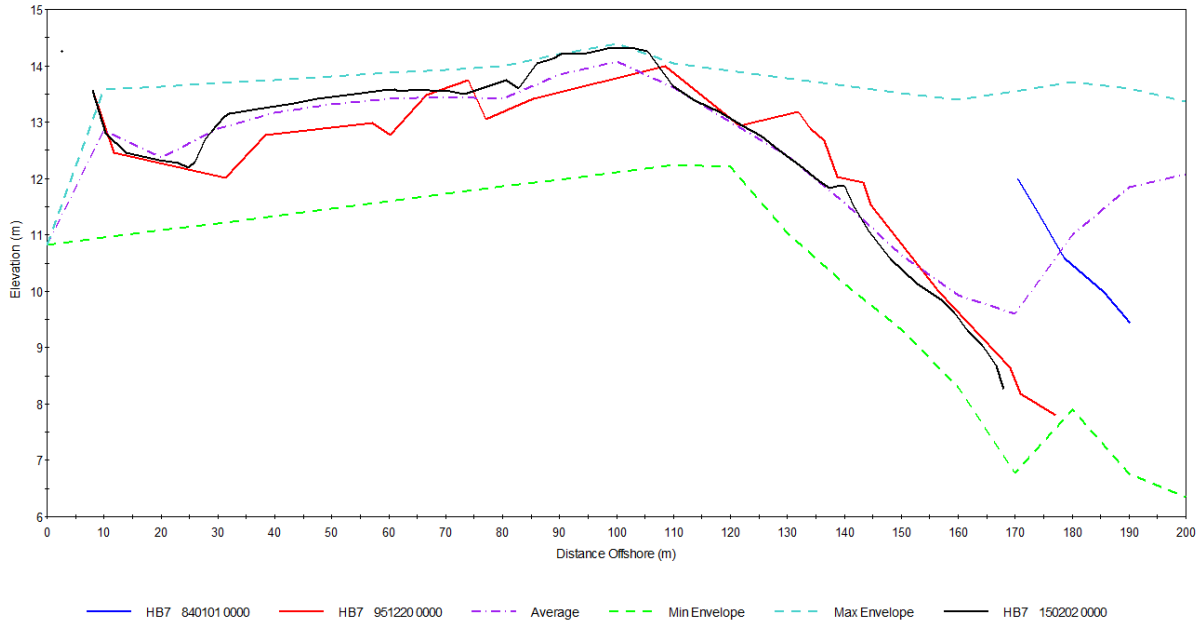

Figure B7: Beach profile plots for HB7

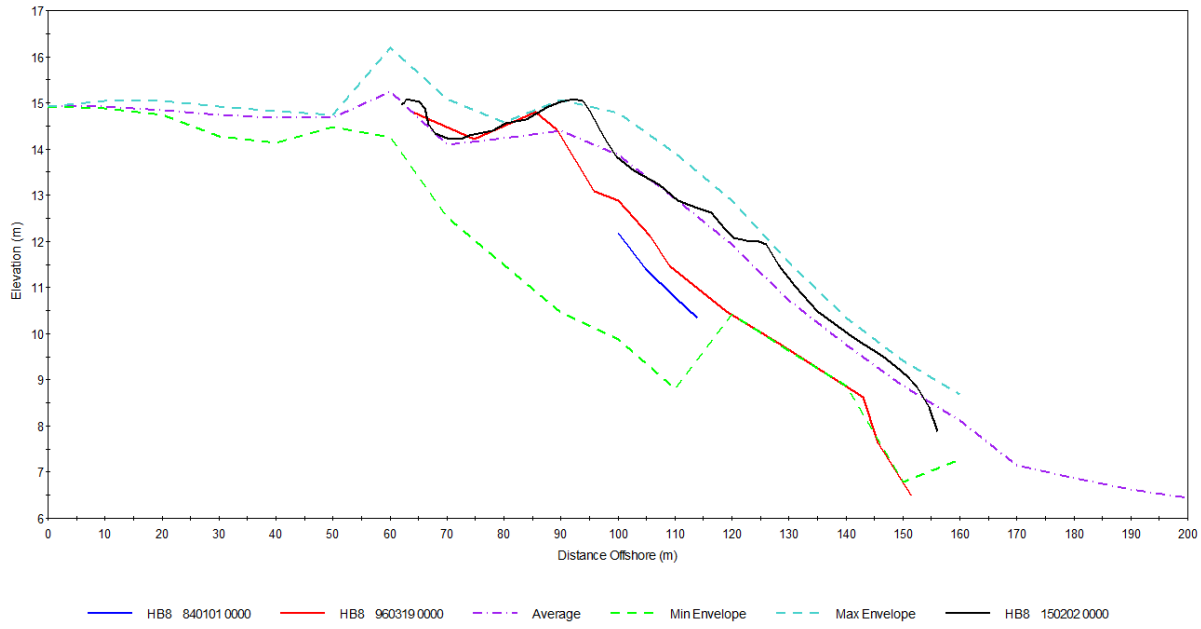

Figure B8: Beach profile plots for HB8

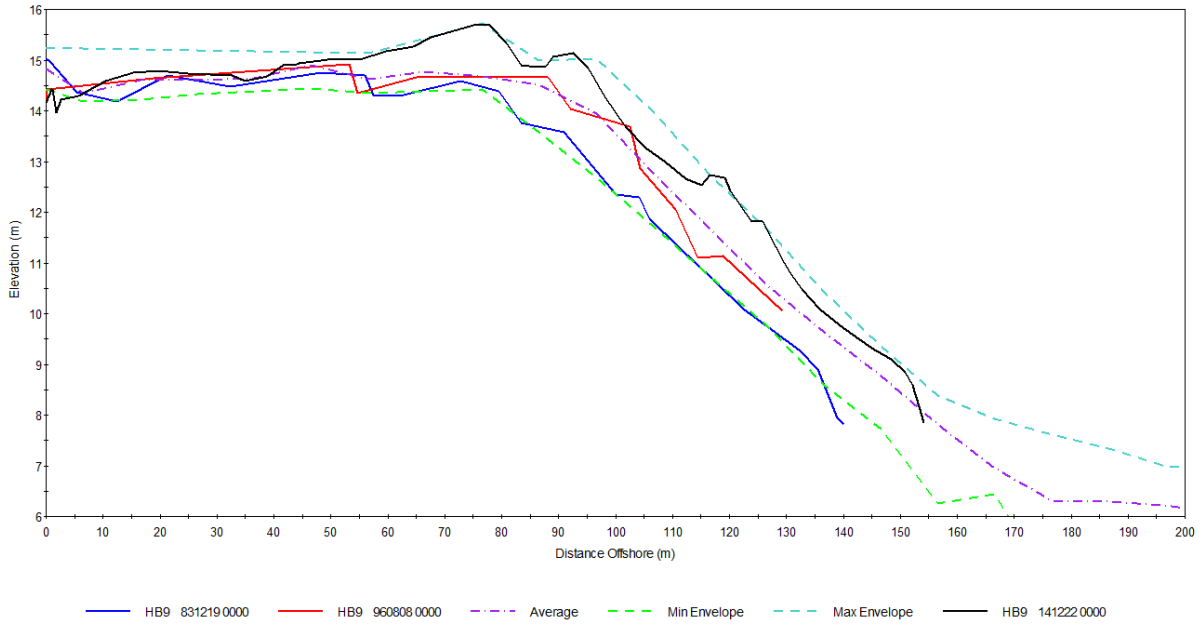

Figure B9: Beach profile plots for HB9

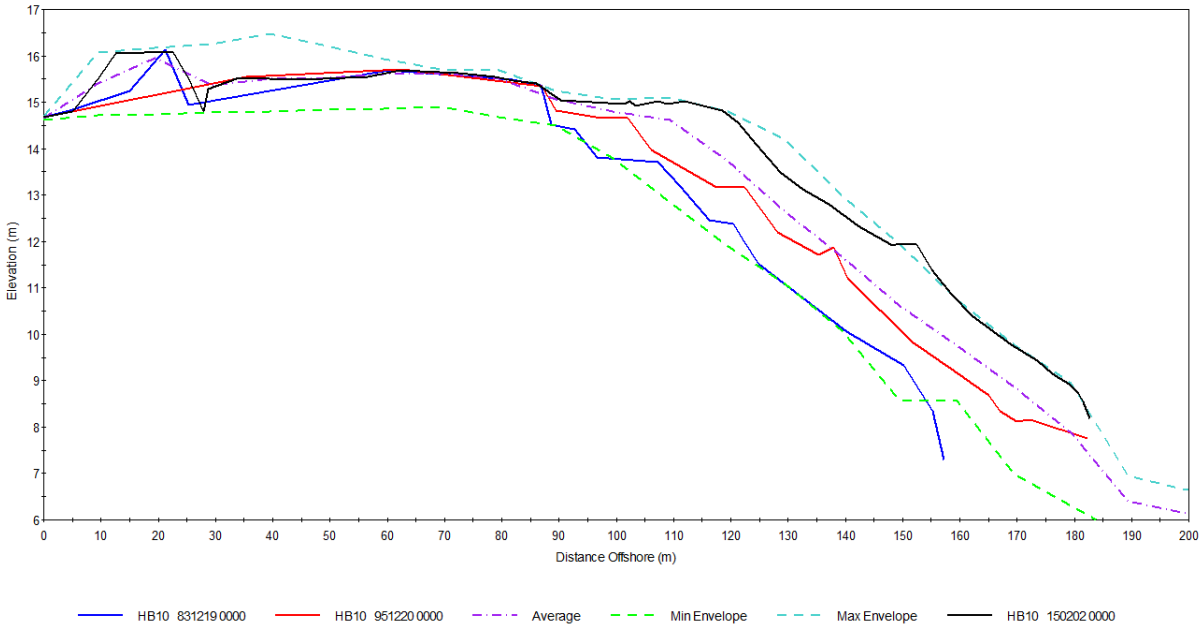

Figure B10: Beach profile plots for HB10

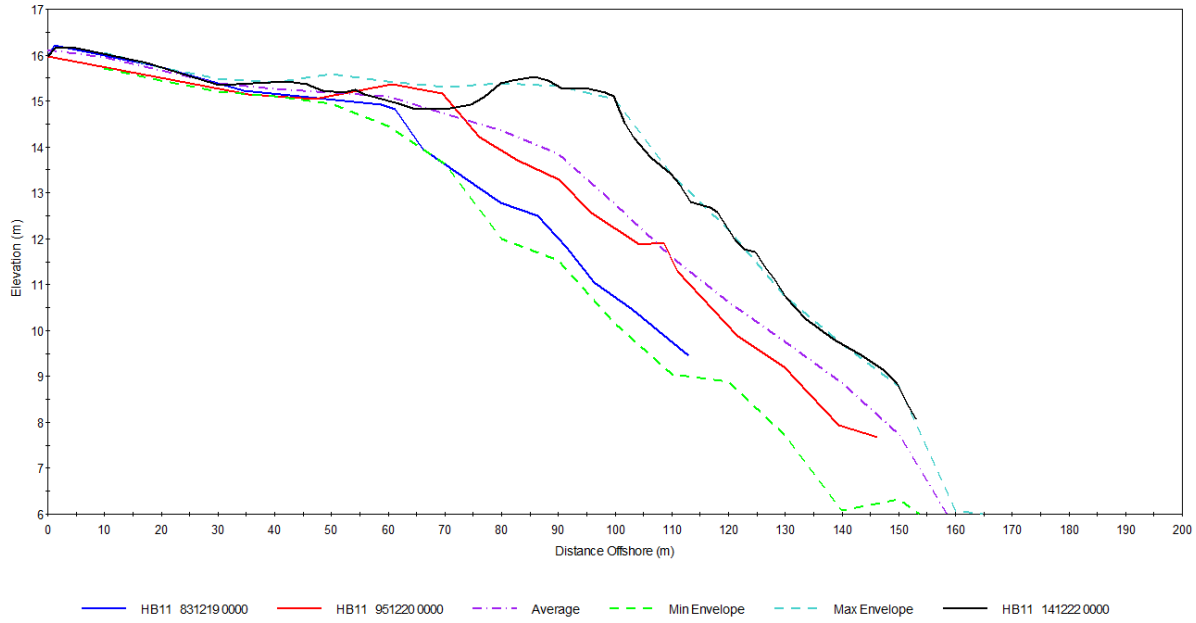

Figure B11: Beach profile plots for HB11

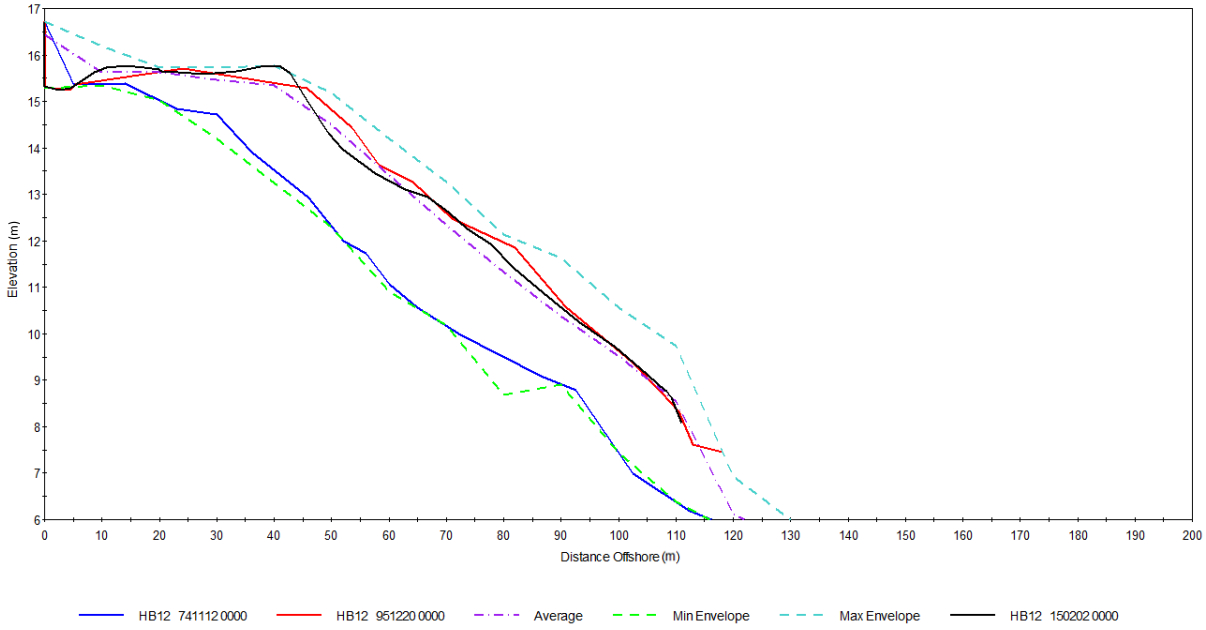

Figure B12: Beach profile plots for HB12

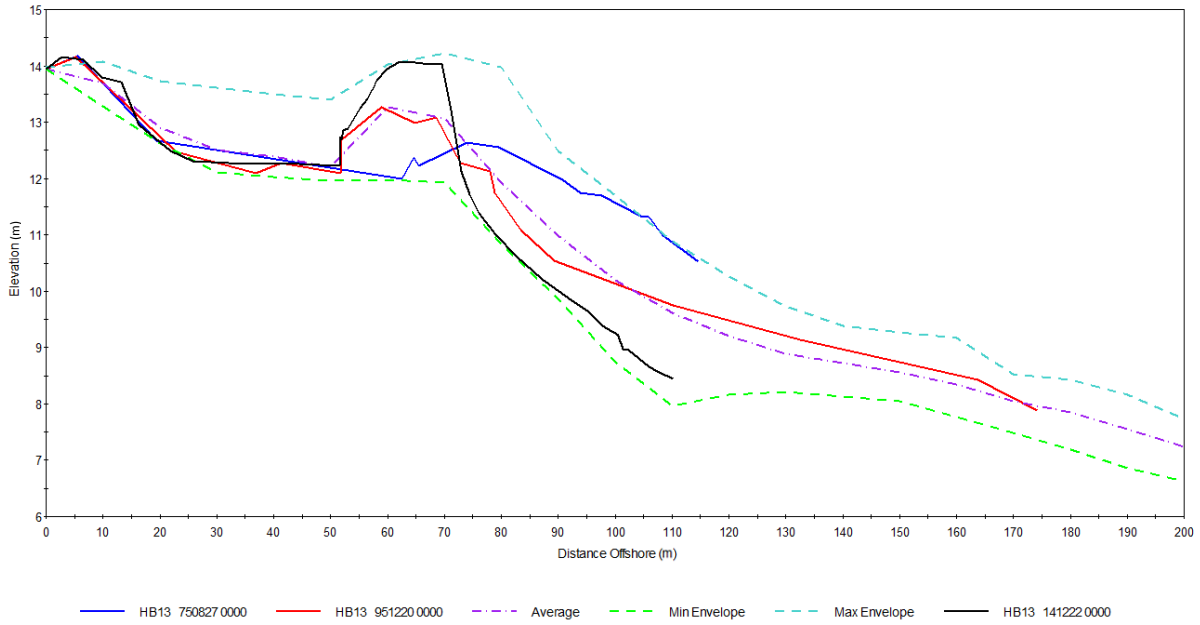

Figure B13: Beach profile plots for HB13

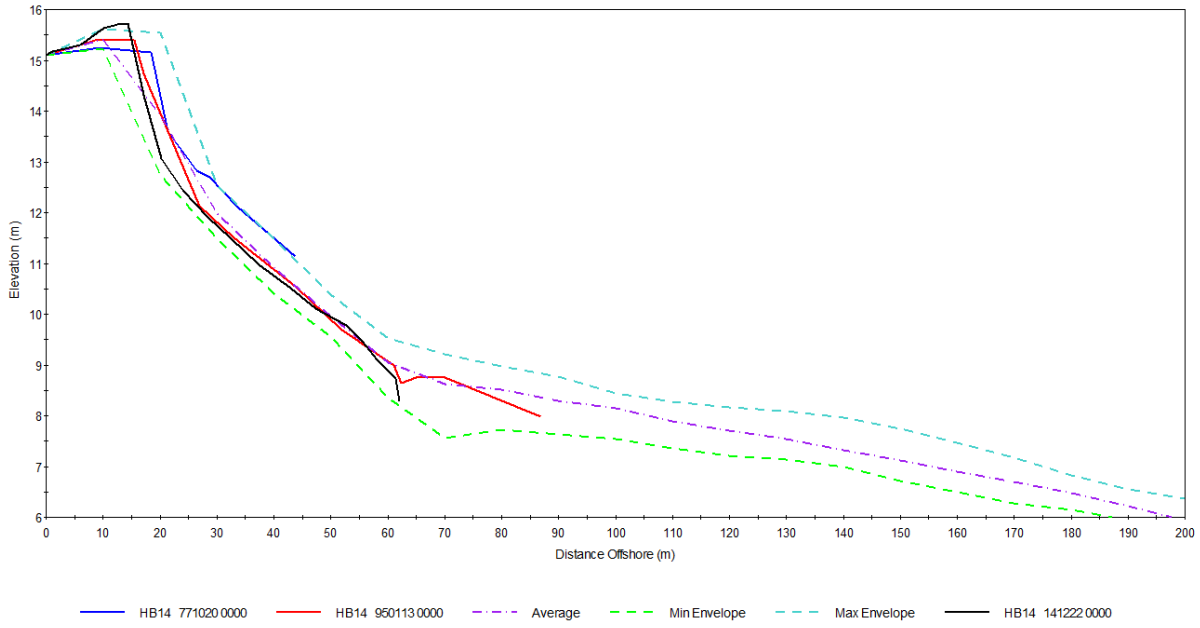

Figure B14: Beach profile plots for HB14

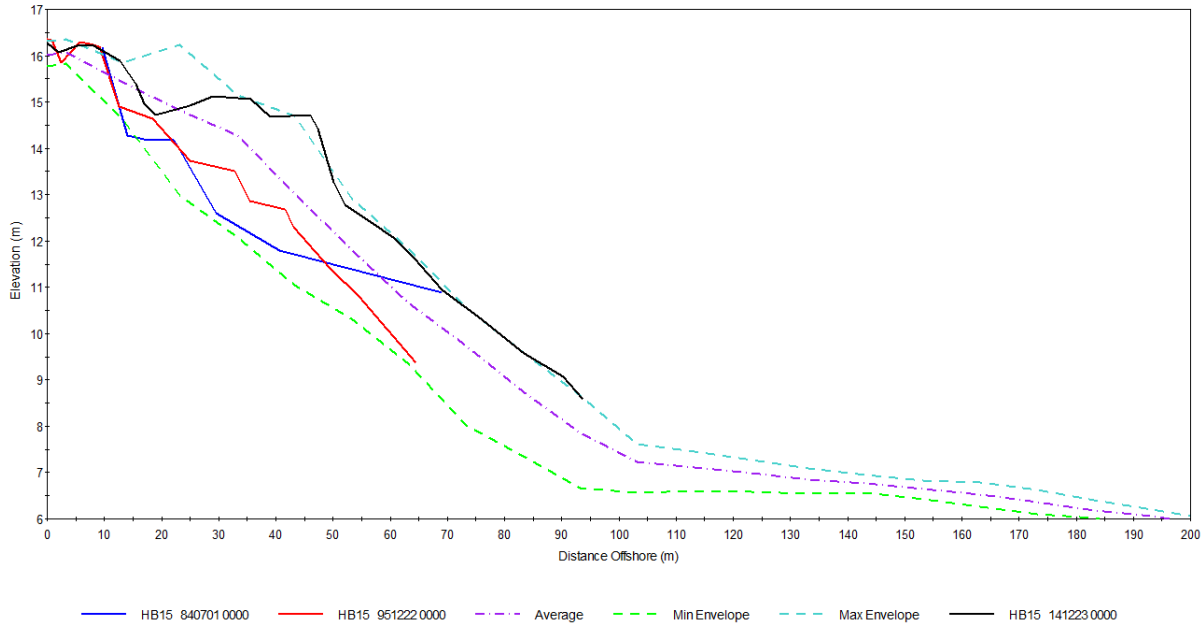

Figure B15: Beach profile plots for HB15

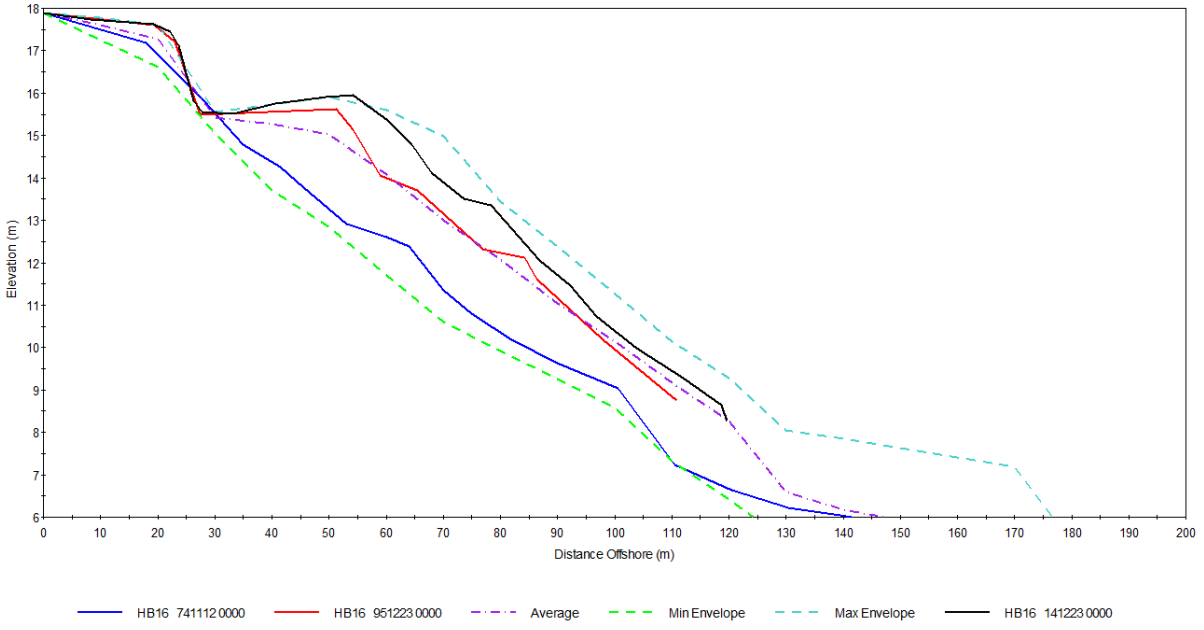

Figure B16: Beach profile plots for HB16

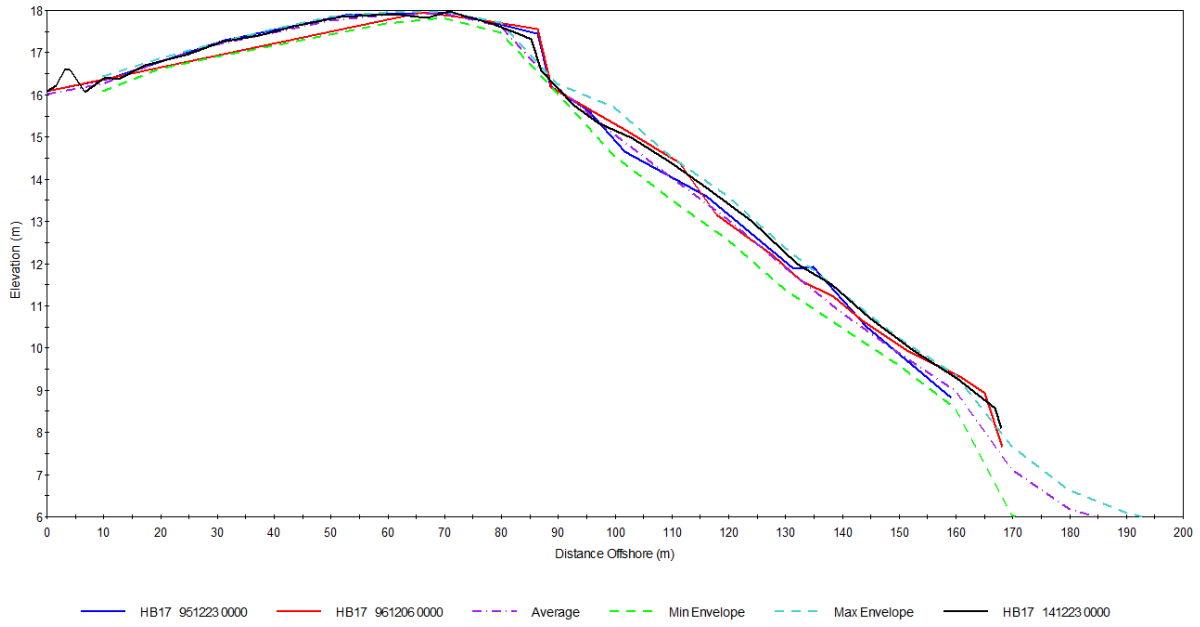

Figure B17: Beach profile plots for HB17

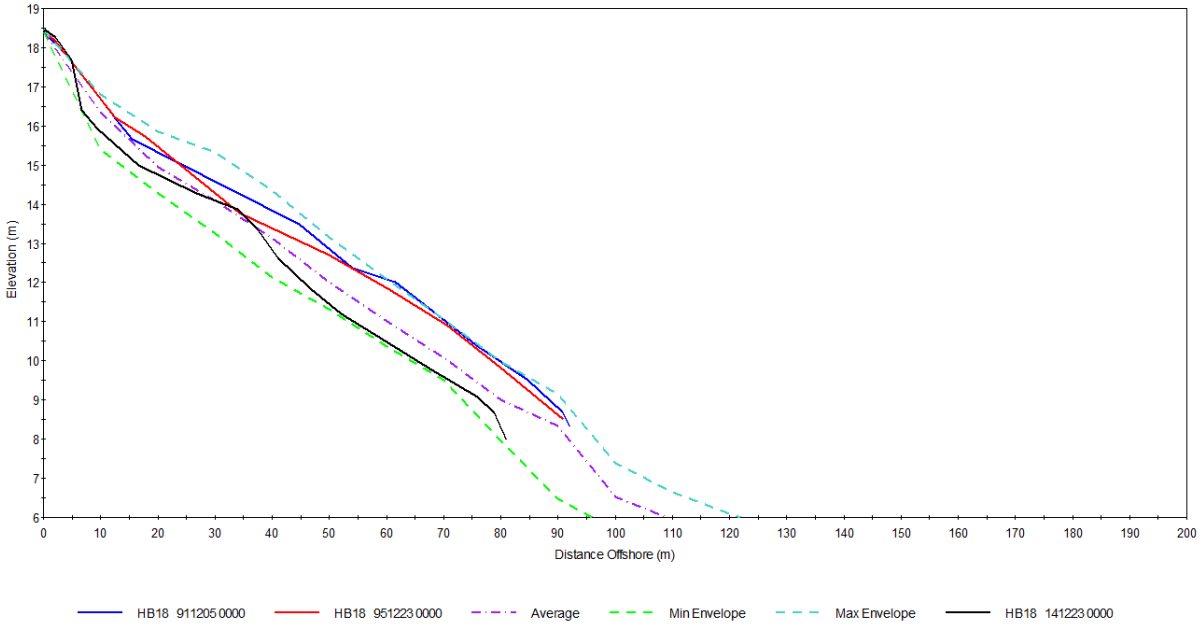

Figure B18: Beach profile plots for HB18

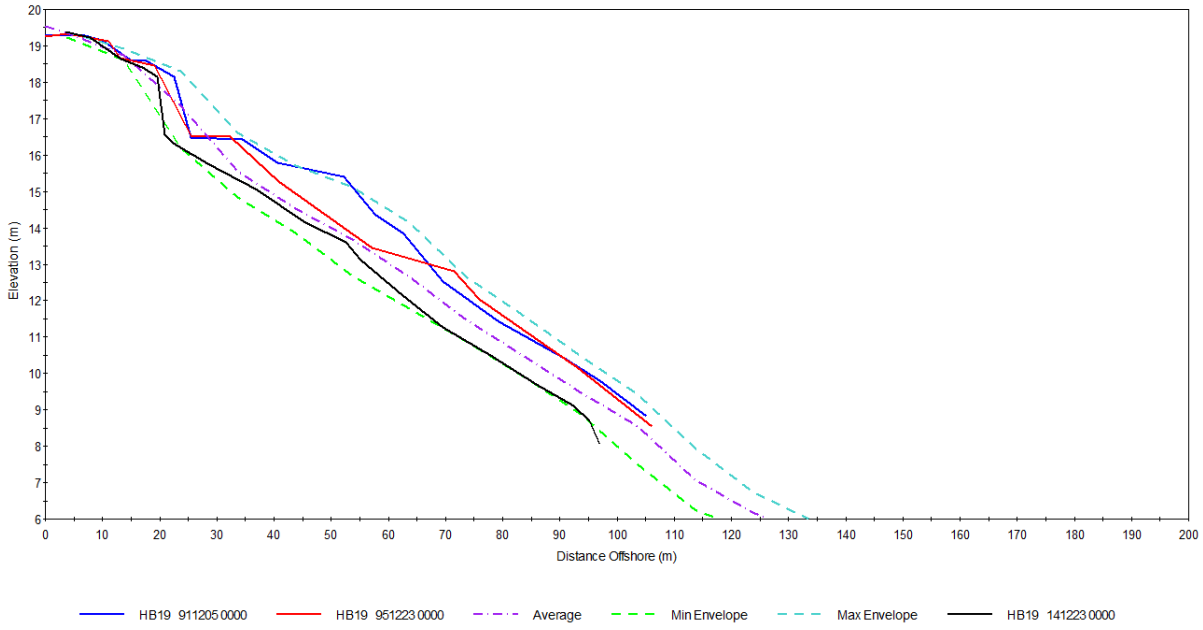

Figure B19: Beach profile plots for HB19

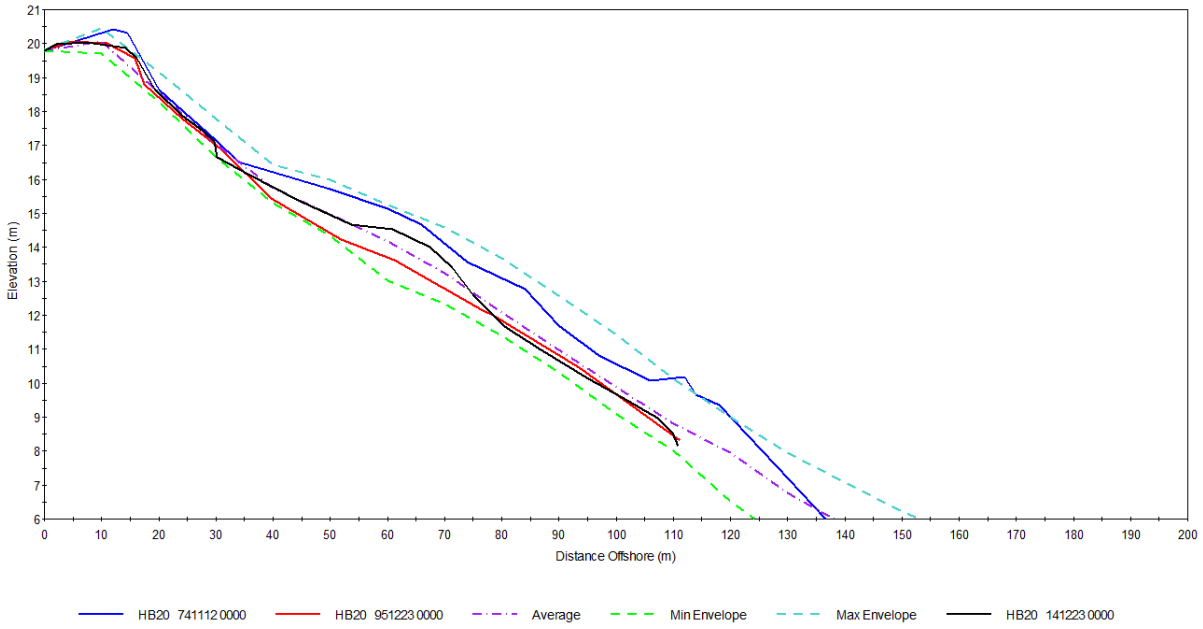

Figure B20: Beach profile plots for HB20

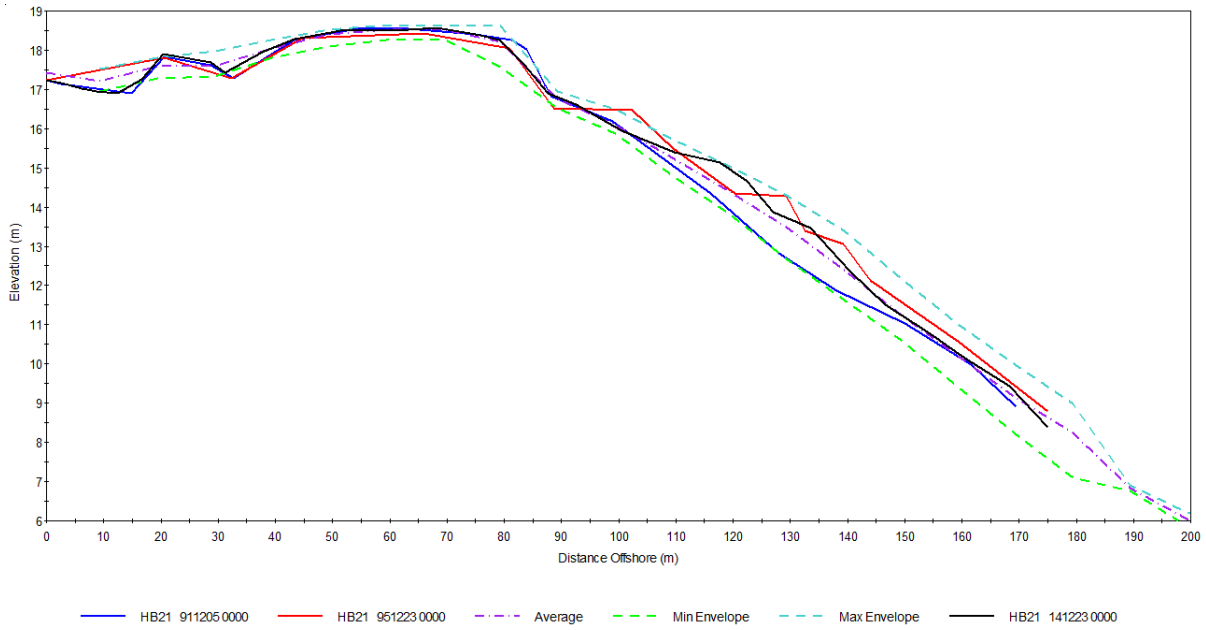

Figure B21: Beach profile plots for HB21

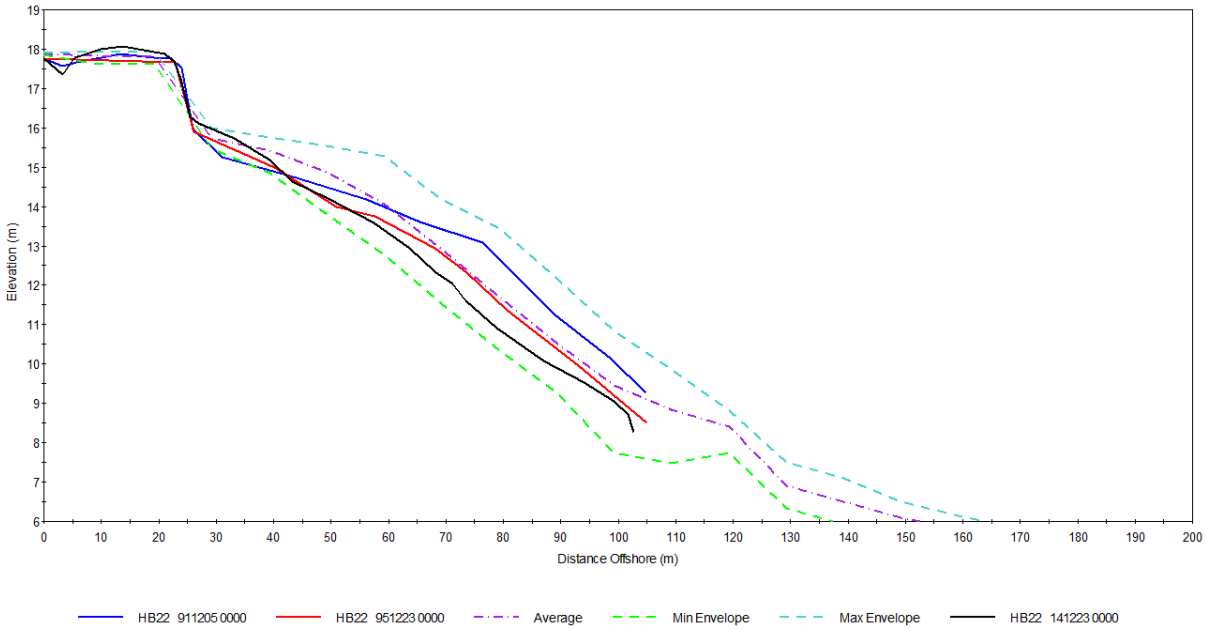

Figure B22: Beach profile plots for HB22

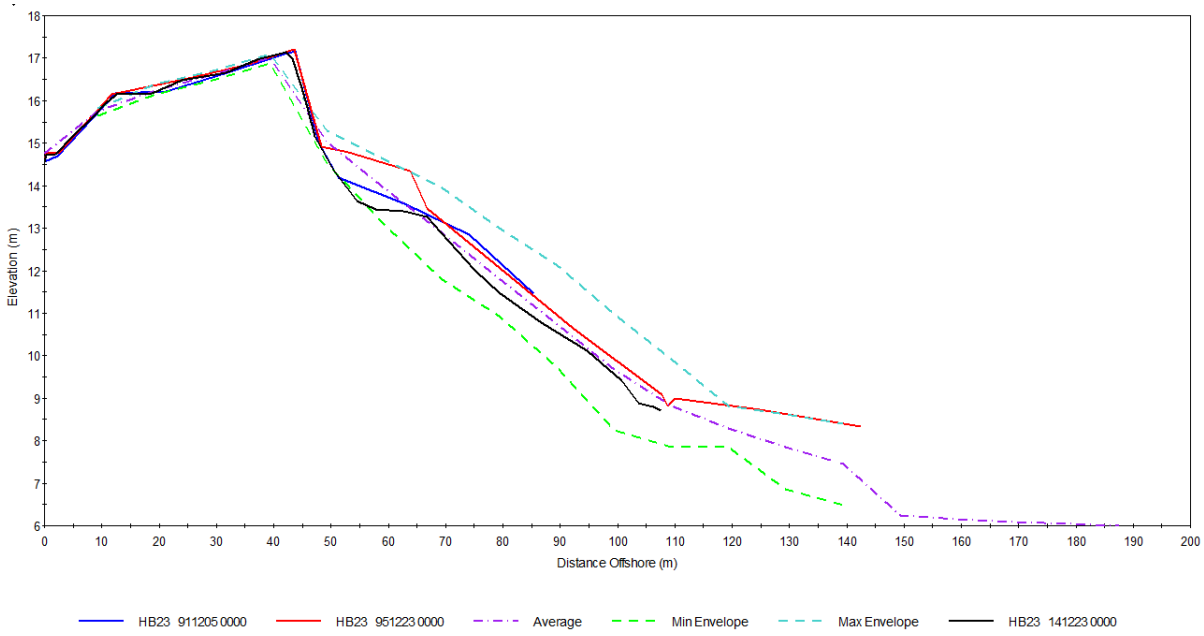

Figure B23: Beach profile plots for HB23

Appendix C: Horizontal excursion trends of 11 m contour

1972-2014

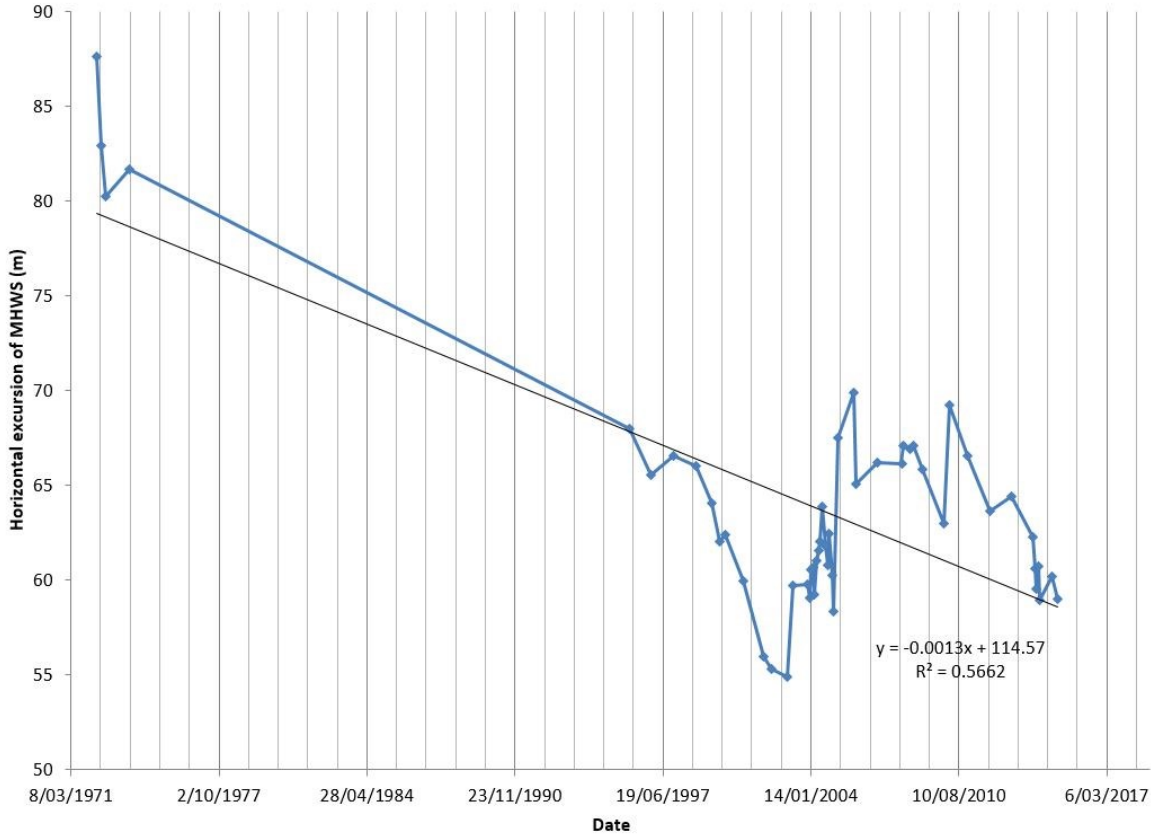

1995-2014

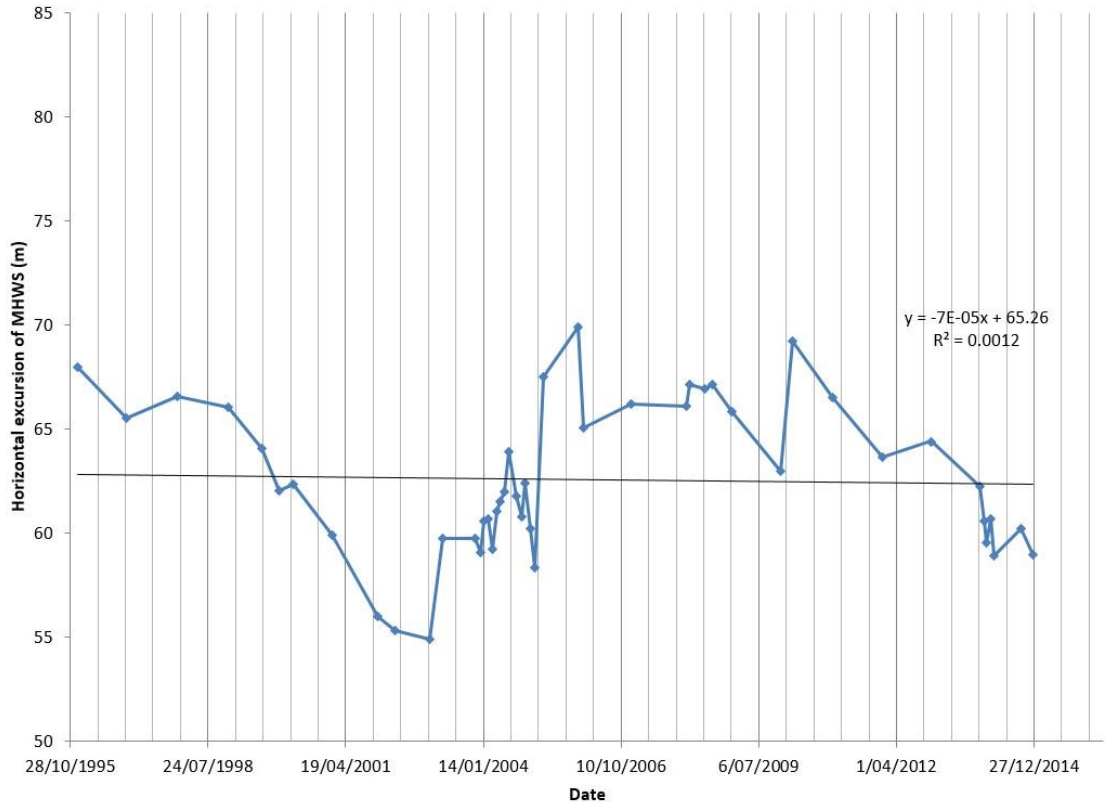

Figure C1: HB1 MHWS Excursion

1973-2014

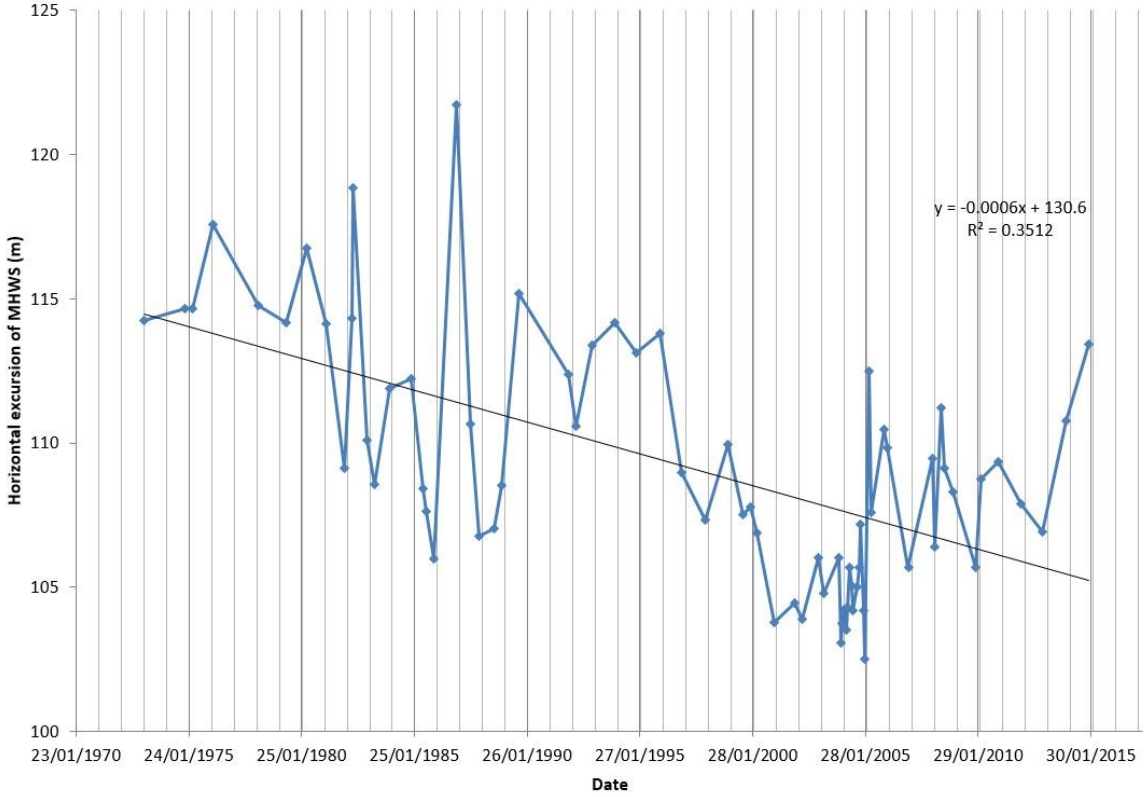

1995-2014

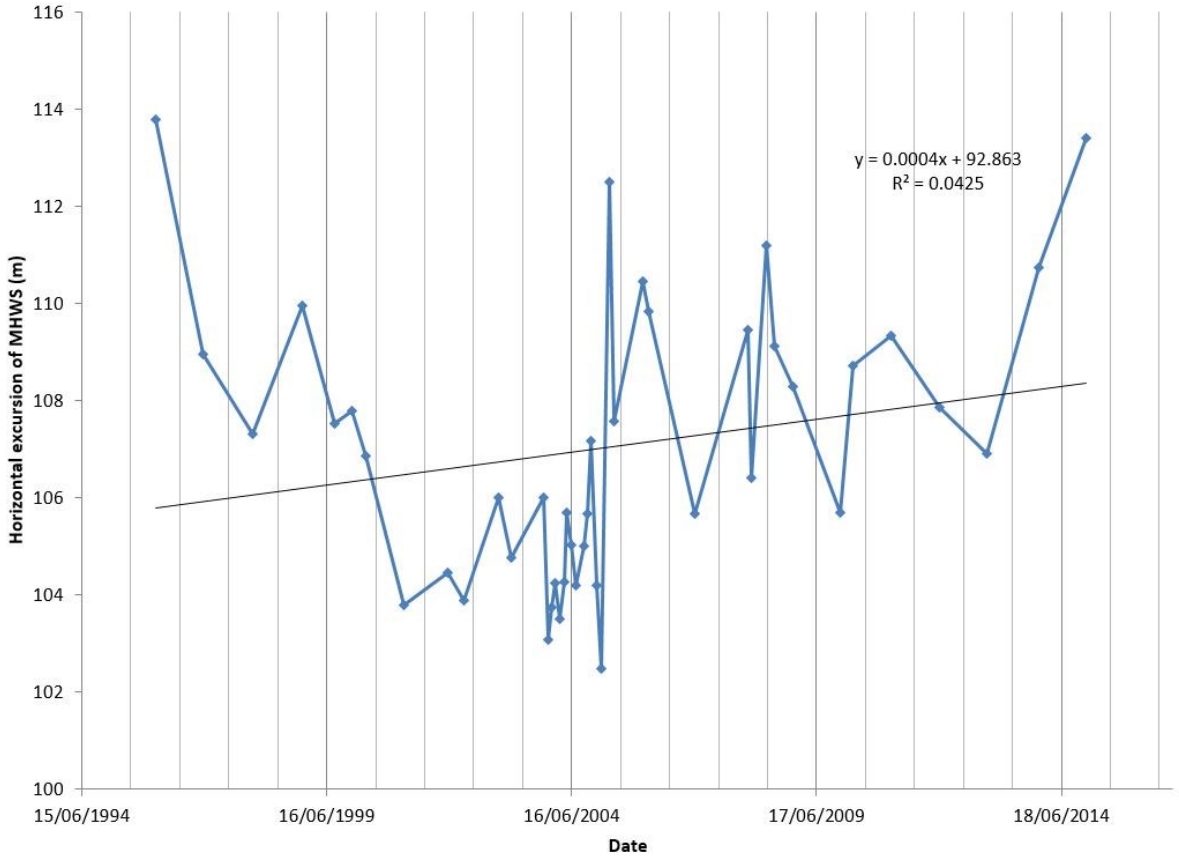

Figure C2: HB2 MHWS Excursion

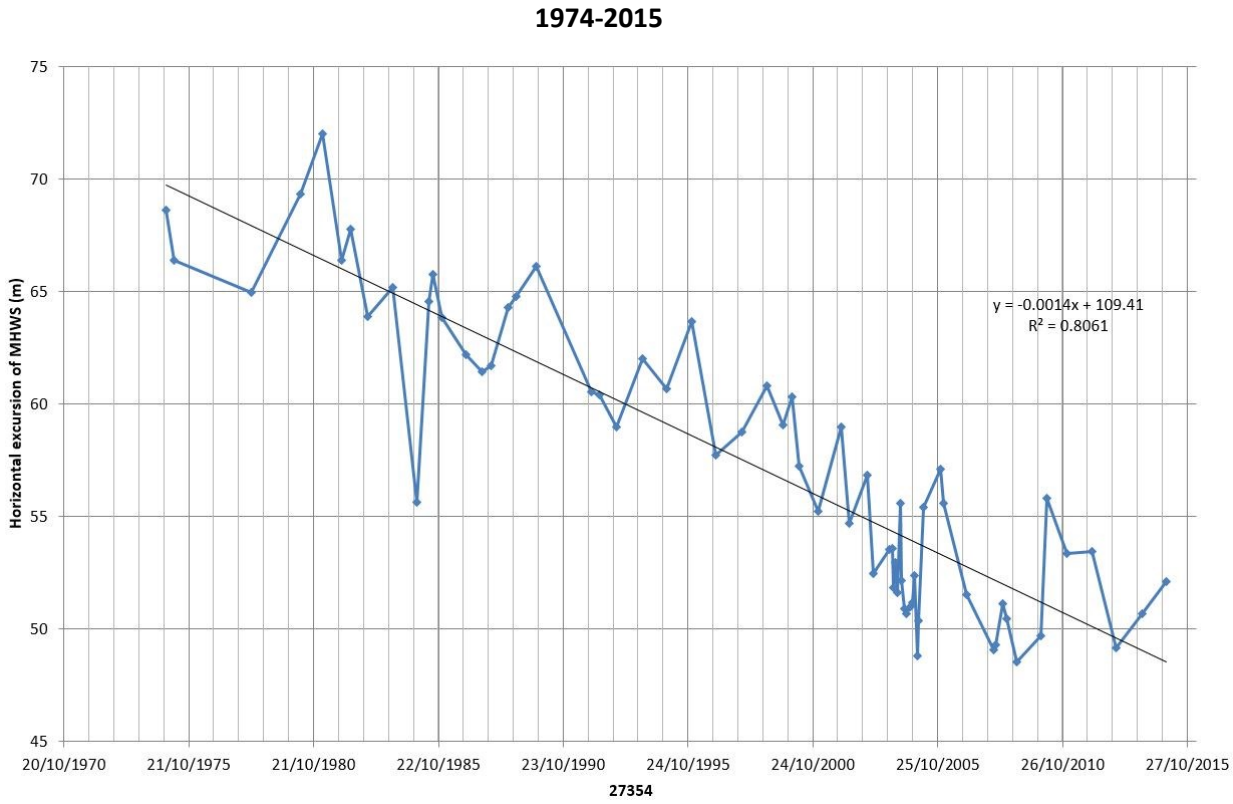

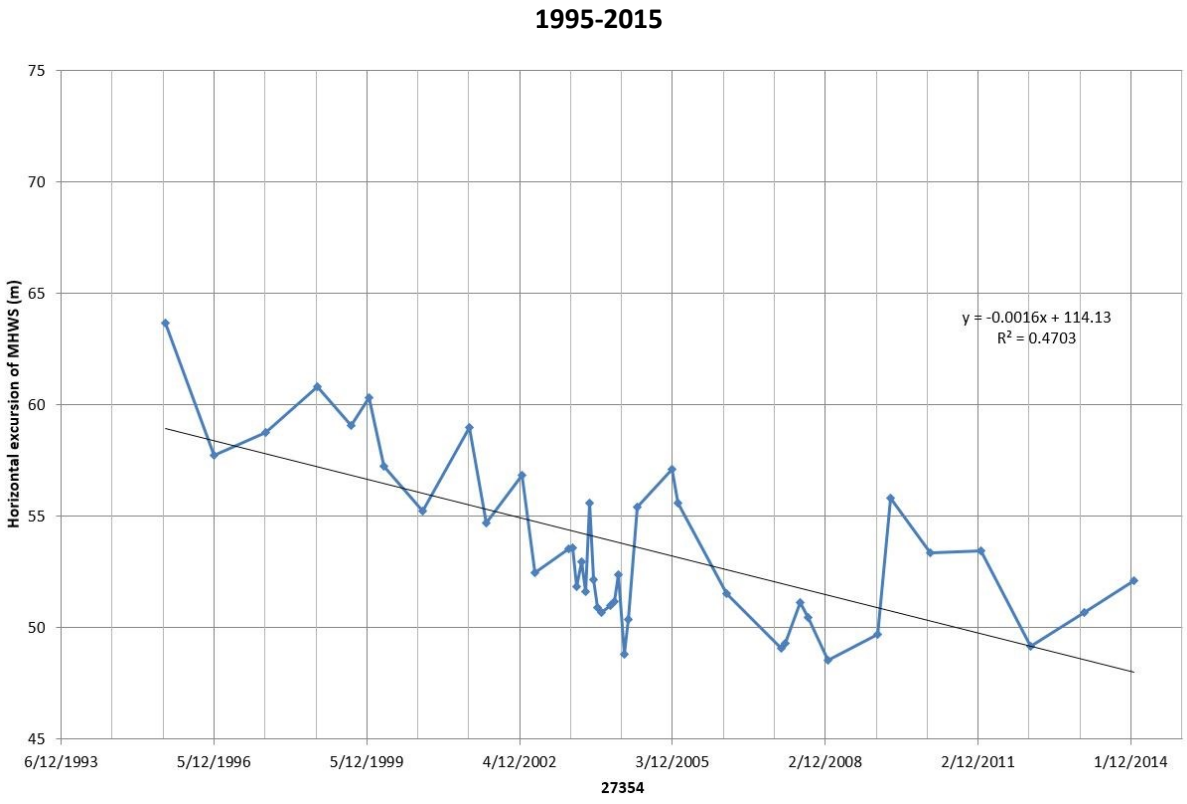

Figure C3: HB3 MHWS Excursion

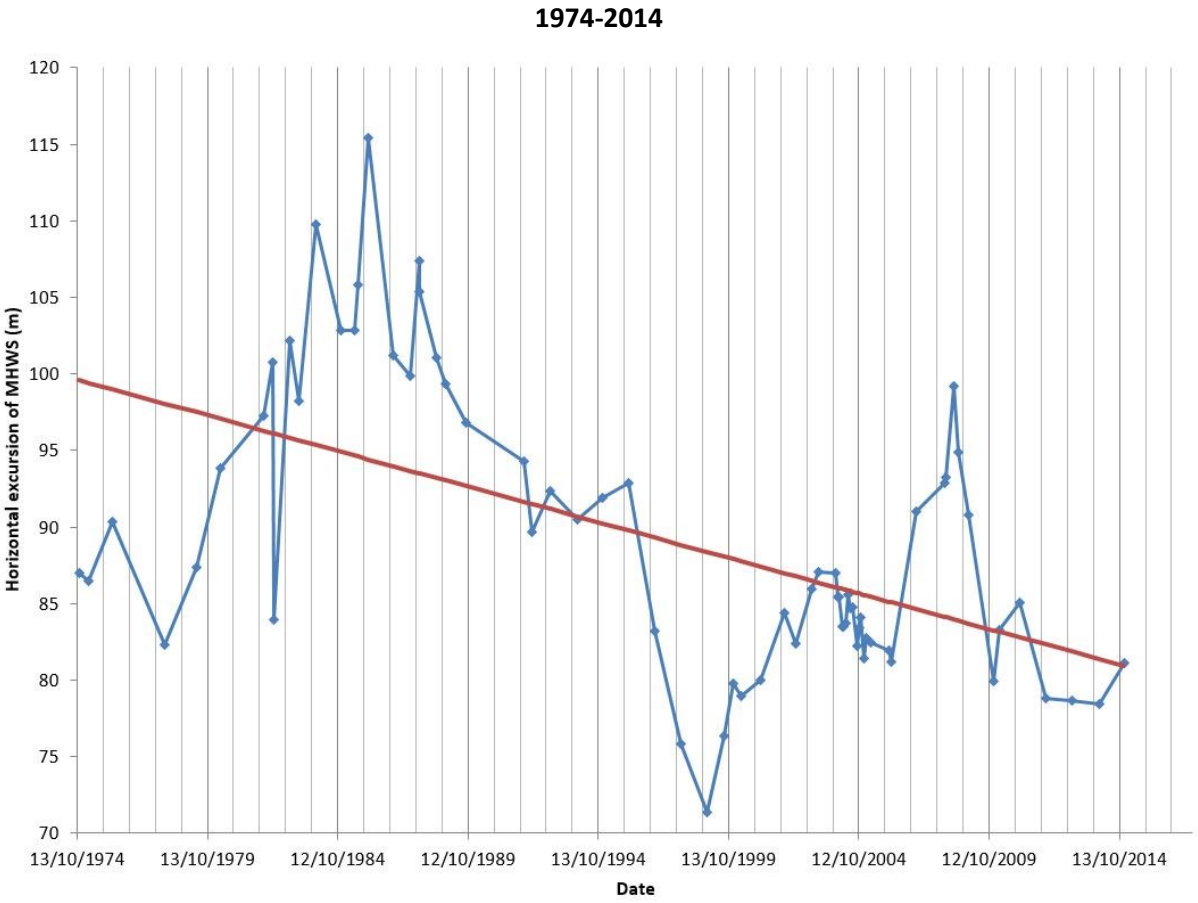

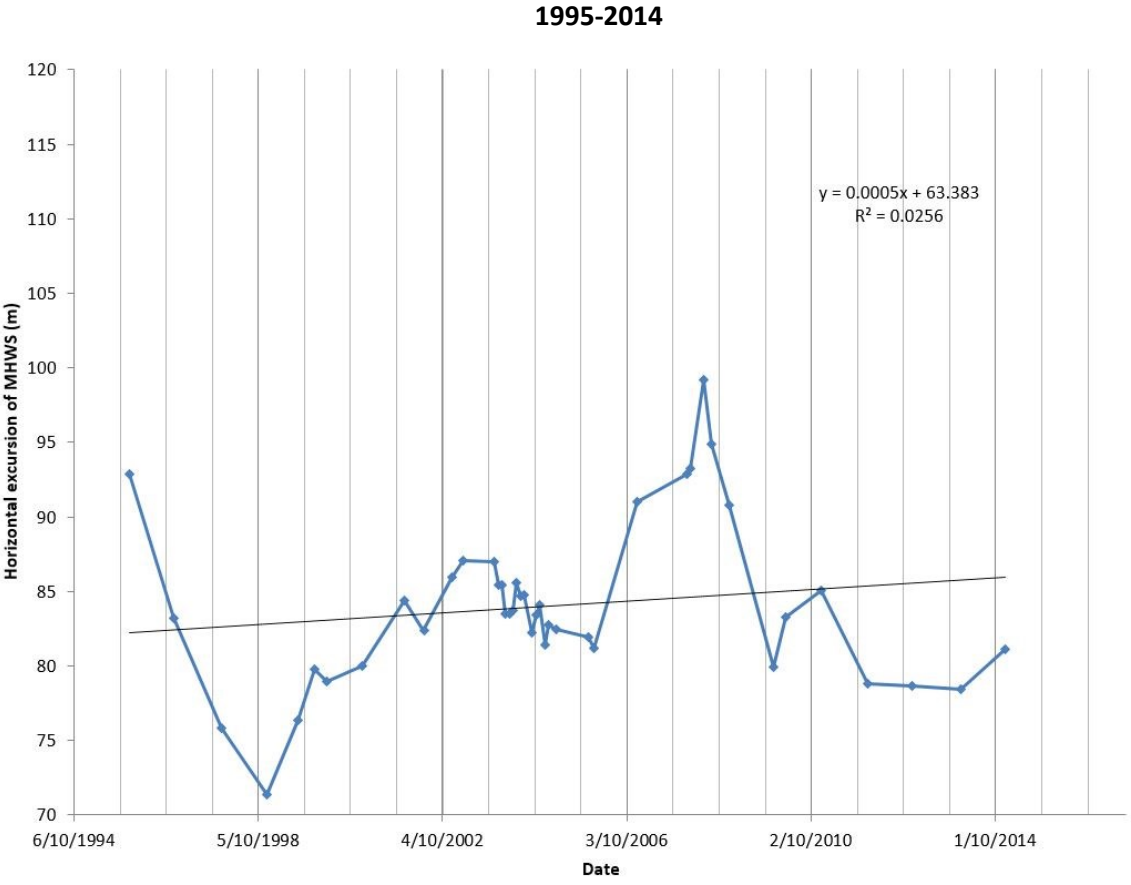

Figure C4: HB4 MHWS Excursion

1989-2015

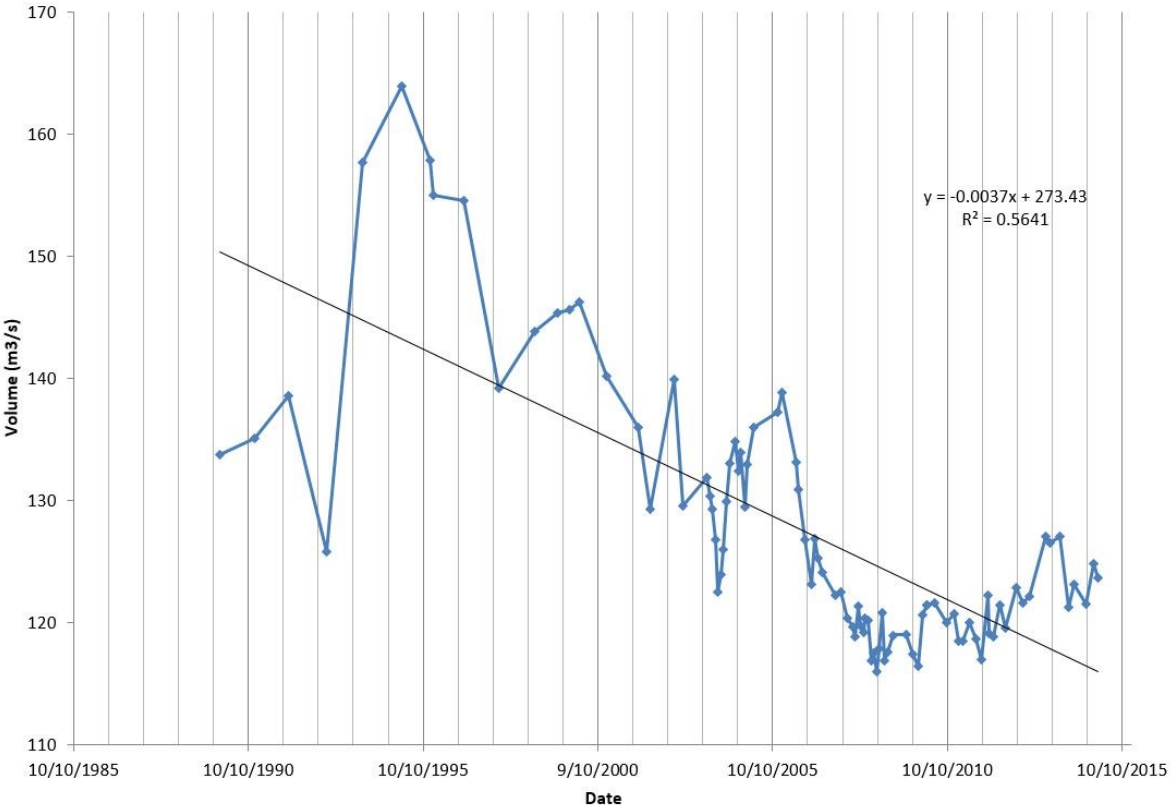

1995-2014

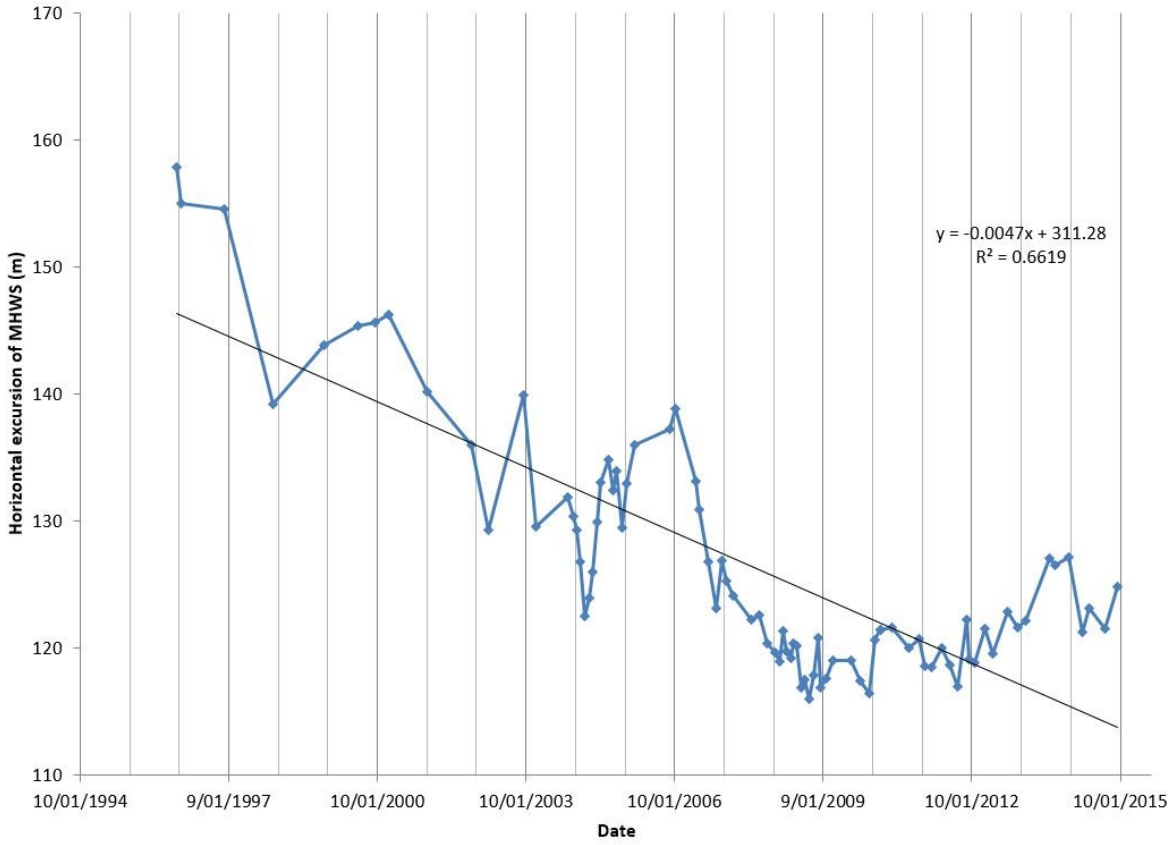

Figure C5: HB5 MHWS Excursion

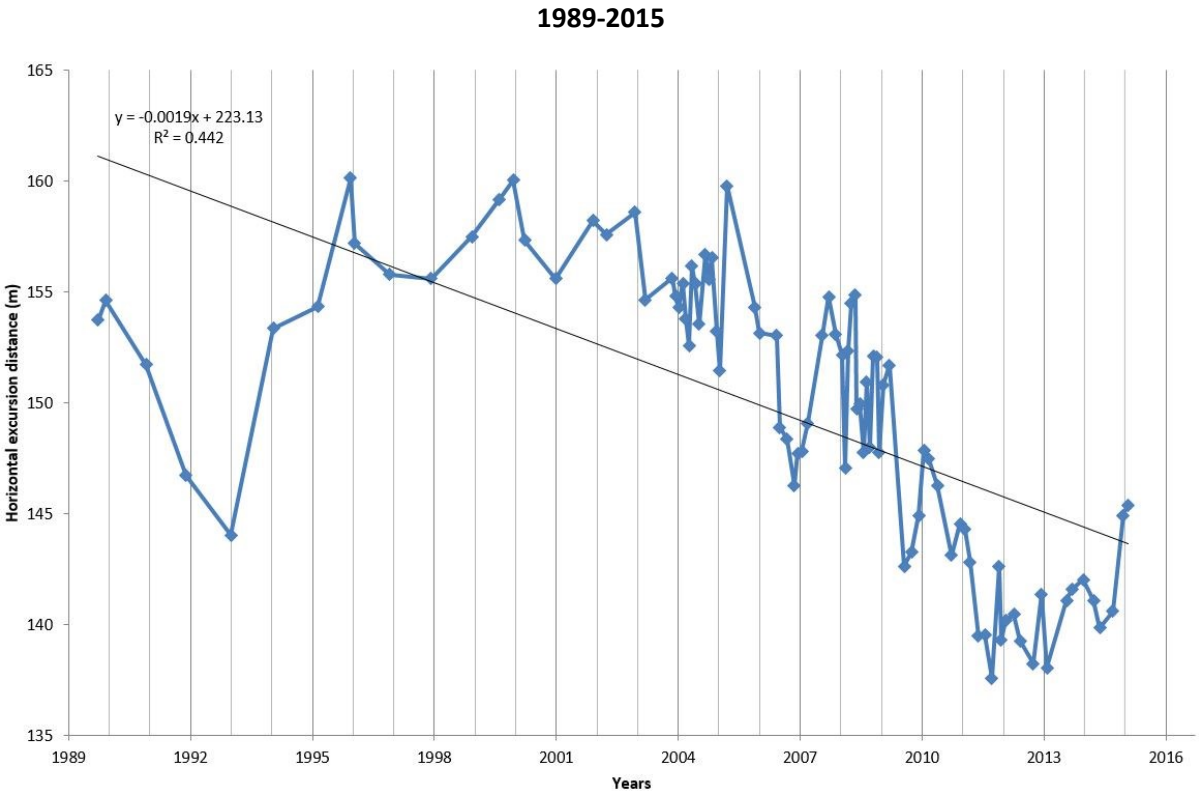

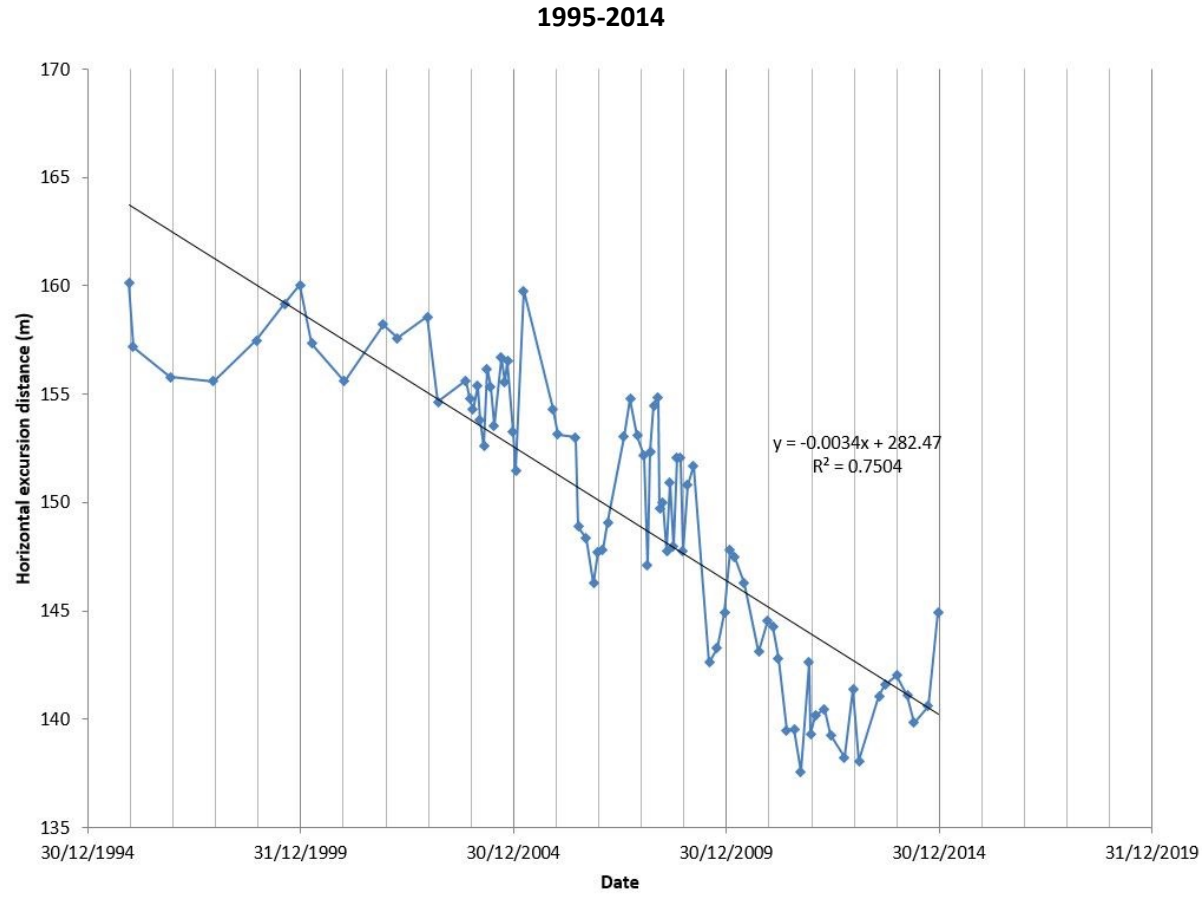

Figure C6: HB6 MHWS Excursion

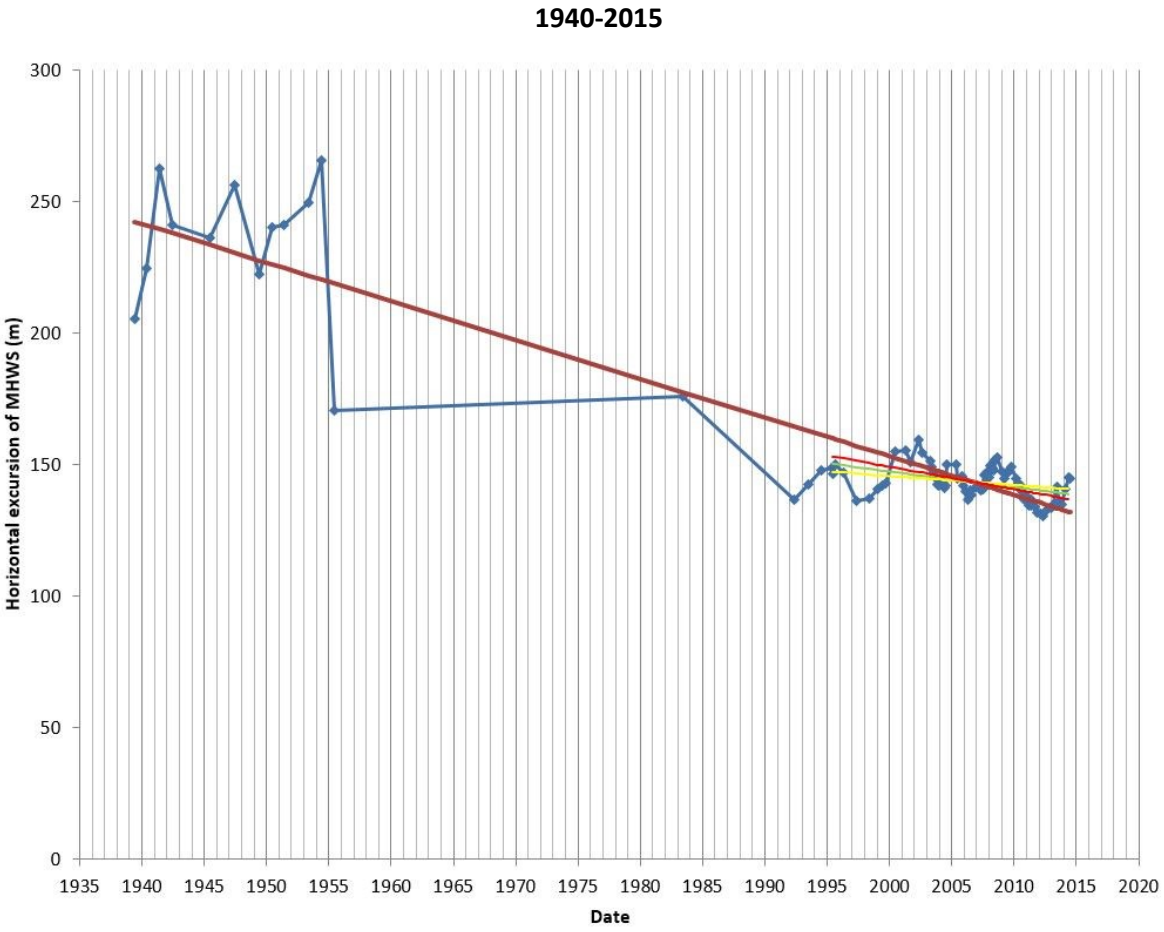

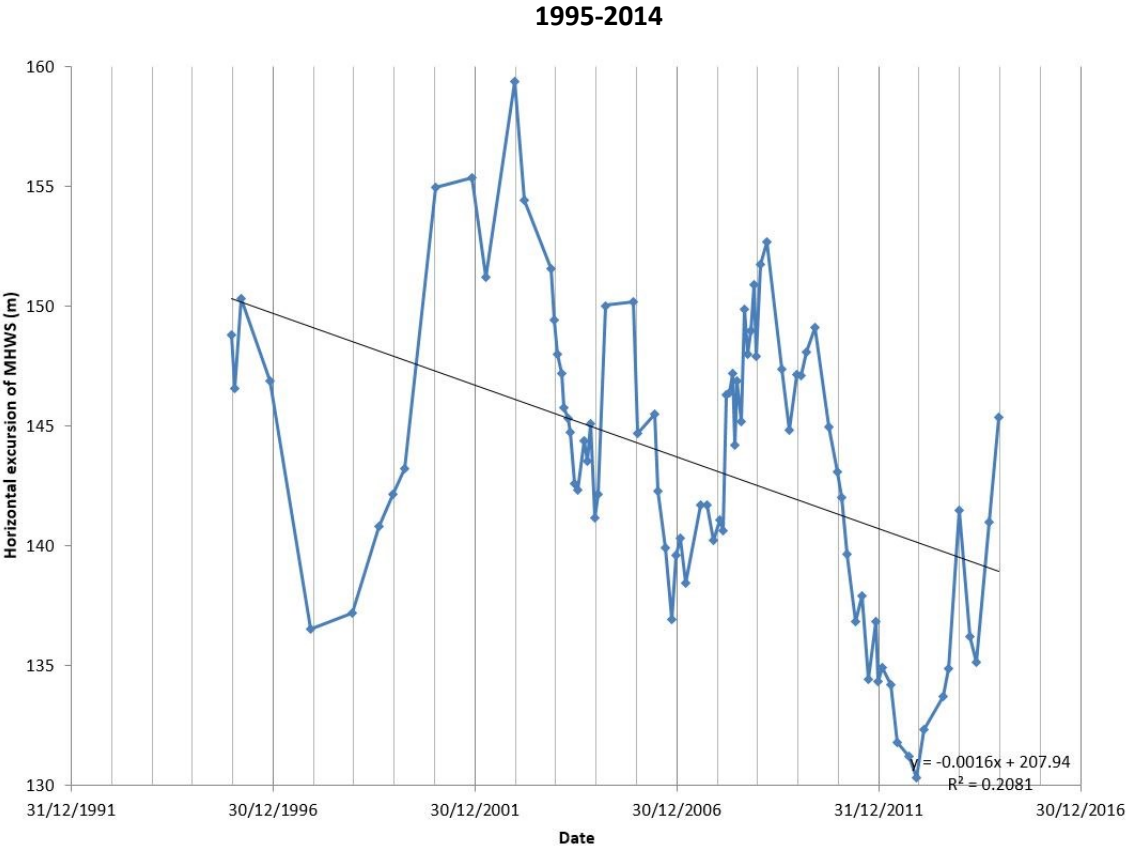

Figure C7: HB7 MHWS Excursion

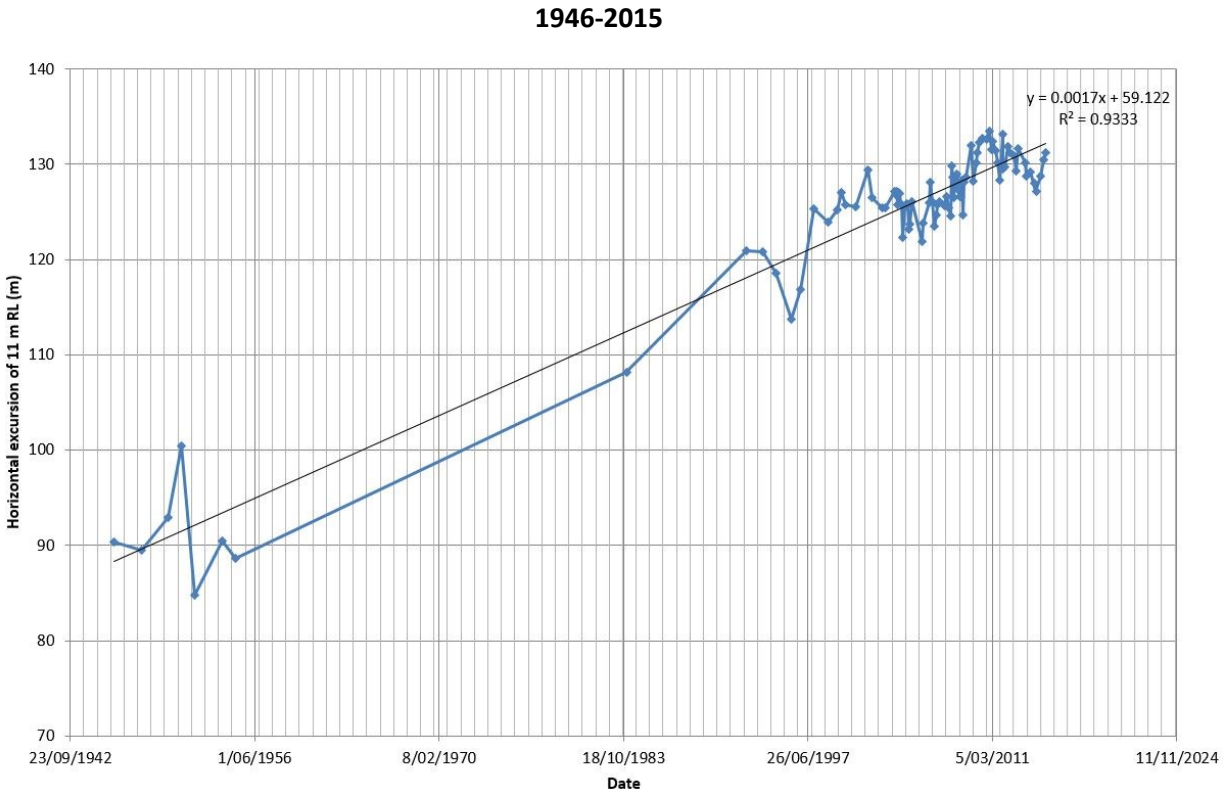

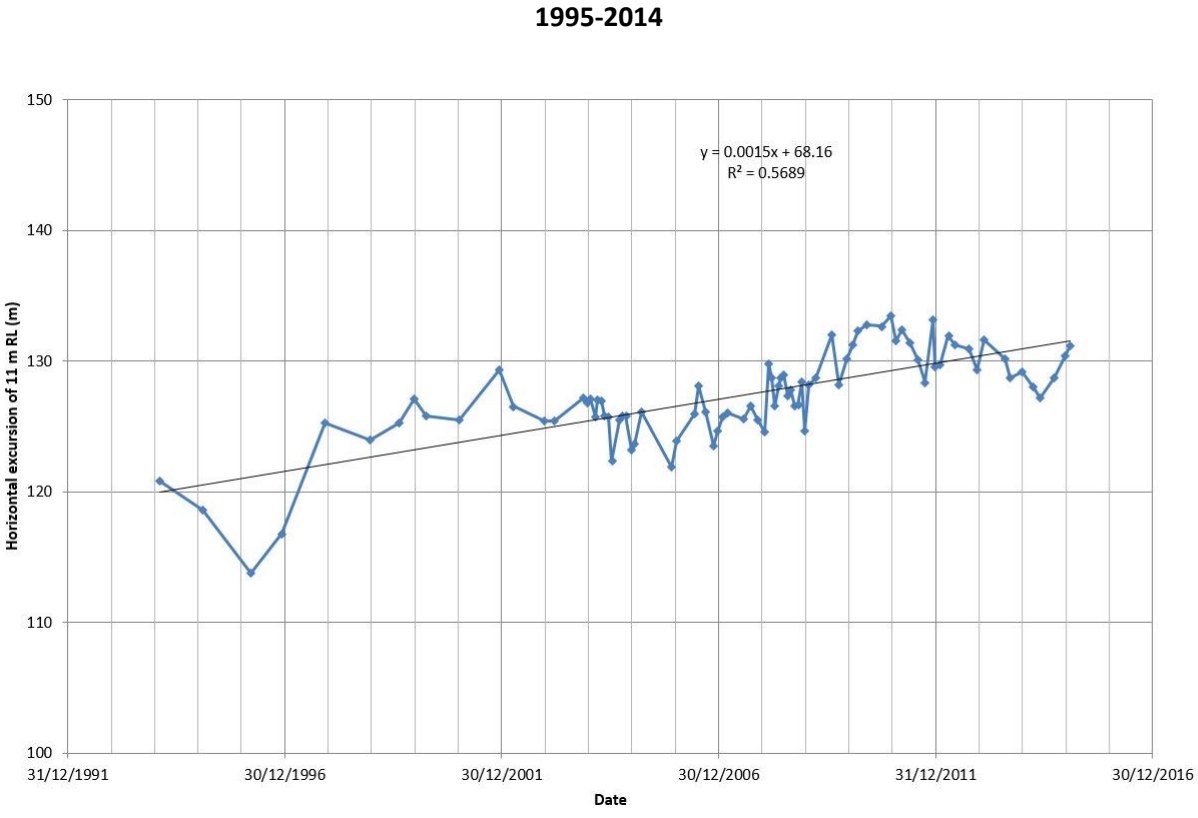

Figure C8: HB8 MHWS Excursion

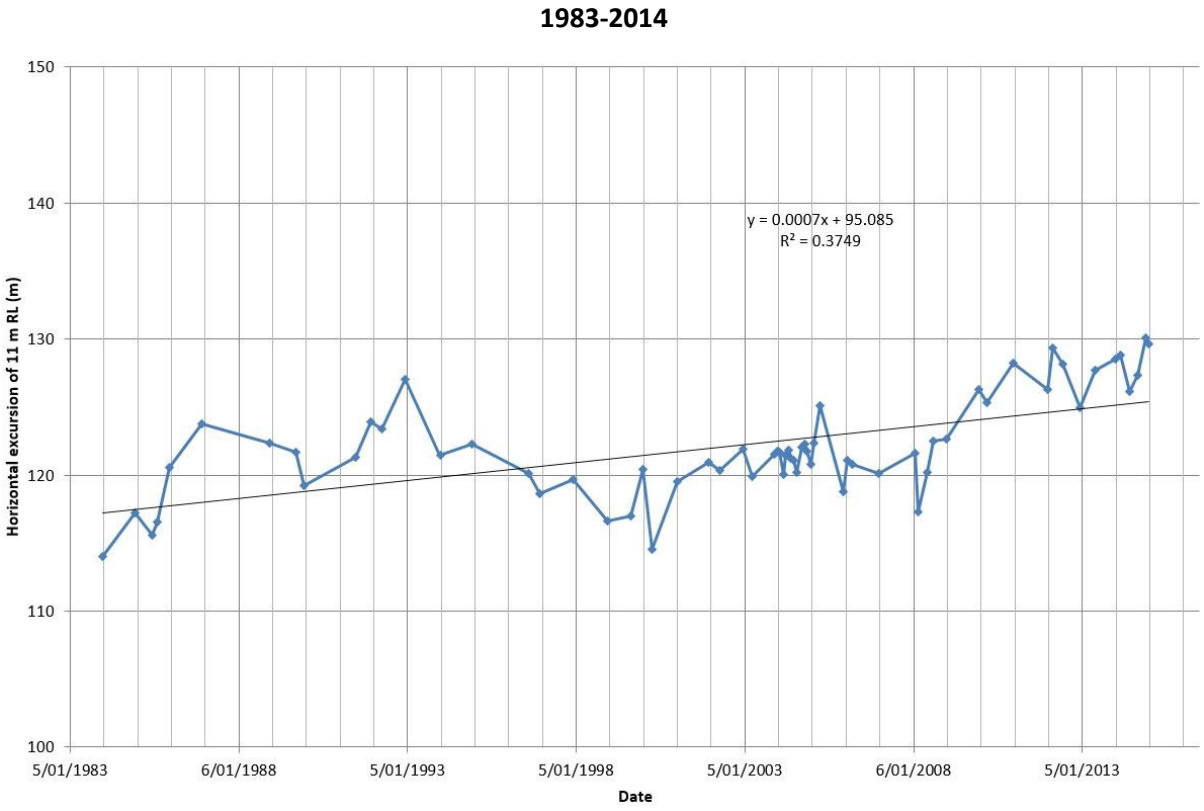

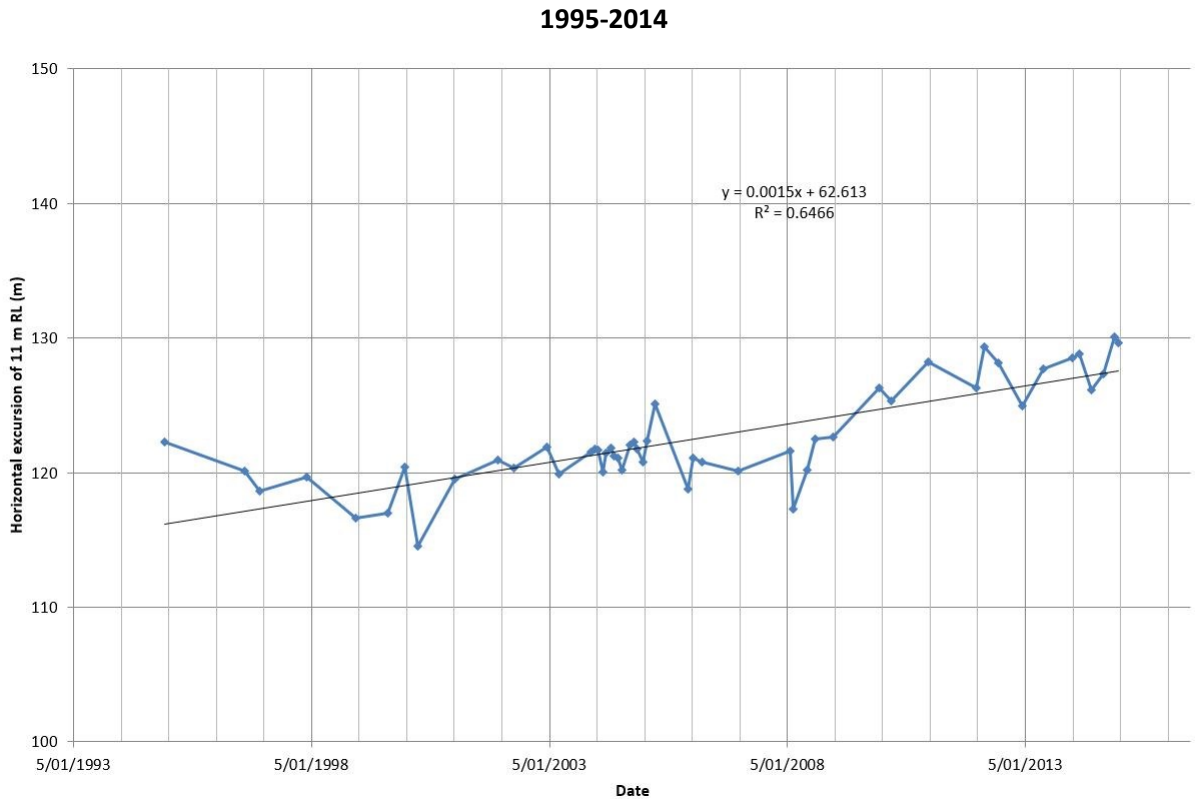

Figure C9: HB9 MHWS Excursion

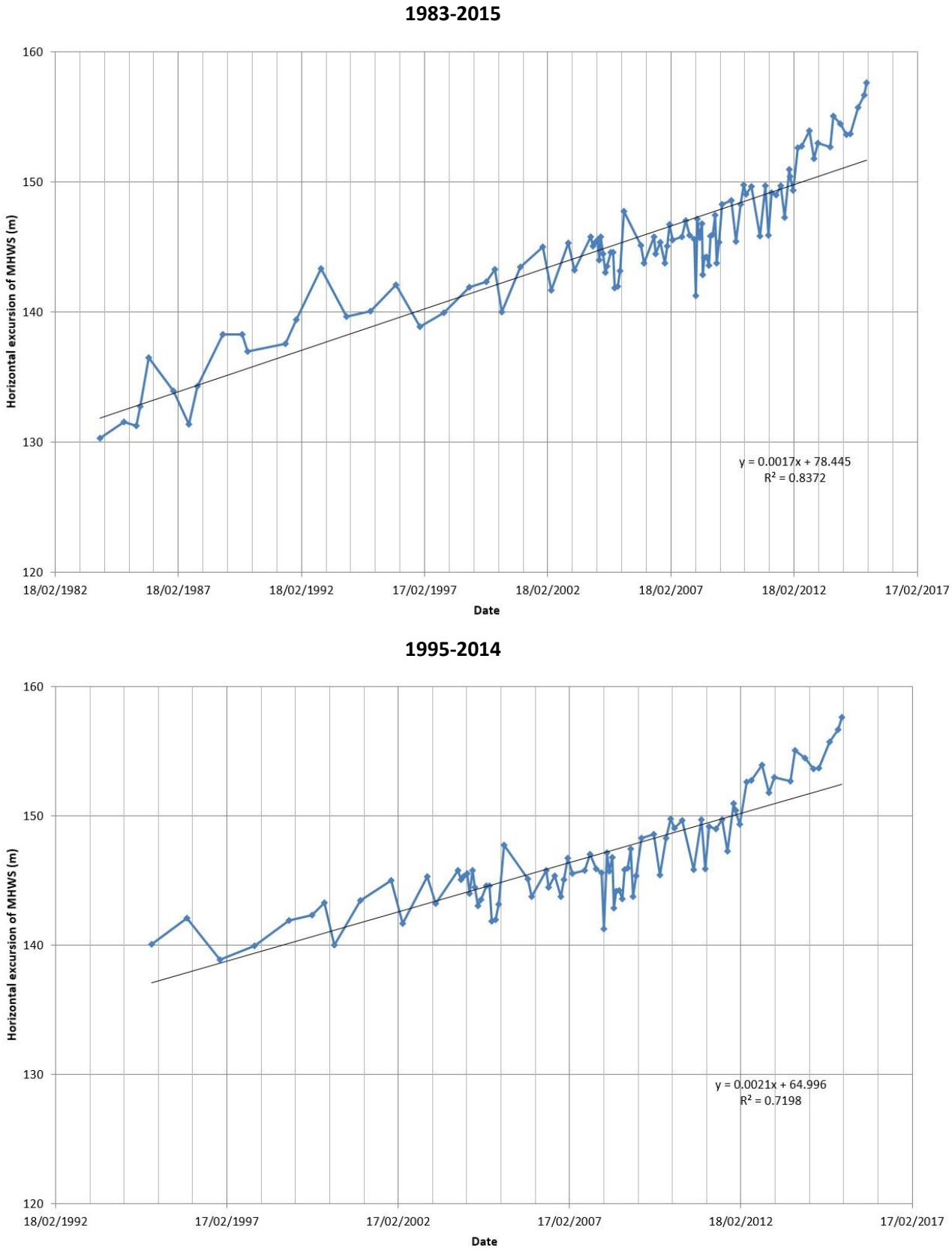

Figure C10: HB10 MHWS Excursion

1930-2014

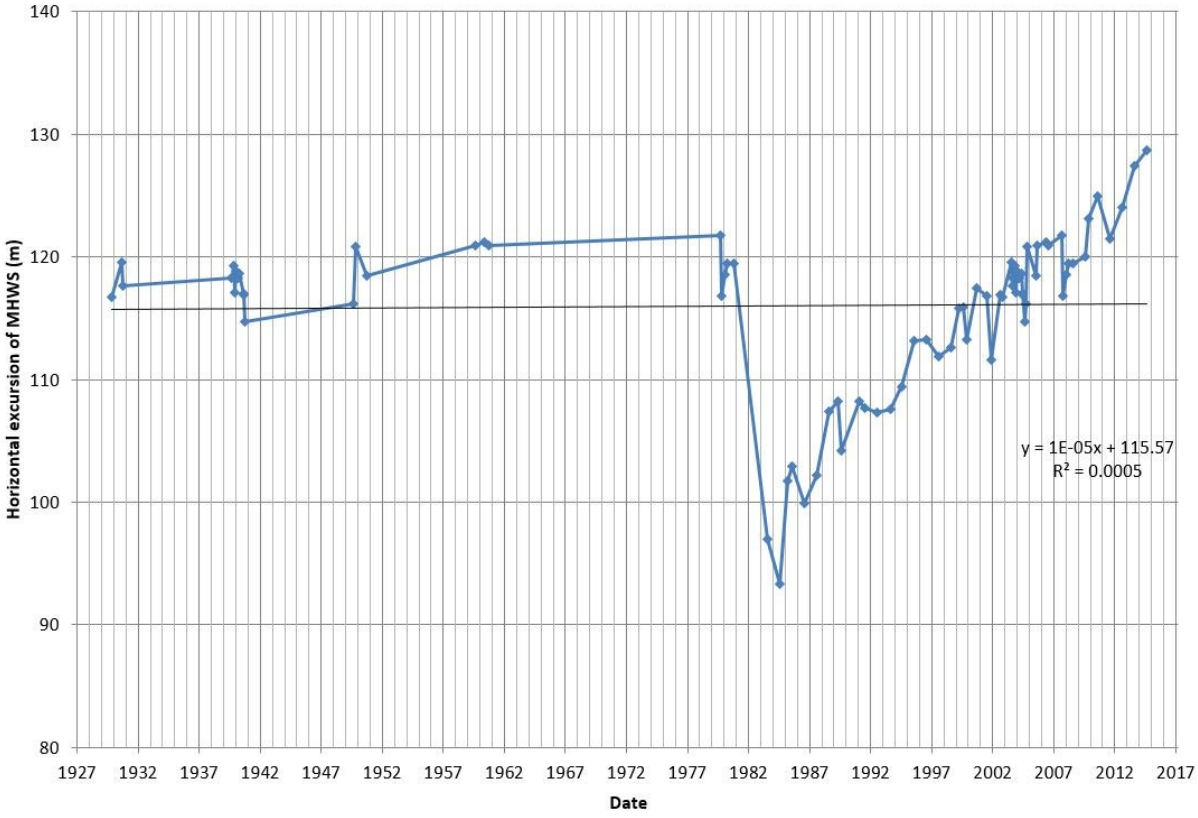

1995-2014

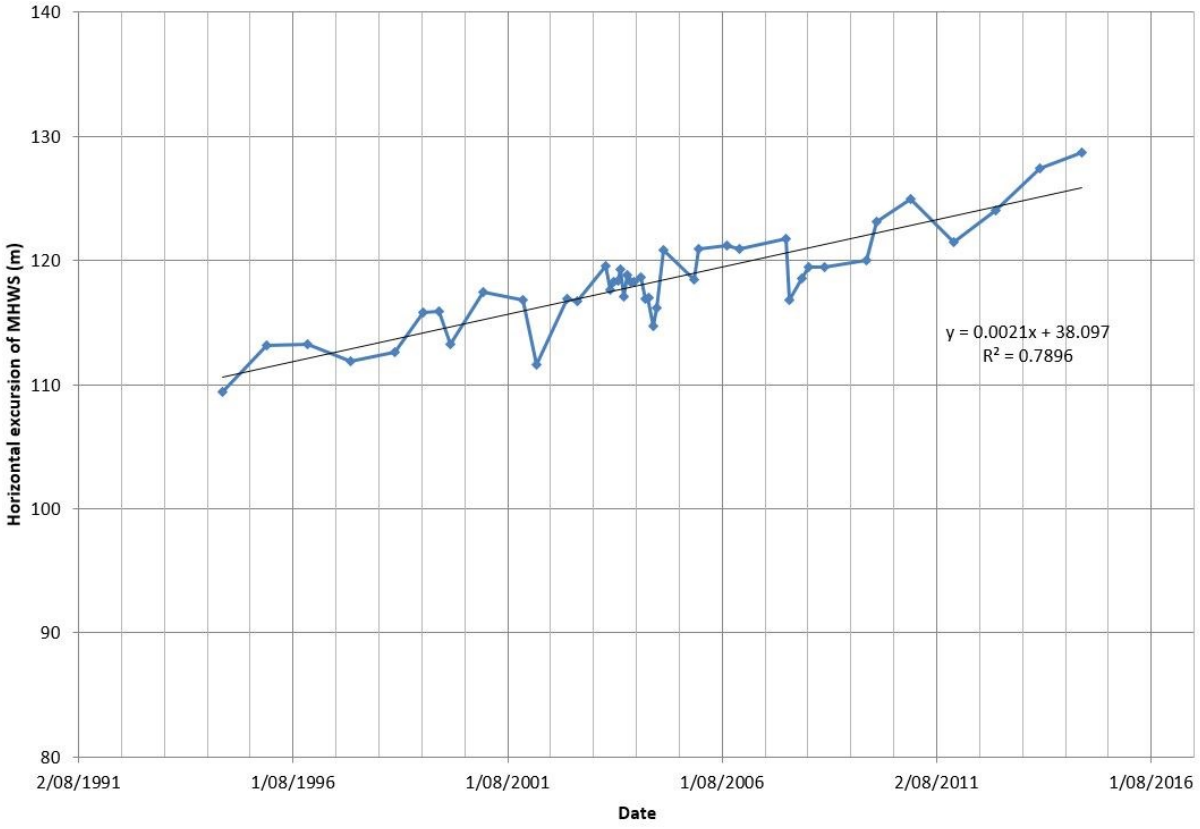

Figure C11: HB11 MHWS Excursion

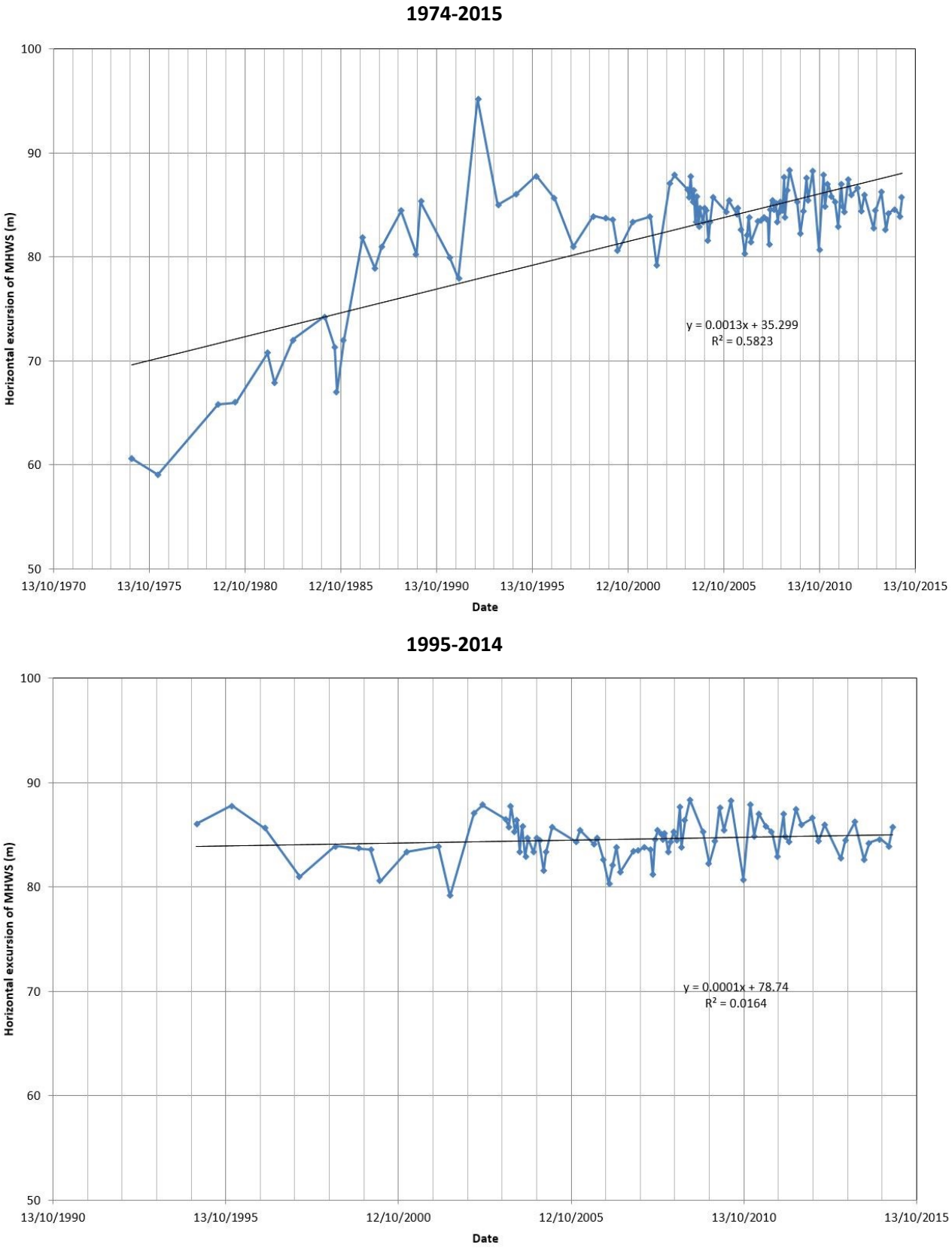

Figure C12: HB12 MHWS Excursion

1974-2014

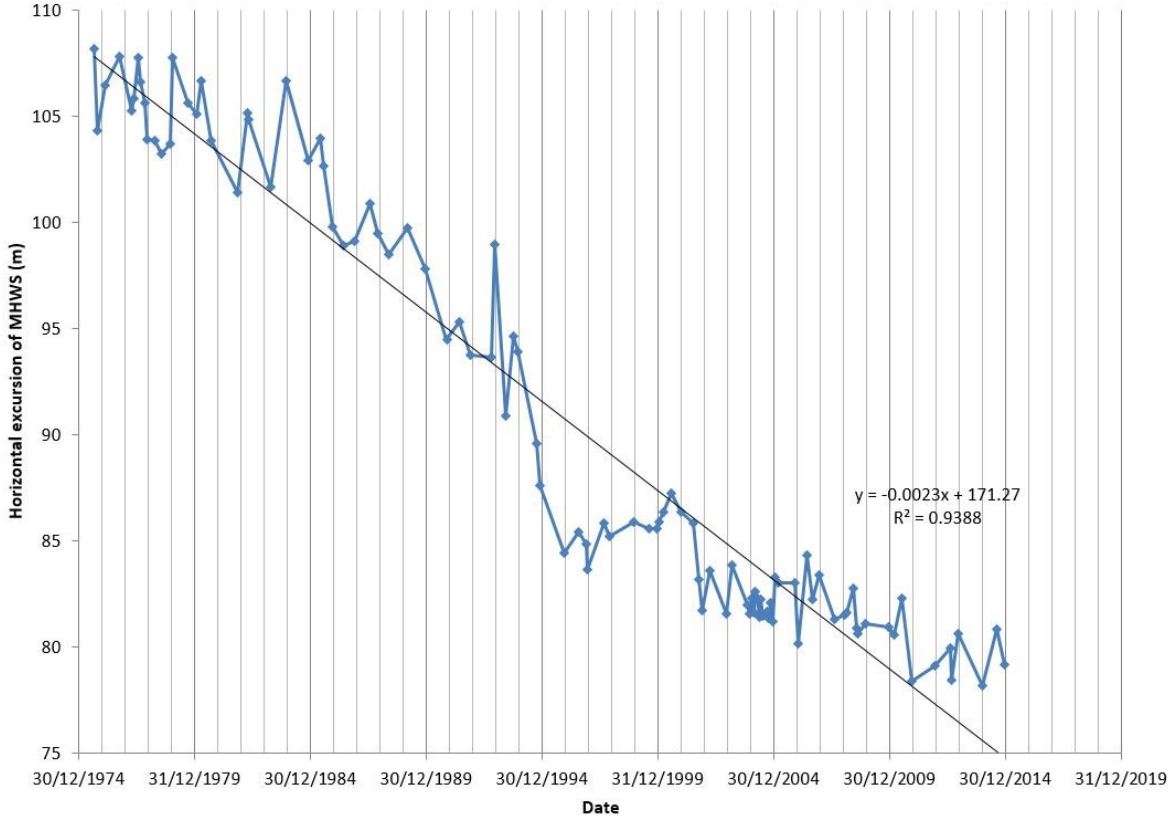

1995-2014

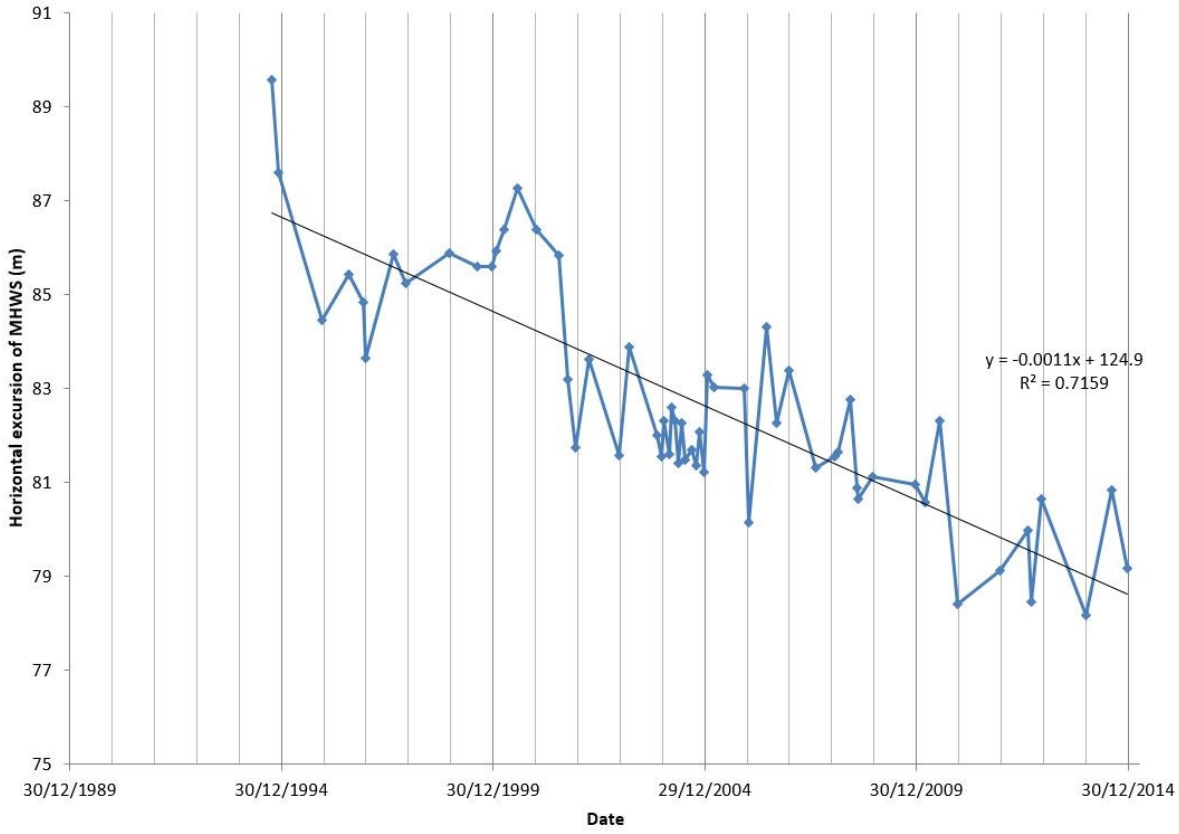

Figure C13: HB13 MHWS Excursion

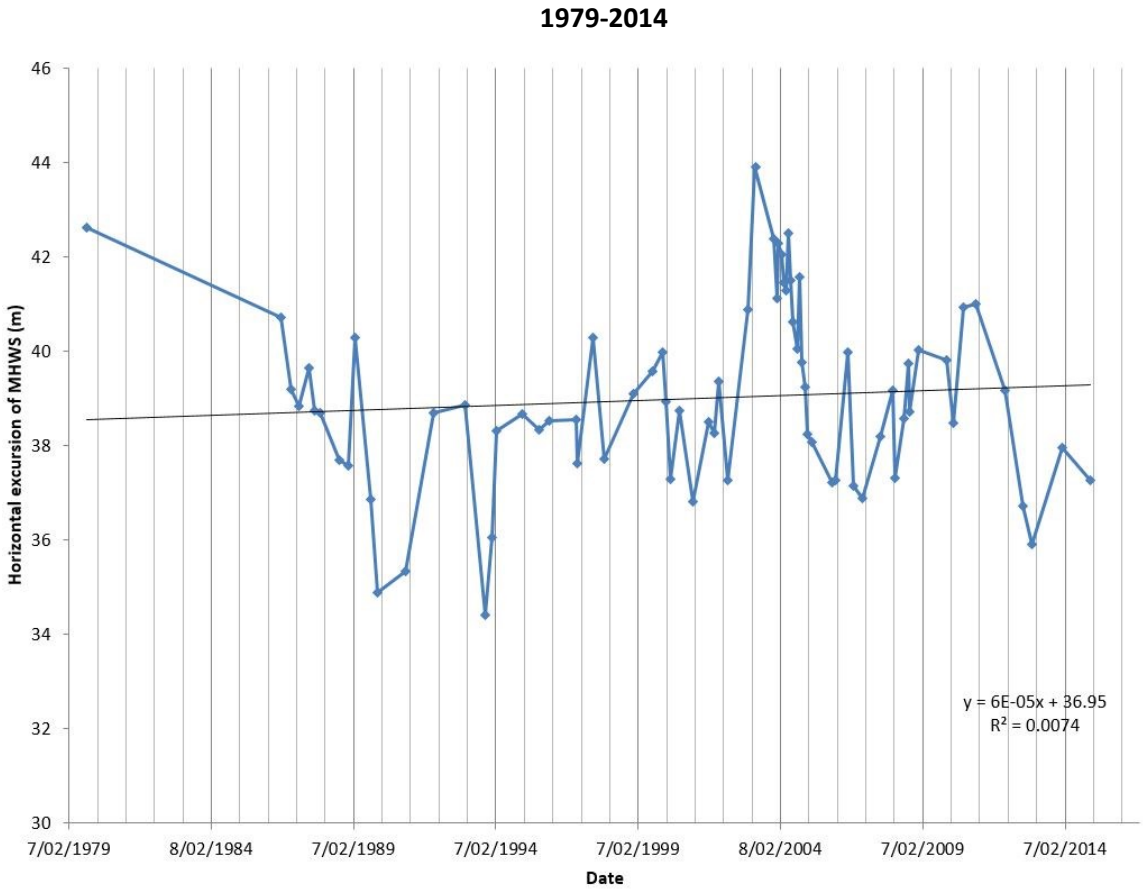

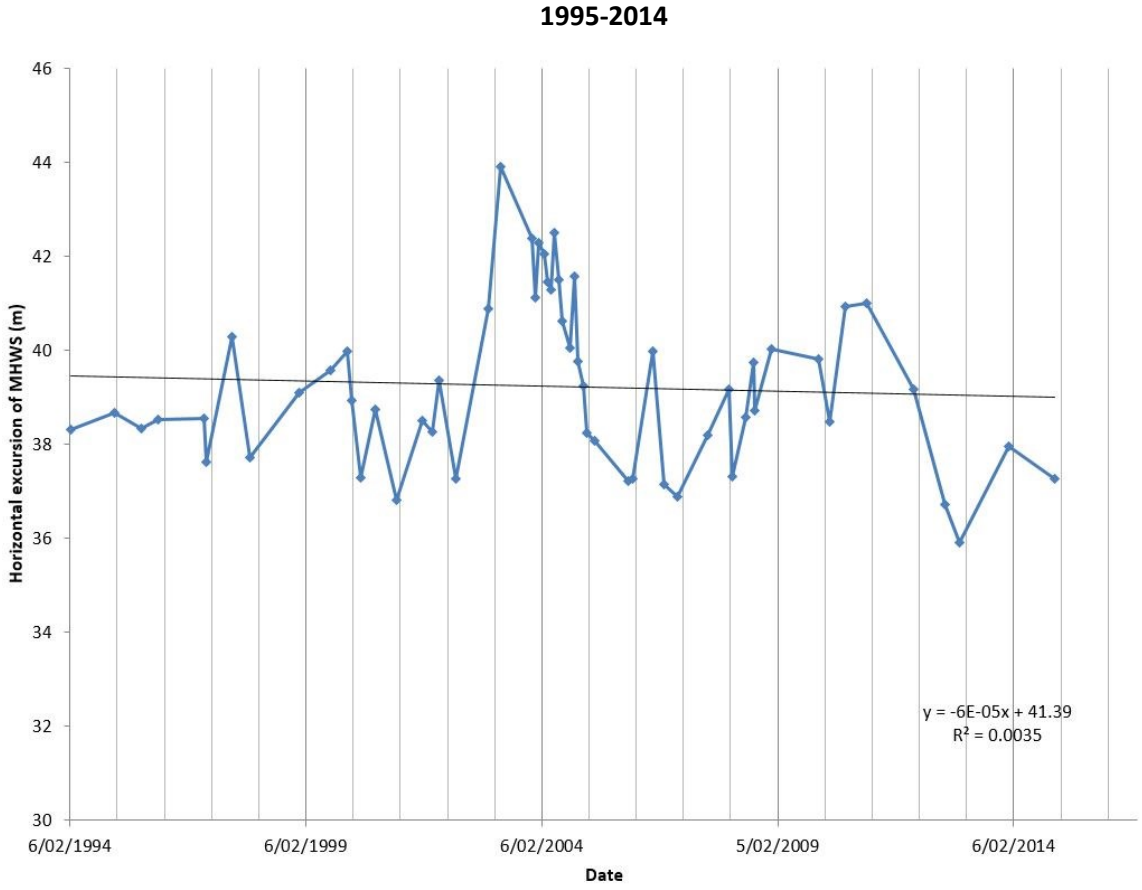

Figure C14: HB14 MHWS Excursion

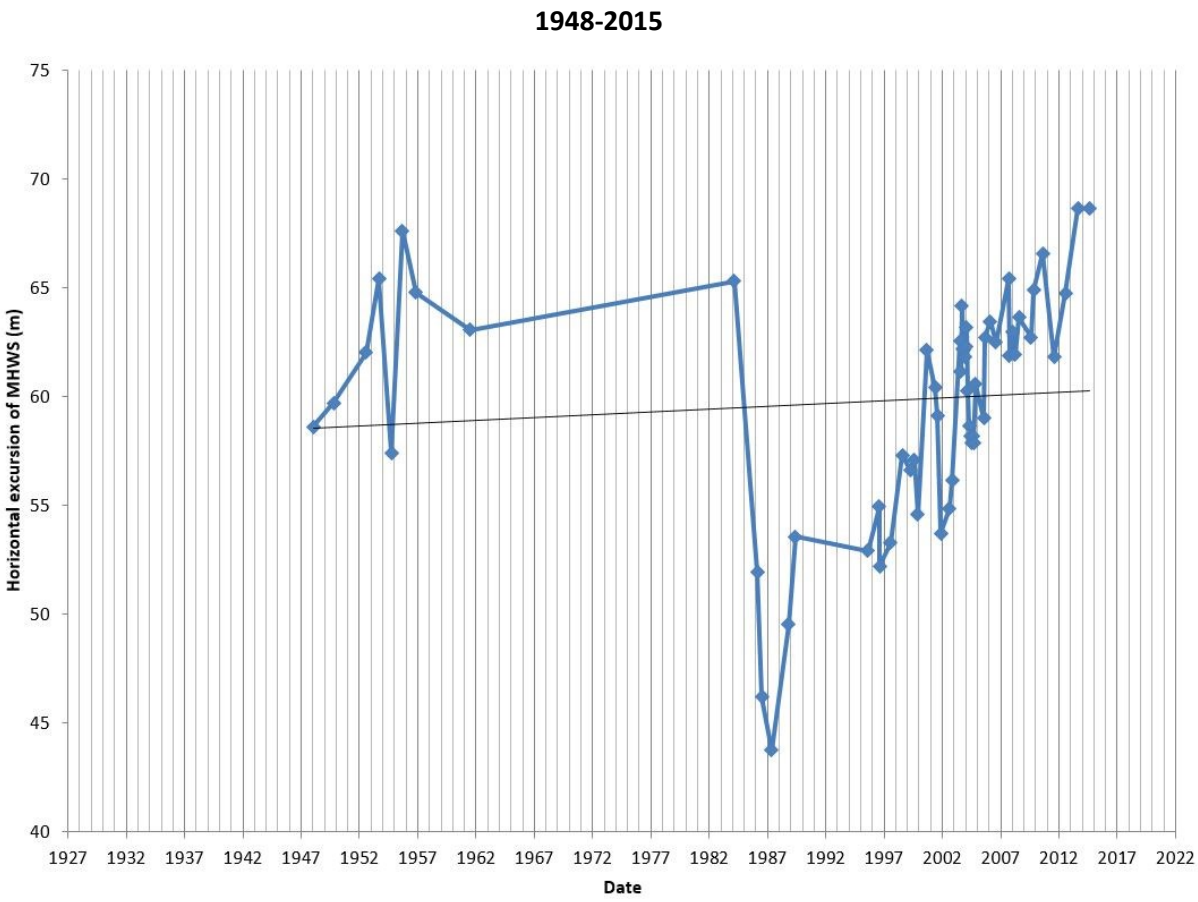

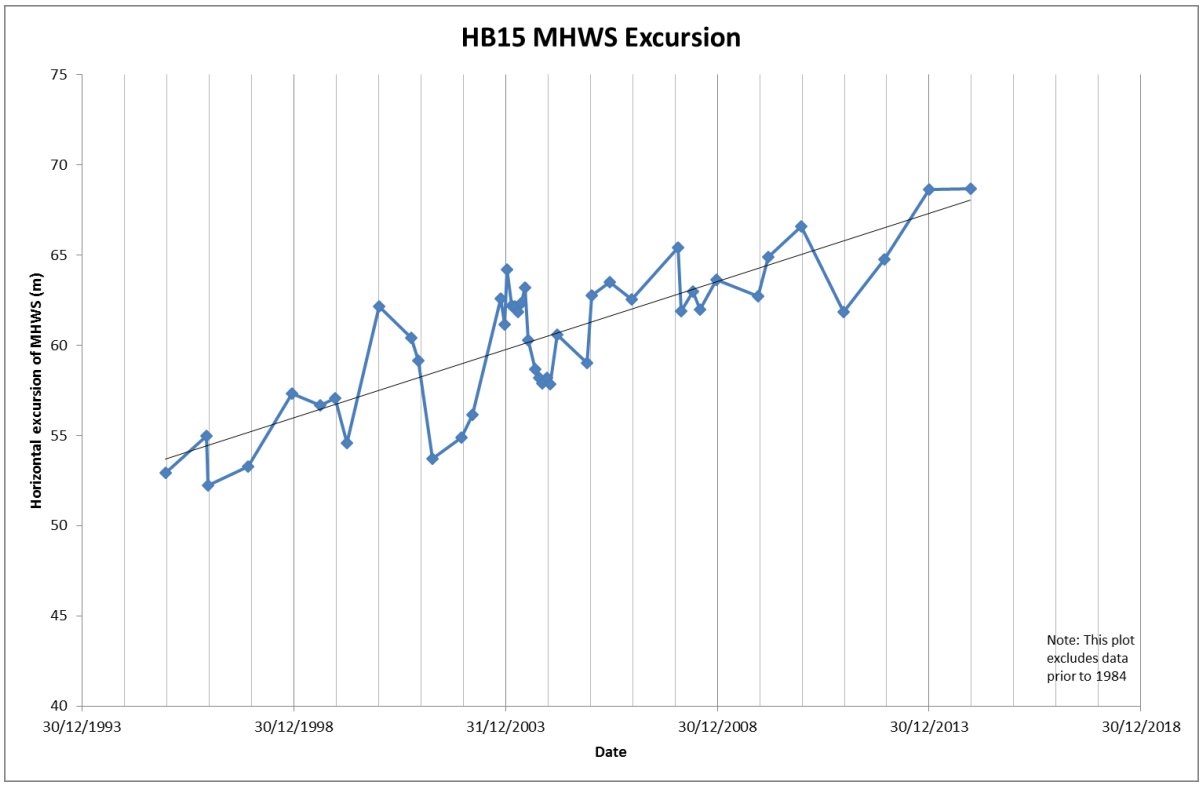

Figure C15: HB15 MHWS Excursion

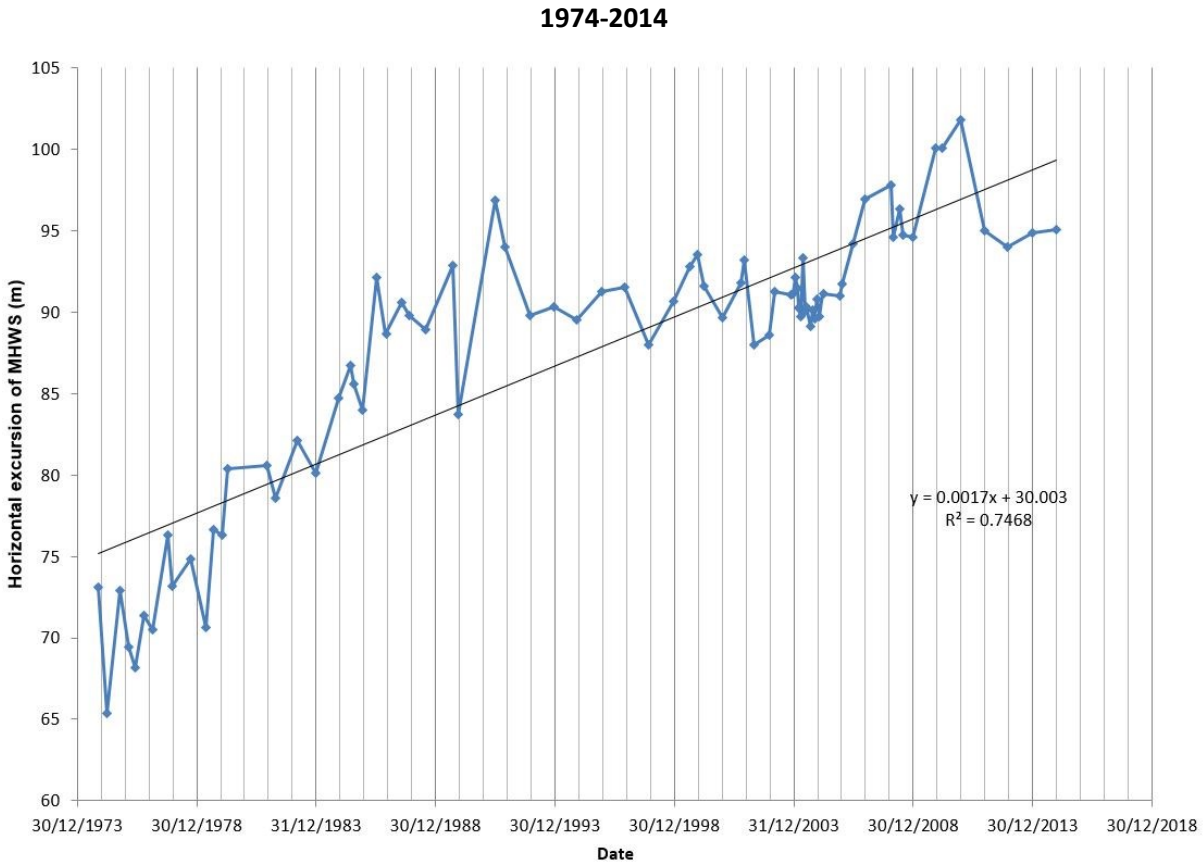

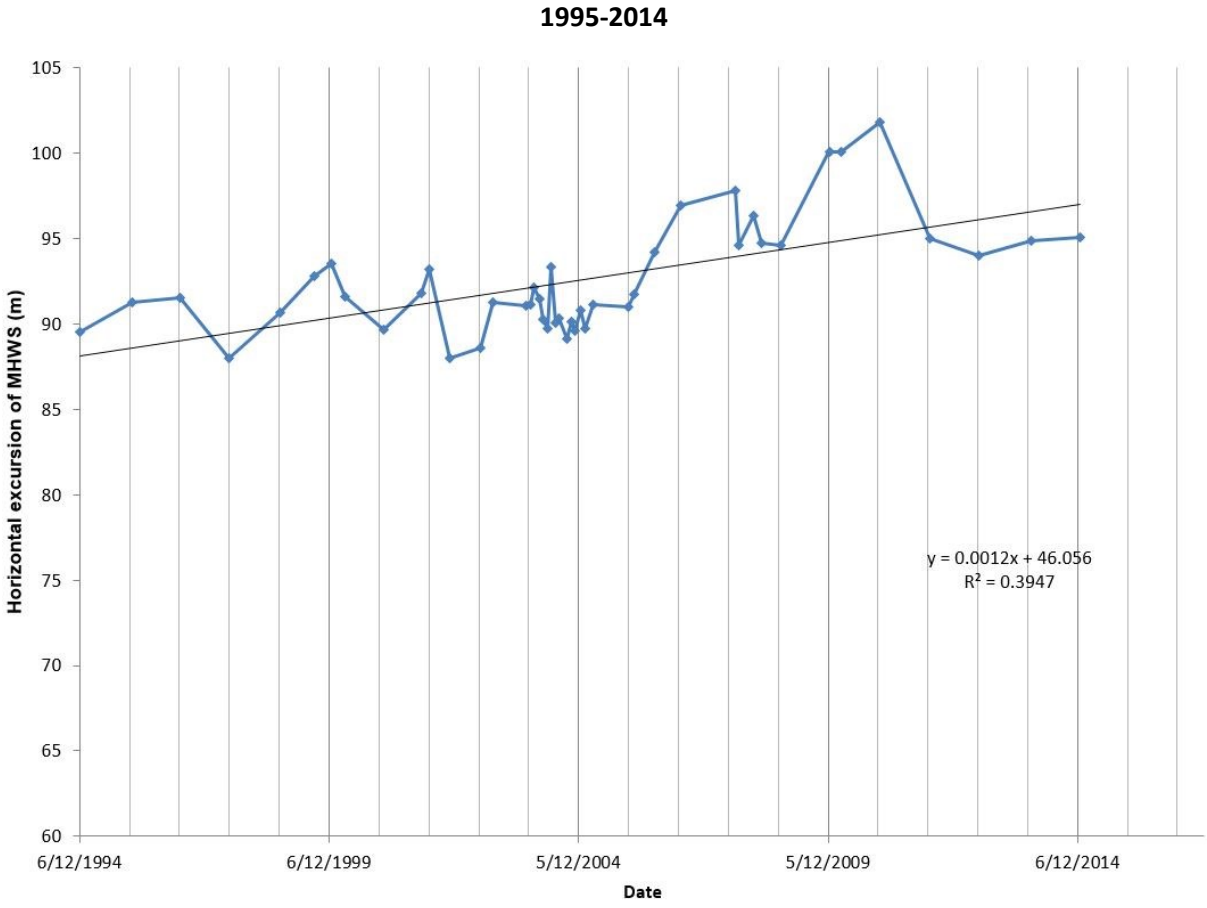

Figure C16: HB16 MHWS Excursion

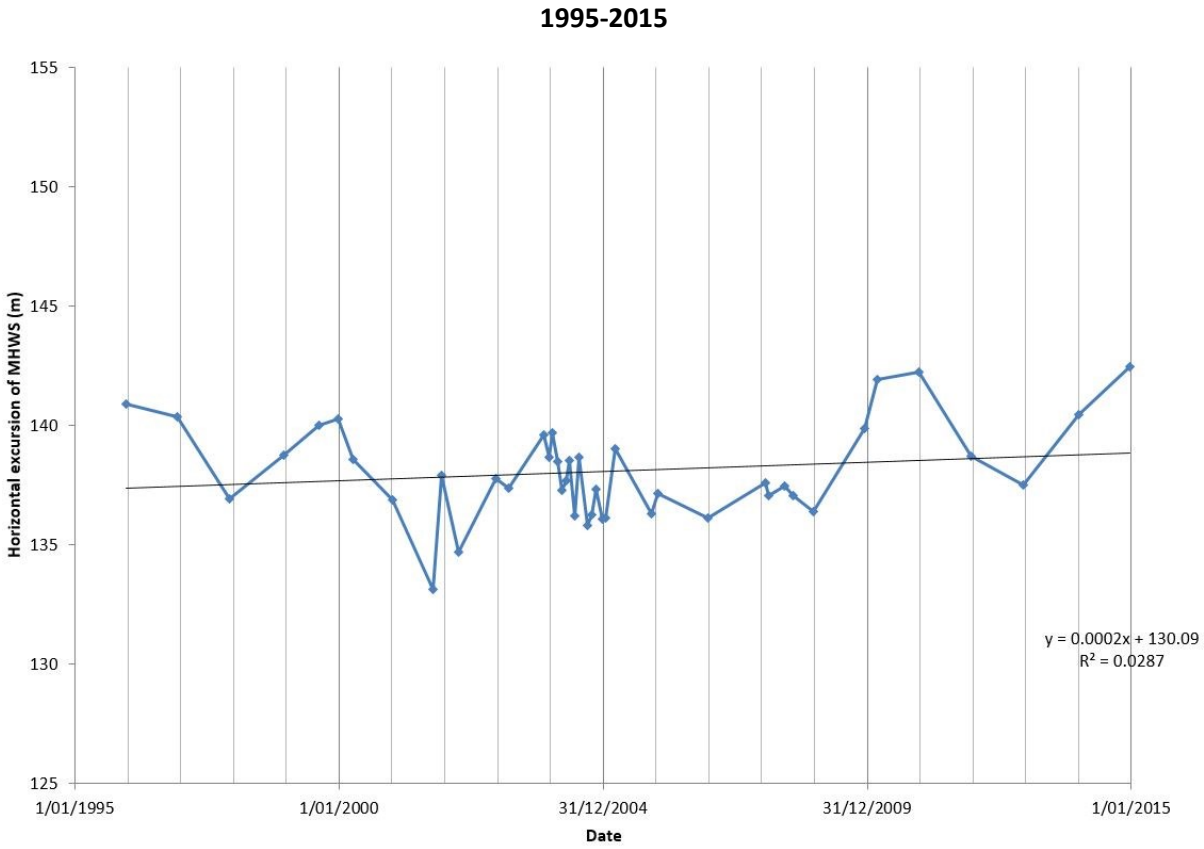

Figure C17: HB17 MHWS Excursion

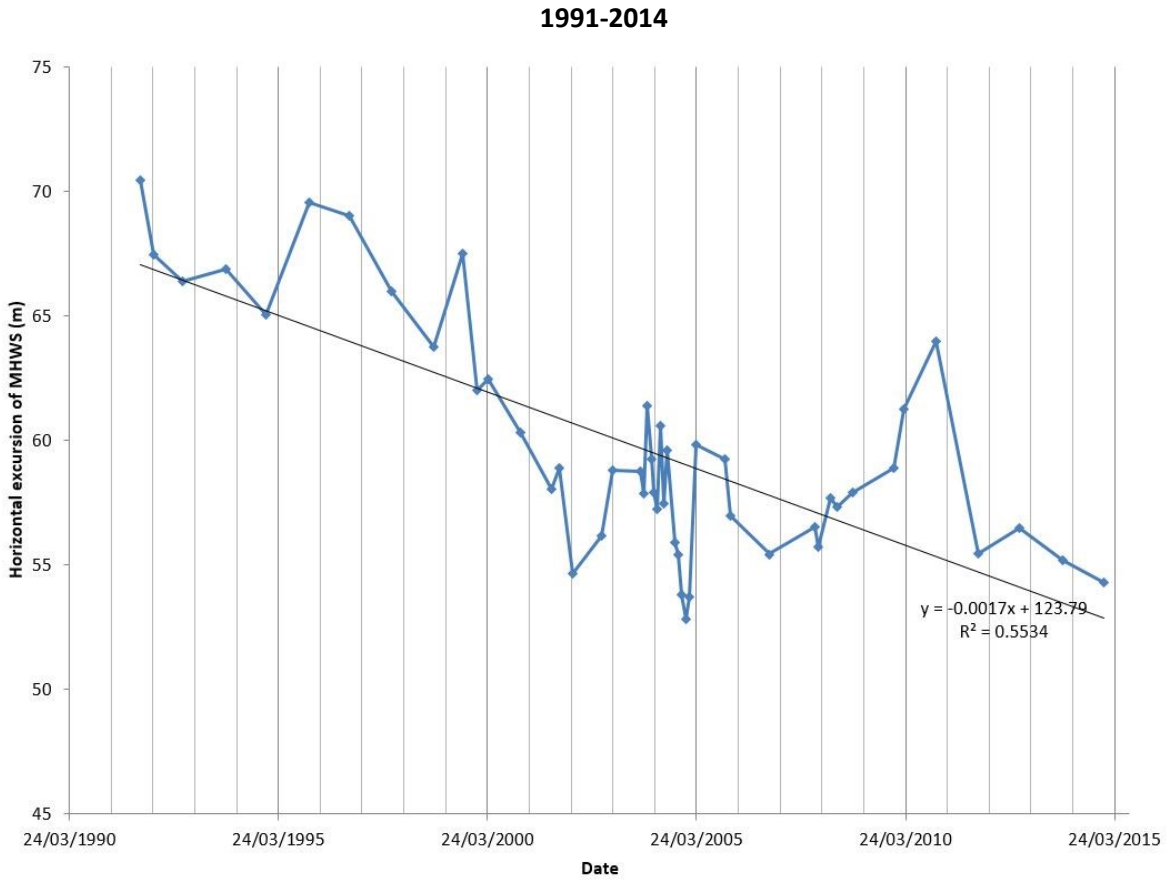

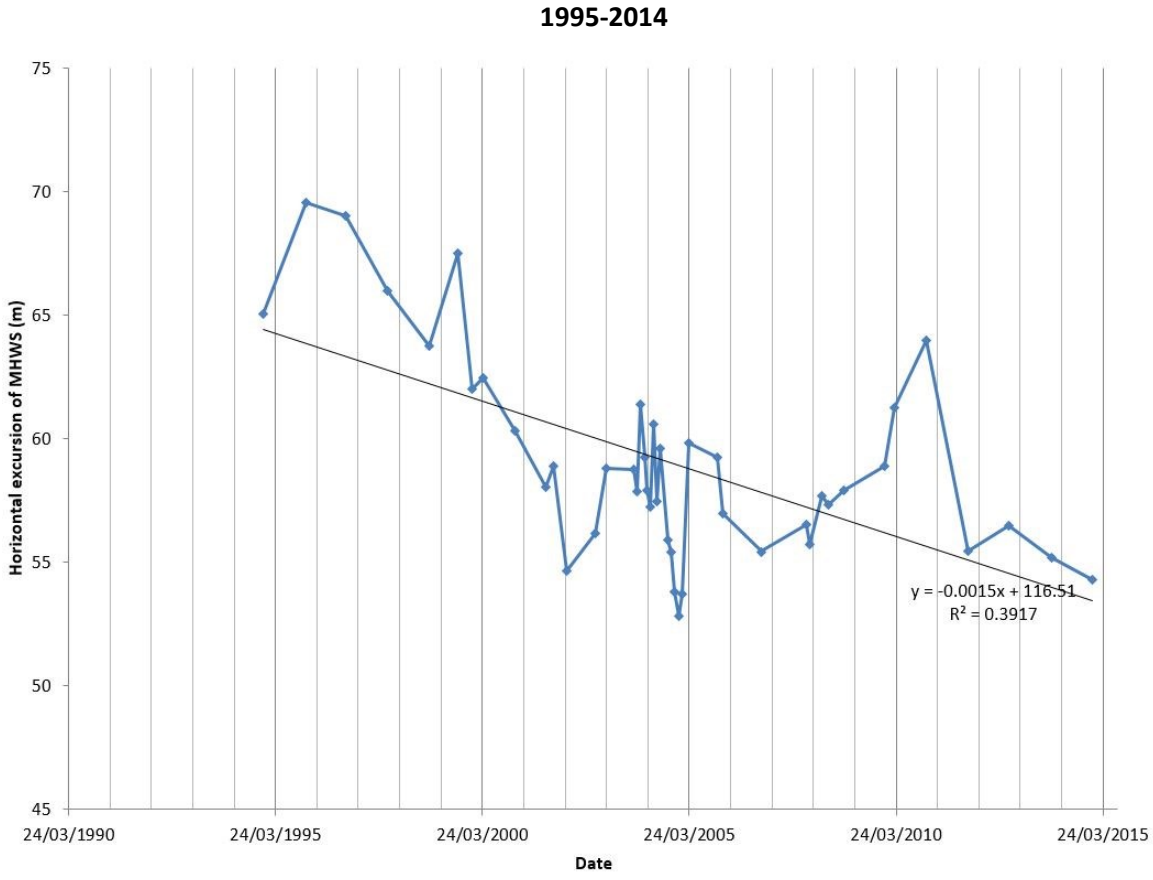

Figure C18: HB18 MHWS Excursion

1991-2014

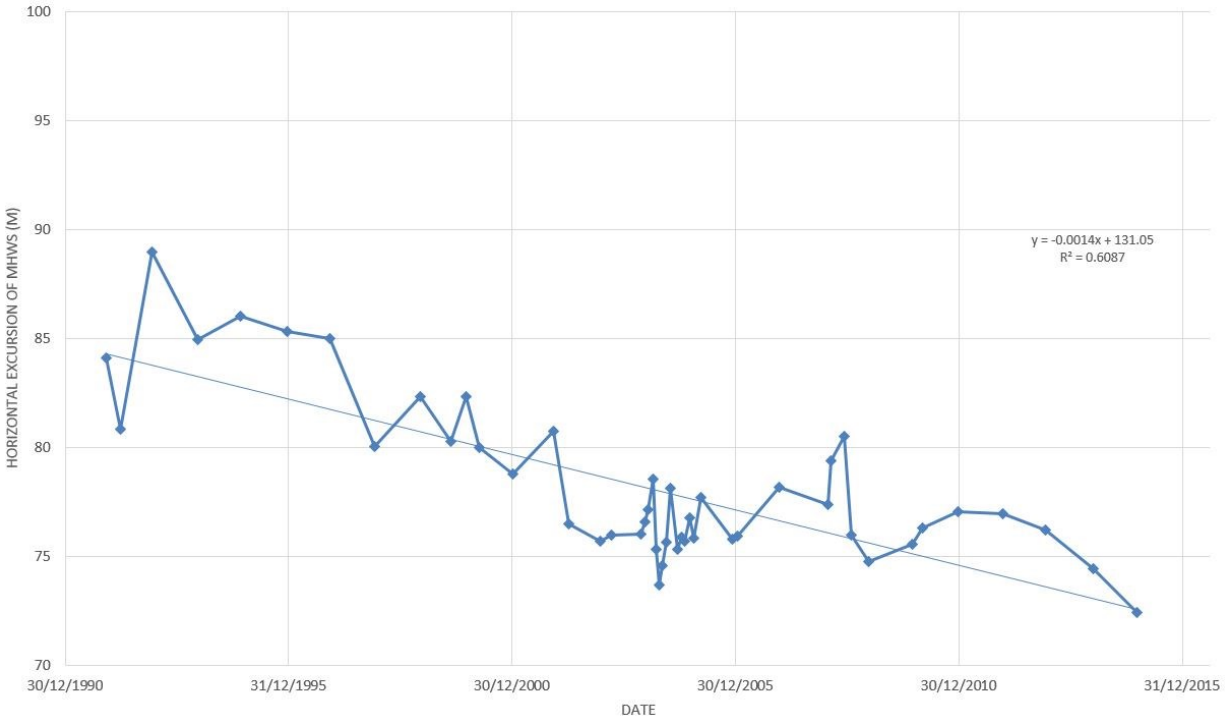

1995-2014

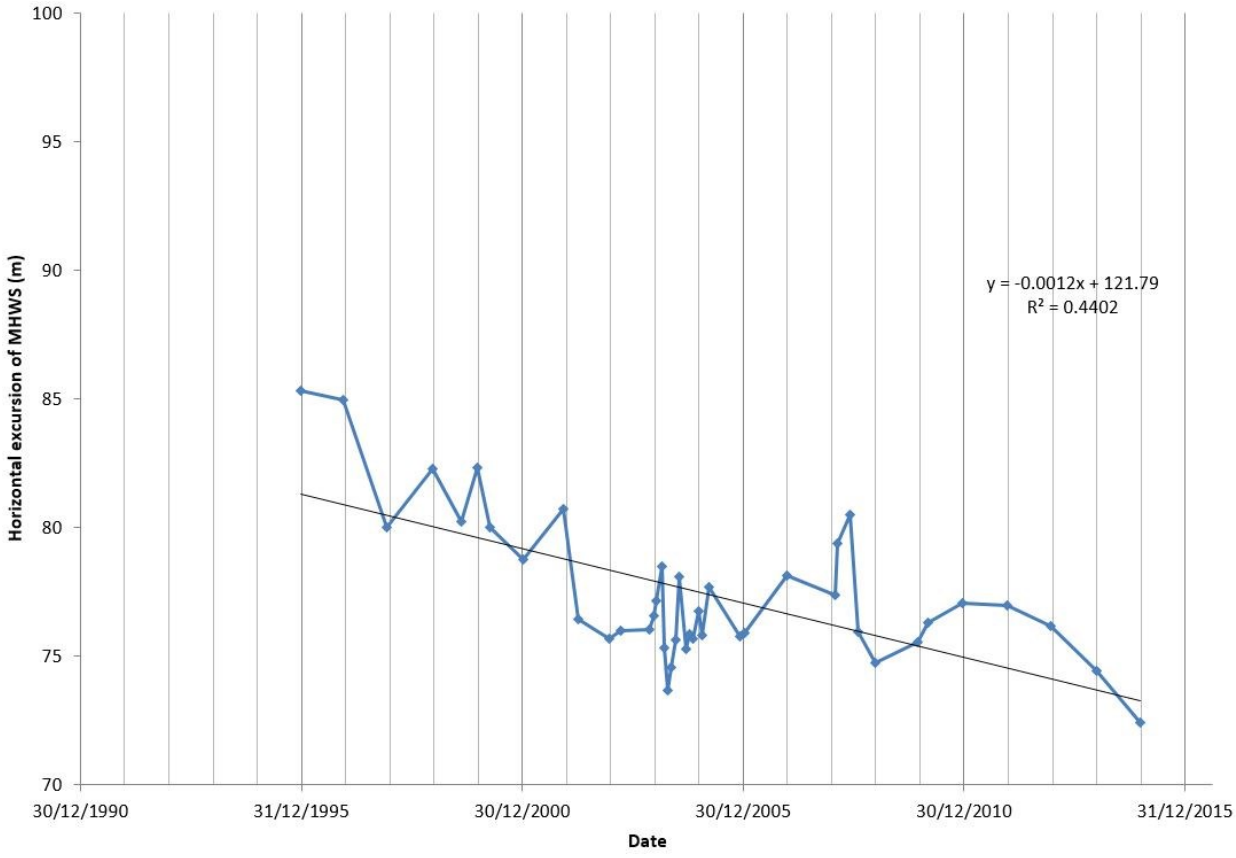

Figure C19: HB19 MHWS Excursion

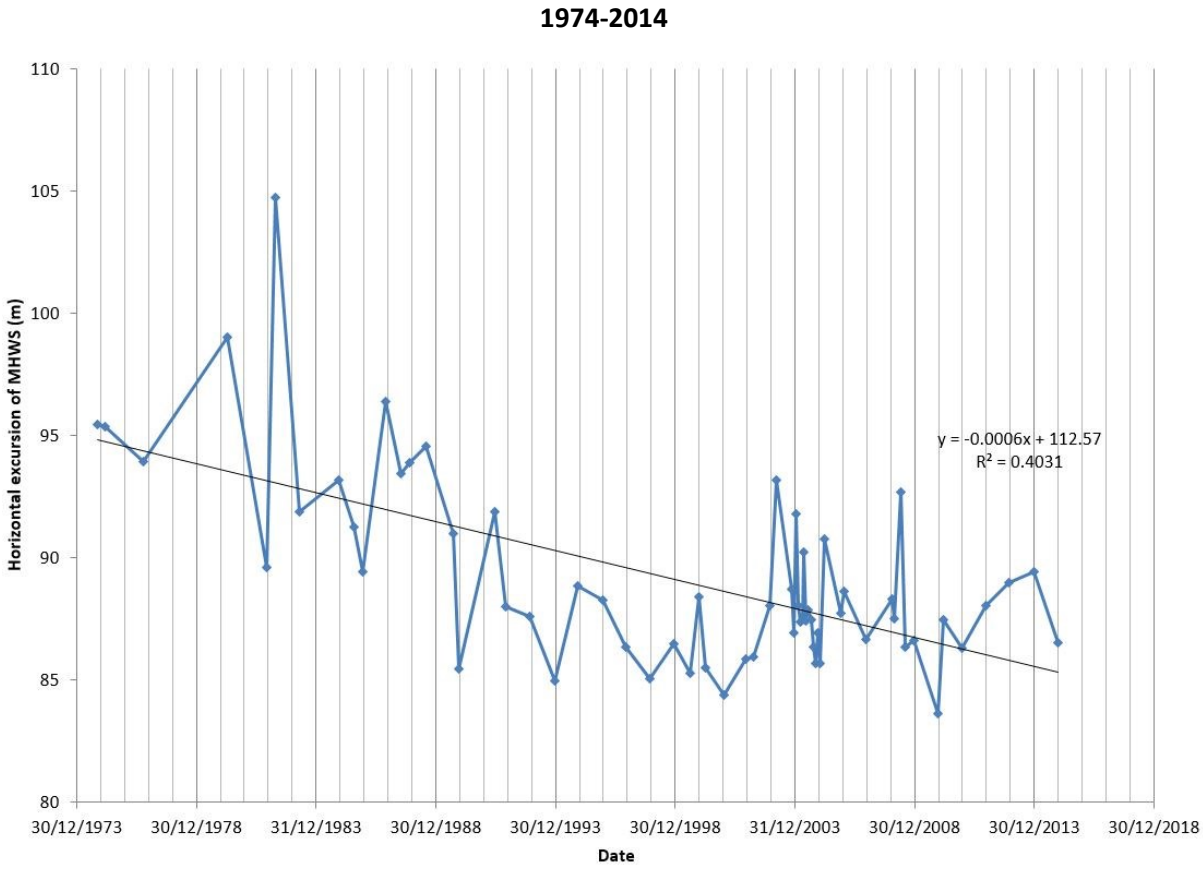

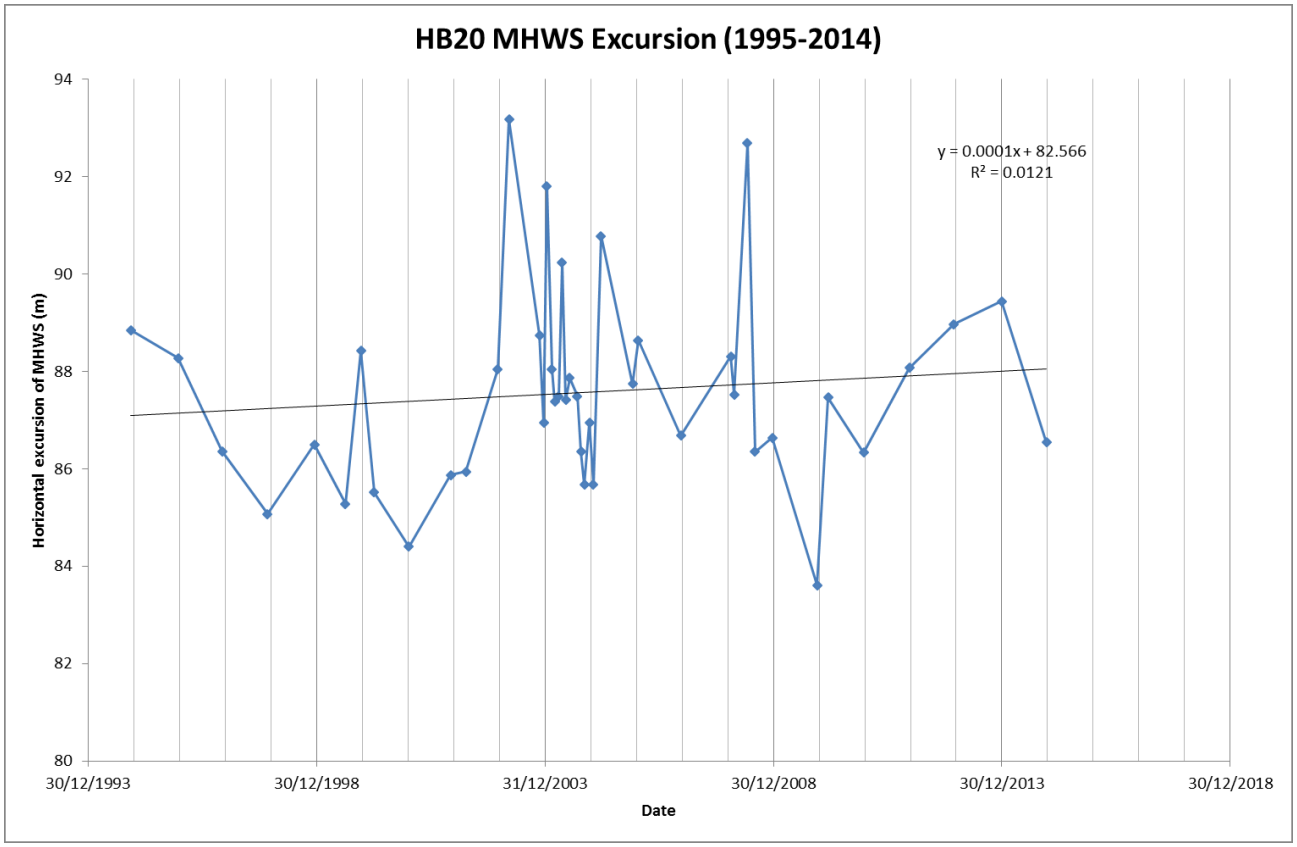

Figure C20: HB20 MHWS Excursion

1991-2015

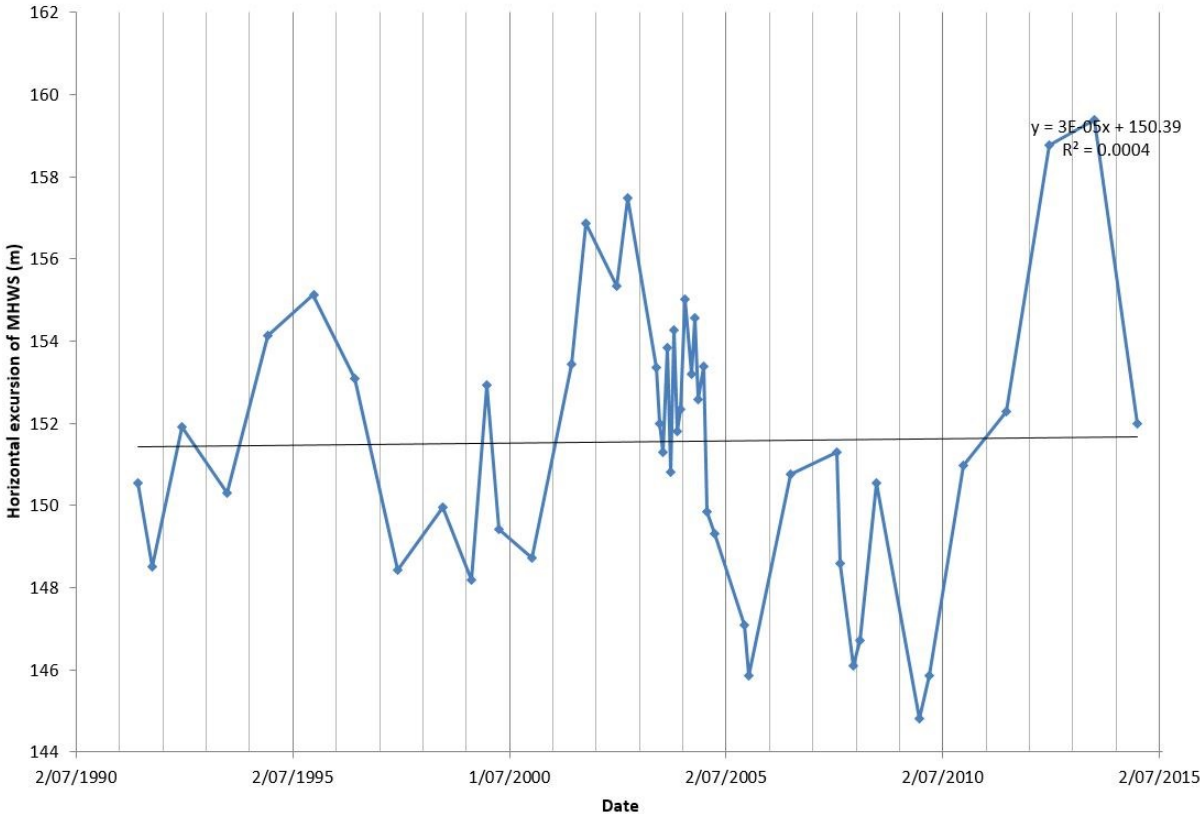

1995-2015

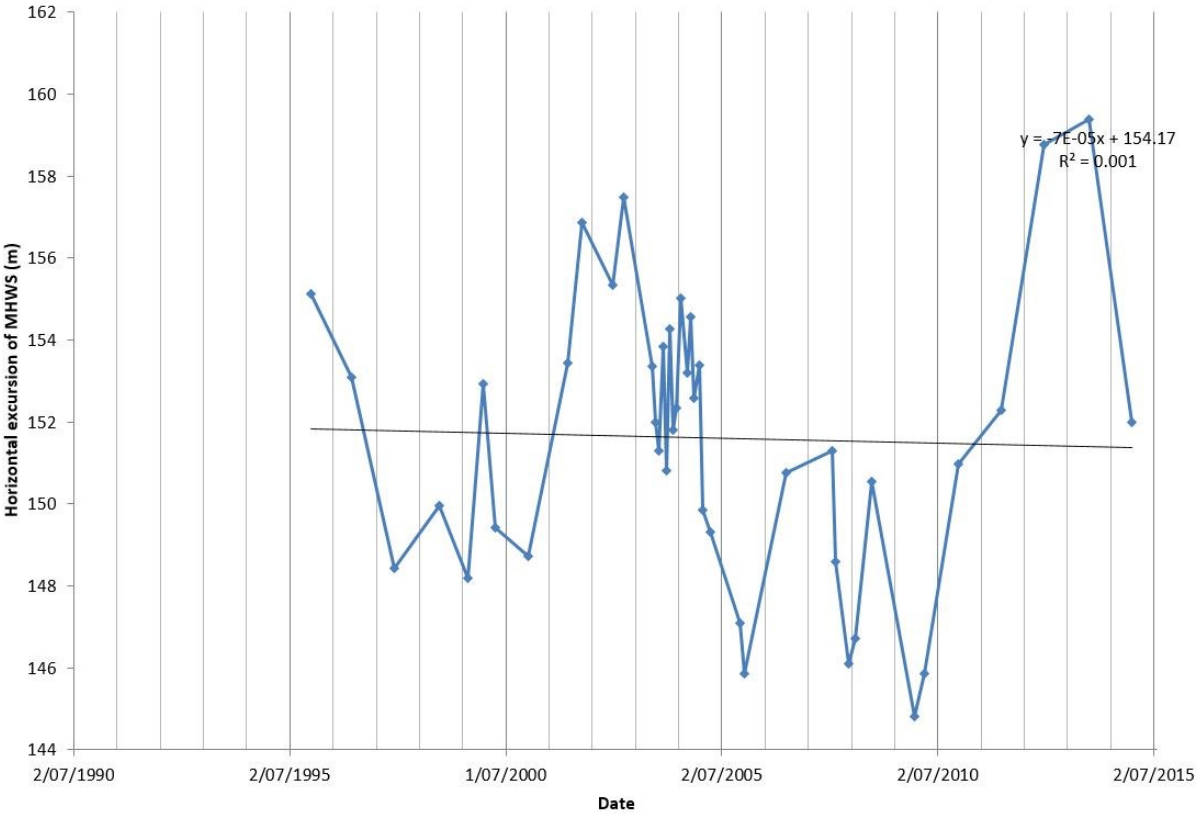

Figure C21: HB21 MHWS Excursion

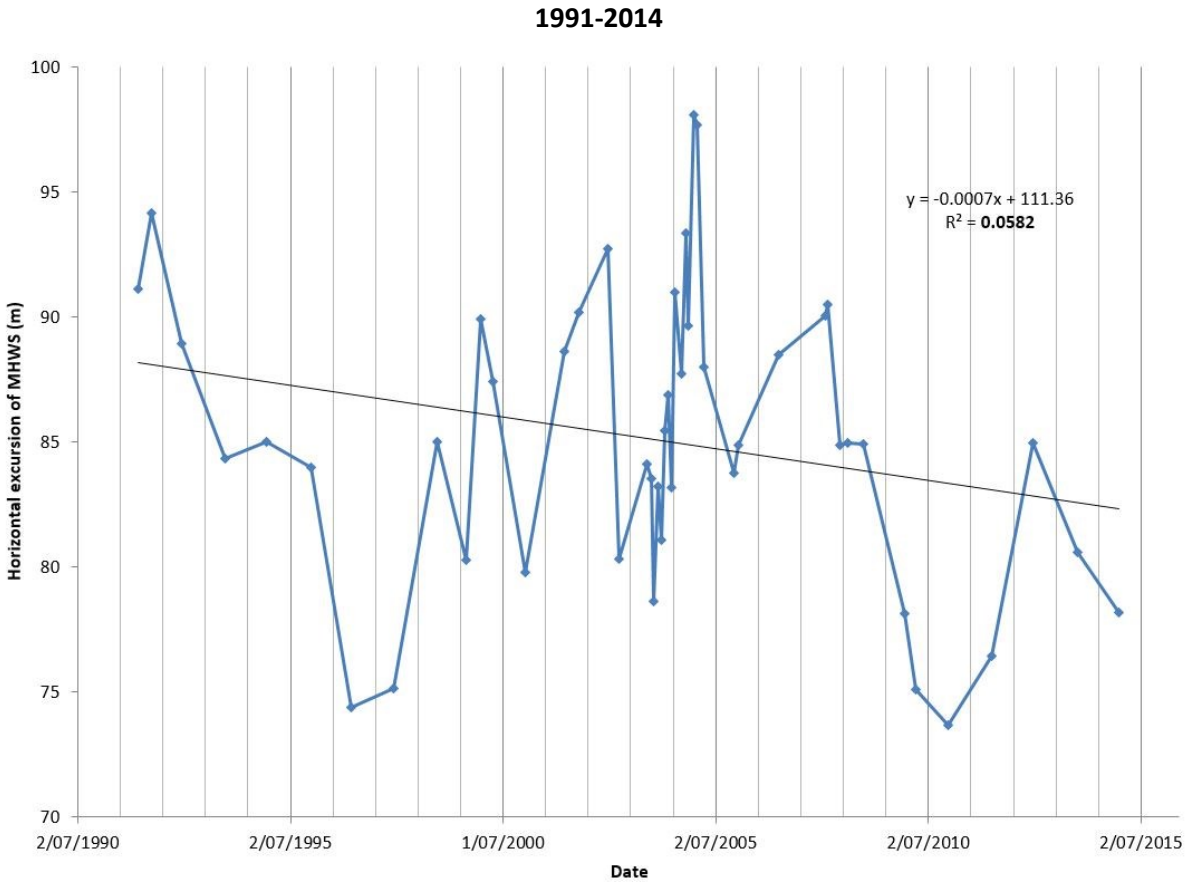

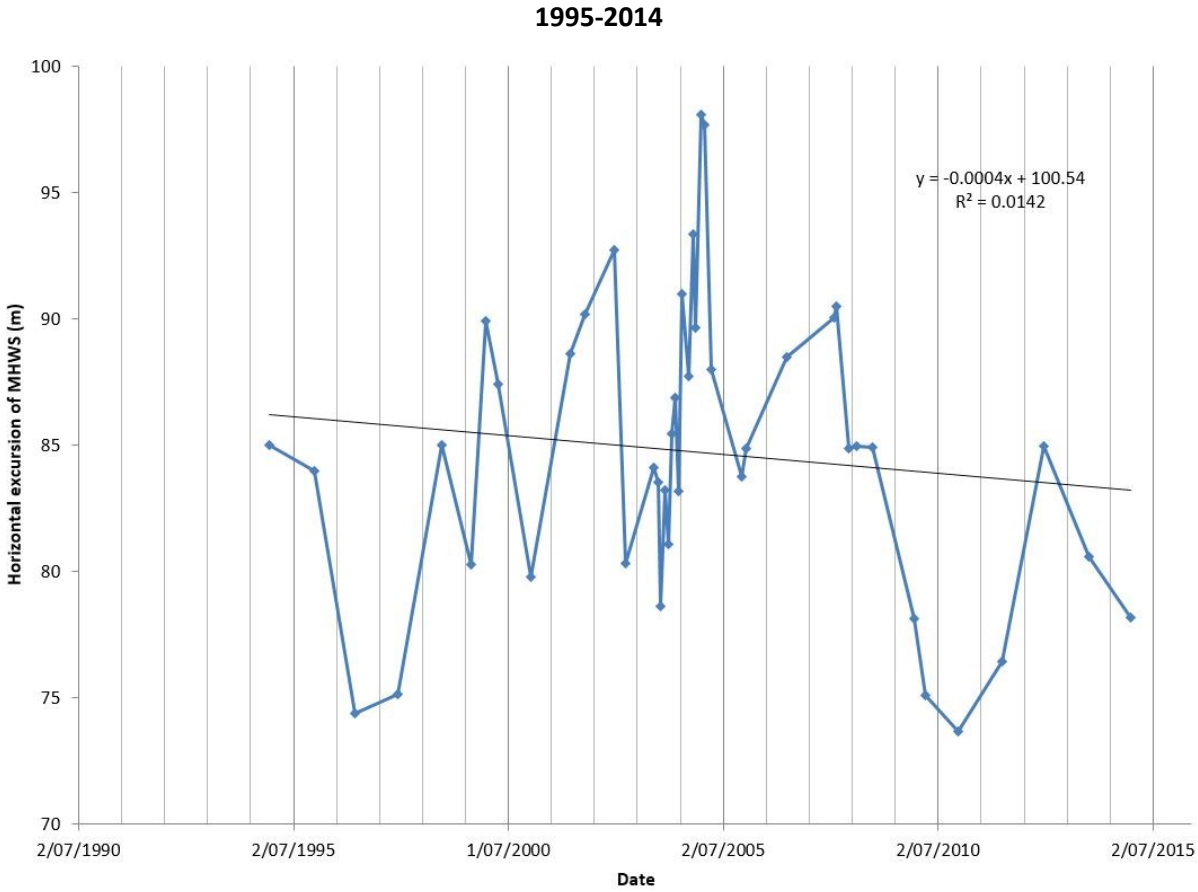

Figure C22: HB22 MHWS Excursion

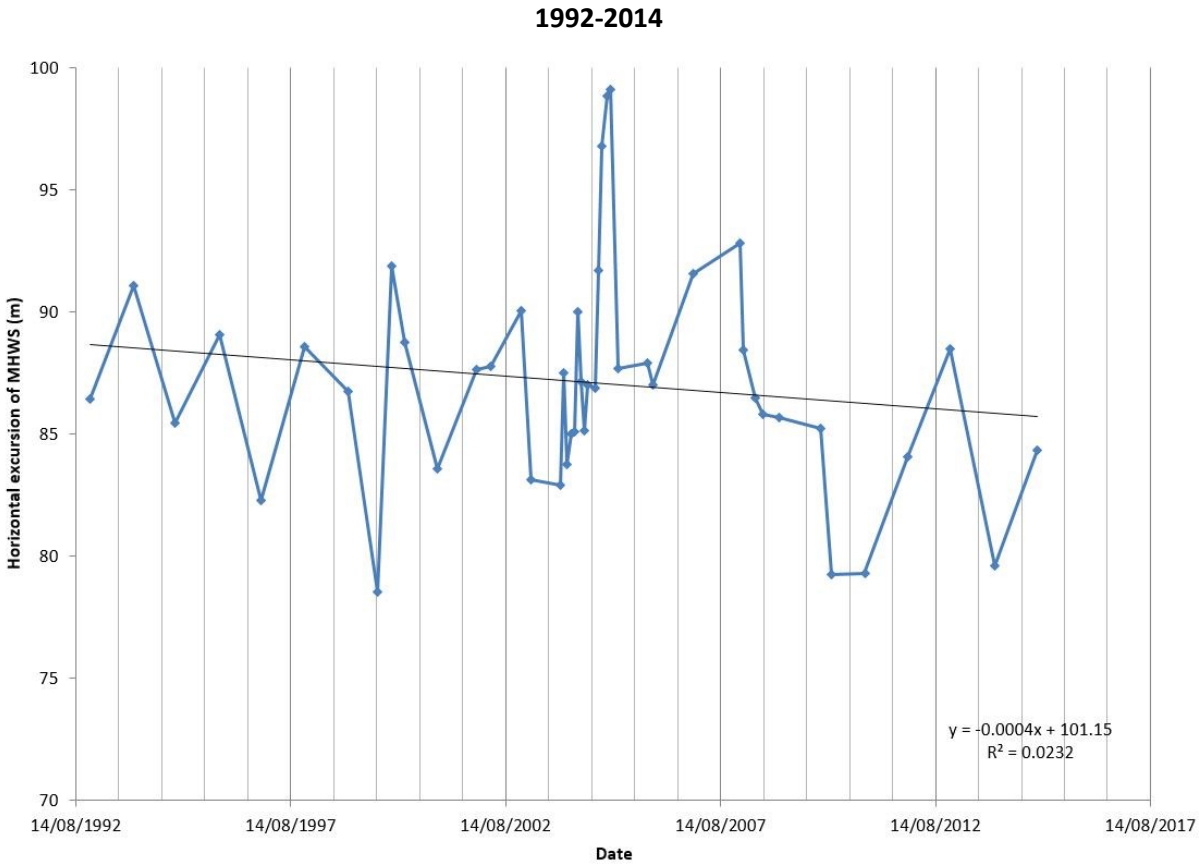

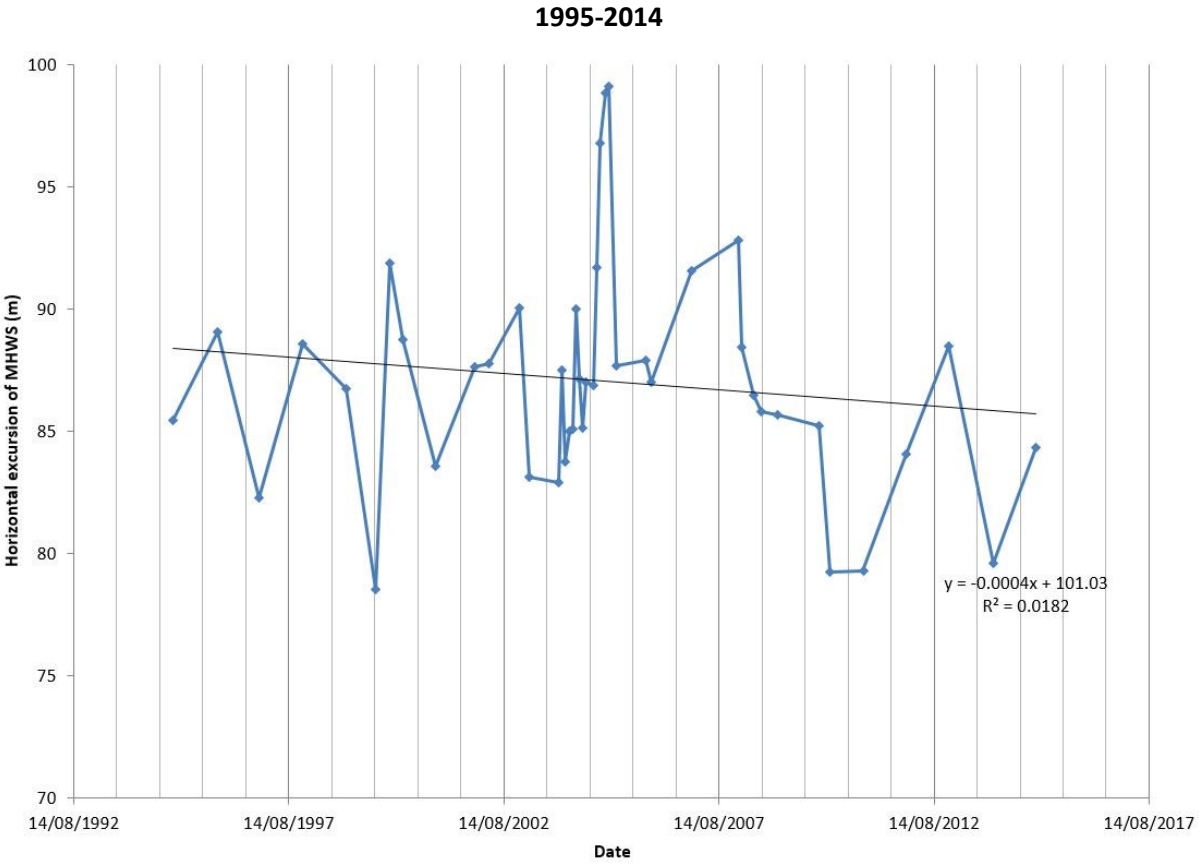

Figure C23: HB23 MHWS Excursion

Appendix D: Derivation design storm

Design storm nearshore time series for 10 yr., 100 yr. and 2x100 yr. events including wave height, period and water level were applied at the outer profile boundary (refer to Section 3.2.2.3). An example design storm is shown in Figure D1.

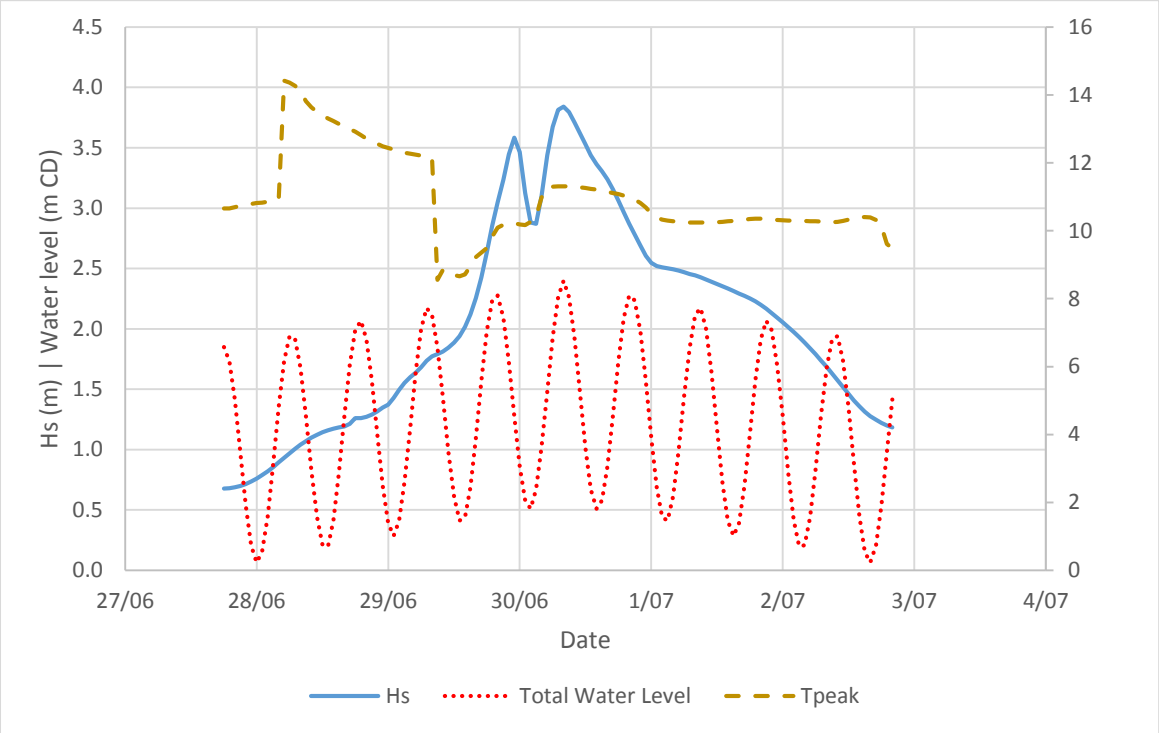

Figure D1 Example design storm

The wave height and period time series were extracted from the WASP data set (refer to Section 2.7). The event that included the largest wave height was used as a basis for the time series. The deep water wave height time series was then scaled down so that the largest wave height matches either the 10 yr. or 100 yr. ARI wave height. That scaling factor was applied to the entire time series. For the wave period it was assumed that wave shoaling and refraction had negligible effect and was therefore not scaled down.

The water level time series has been based on the spring tide range (refer to Section 2.6.1) and includes a synthetic storm surge. The storm surge is both zero at the start and the end of the time series and reaches a maximum at the same time as the wave height reaches its maximum (see Figure D1). The maximum water level is set so that it matches either the 10 yr. or 100 yr. ARI level (refer to Section 2.6.4).

Appendix E Short-Term component values

Profile	AEP Storm	Storm cut					Overwash/Overtopping
		Xbeach-G		BMAP			
		11m	12m	Standard Deviation	Maximum observed	Time between surveys	
HB1	10%	5.5	9	4.3	-4.83	1month	Overtopping/Overwash
	1%	8	15	8.6			
	2x1%	9	18	12.9			
HB2	10%	8.5	8.5	3.2	-4.2	4weeks	Overtopping
	1%	9.5	10	6.4			
	2x1%	9.5	11.5	9.6			
HB3	10%			2.7	-4.4	4months	
	1%			5.4			
	2x1%	1.5	4	8.1			
HB4	10%	4	9	6.1	-4.7	3months	Little overtopping - Overtopping for 2x1% storm
	1%	4.5	11	12.2			
	2x1%	5	15	18.3			
HB5	10%	7	10	6.1	-10.3	3months	
	1%	7.5	11	12.2			
	2x1%	10	16	18.3			
HB6	10%	8.5	11.5	4	-9	4months	Overwash
	1%	8.5	13.5	8			
	2x1%	8.5	17	12			
HB7	10%			6.7	-5.5	1month	
	1%			13.4			
	2x1%	12.5	18.5	20.1			
HB8	10%			2.3	-4.2	3months	
	1%			4.6			
	2x1%	3.5	11.5	6.9			
HB9	10%			2.7	-5.8	4months	
	1%			5.4			
	2x1%	0.5	11.5	8.1			
HB10	10%			2.2	-4.3	1month	
	1%			4.4			
	2x1%	12	14	6.6			
HB11	10%			3.7	-5	1month	
	1%			7.4			
	2x1%	12	16	11.1			
HB12	10%	14	15.5	2.6	-7.5	4months	
	1%	14	16.5	5.2			
	2x1%	12.5	17	7.8			
HB13	10%	0	4.5	2.6	-8.1	6months	Stable for 10%, Front berm washed away for 2x1% storm
	1%	0	11	5.2			
	2x1%	8.5	32	7.8			
HB14	10%			1.8	-3	3months	
	1%	accretion	1.5	3.6			
	2x1%	accretion	accretion	5.4			
HB15	10%	1.5	6.5	4	-5.7	5months	
	1%	accretion	7	8			
	2x1%	accretion	3	12			
HB16	10%			2.6	-9	3months	
	1%			5.2			
	2x1%	6	11	7.8			
HB17	10%	12	12	2	-3.2	3months	
	1%	12.5	13	4			
	2x1%	12.5	13	6			
HB18	10%			3.2	-5.5	4months	
	1%			6.4			
	2x1%	9	12.5	9.6			
HB19	10%	14	14	2.1	-4.5	2months	
	1%	14	15	4.2			
	2x1%	15.5	17	6.3			
HB20	10%	12	12	2.4	-6.3	2months	
	1%	12	13.5	4.8			
	2x1%	12.5	15	7.2			
HB21	10%			3.5	-3.5	4months	
	1%			7			
	2x1%	12	14	10.5			
HB22	10%	9	12	5.9	-9.7	2months	
	1%	9	13	11.8			
	2x1%	9	14	17.7			
HB23	10%	6	9	4.6	-11.4	2months	
	1%	6	10.5	9.2			
	2x1%	2	9	13.8			

Appendix F: Closure depth information

Site	Wave output point	H12% [m]	Ts [sec]		Inner closure depth below MLWS [m]	Reference depth (m RL)		Inner closure slope	Beach face
HB1	Clifton	2.9	11.0		6.06	3.1		0.005	0.093
HB2	Te Awanga	2.7	10.5		5.65	3.5		0.010	0.096
HB3	Te Awanga	2.7	10.5		5.65	3.5		0.018	0.110
HB4	Haumoana	2.5	9.4		5.28	3.9		0.019	0.087
HB5	Haumoana	2.5	9.4		5.28	3.9		0.019	0.081
HB6	Haumoana	2.5	9.4		5.28	3.9		0.030	0.086
HB7	Haumoana	2.5	9.4		5.28	3.9		0.046	0.090
HB8	Napier	2.8	11.2		5.93	3.2		0.046	0.096
HB9	Napier	2.8	11.2		5.93	3.2		0.045	0.095
HB10	Napier	2.8	11.2		5.93	3.2		0.038	0.095
HB11	Napier	2.8	11.2		5.93	3.2		0.043	0.090
HB12	Napier	2.8	11.2		5.93	3.2		0.044	0.091
HB13	Westshore	2.6	13.2		5.59	3.5		0.008	0.070
HB14	Westshore	2.6	13.2		5.59	3.5		0.026	0.100
HB15	Westshore	2.6	13.2		5.59	3.5		0.038	0.103
HB16	Bay View	2.6	12.5		5.67	3.5		0.050	0.070
HB17	Bay View	2.6	12.5		5.67	3.5		0.057	0.100
HB18	Bay View	2.6	12.5		5.67	3.5		0.069	0.094
HB19	Bay View	2.6	12.5		5.67	3.5		0.078	0.100
HB20	Bay View	2.6	12.5		5.67	3.5		0.088	0.100
HB21	Bay View	2.6	12.5		5.67	3.5		0.059	0.107
HB22	Bay View	2.6	12.5		5.67	3.5		0.043	0.106
HB23	Bay View	2.6	12.5		5.67	3.5		0.039	0.100

Appendix G Graphs

- **CEHZ present day**
- **CEHZ 2065**
- **CEHZ 2120**

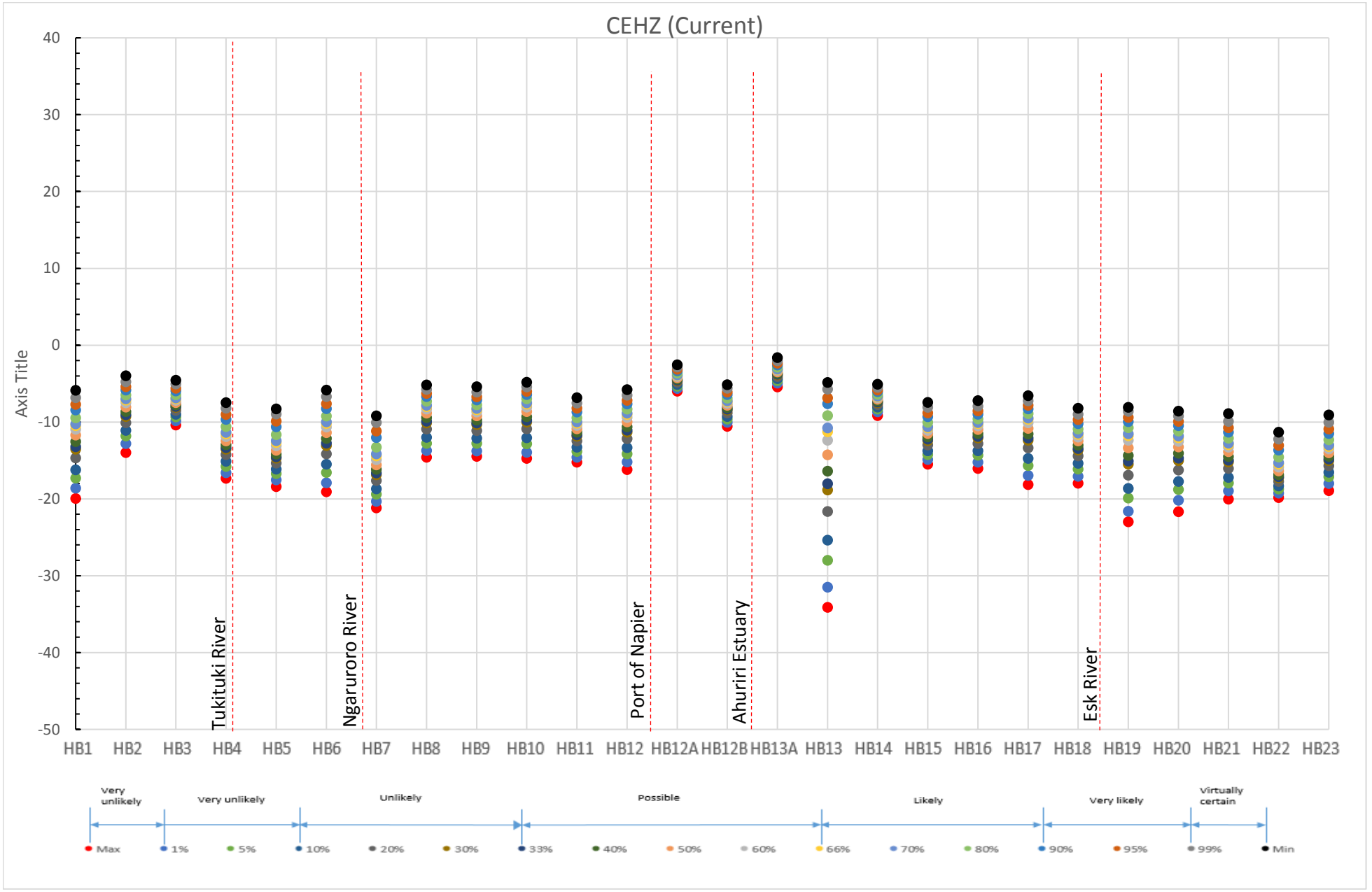
CEHZ (Current)
Axis Title
40
30
20
10
0
-10
-20
-30
-40
-50
HB1
HB2
HB3
HB4
HB5
HB6
HB7
HB8
HB9
HB10
HB11
HB12
HB12A
HB12B
HB13A
HB13
HB14
HB15
HB16
HB17
HB18
HB19
HB20
HB21
HB22
HB23
Tukituki River
Ngaruroro River
Port of Napier
Ahuriri Estuary
Esk River
Very unlikely
Very unlikely
Unlikely
Possible
Likely
Very likely
Virtually certain
Max
1%
5%
10%
20%
30%
33%
40%
50%
60%
66%
70%
80%
90%
95%
99%
Min

Appendix H: Cell division based on dune crest elevation

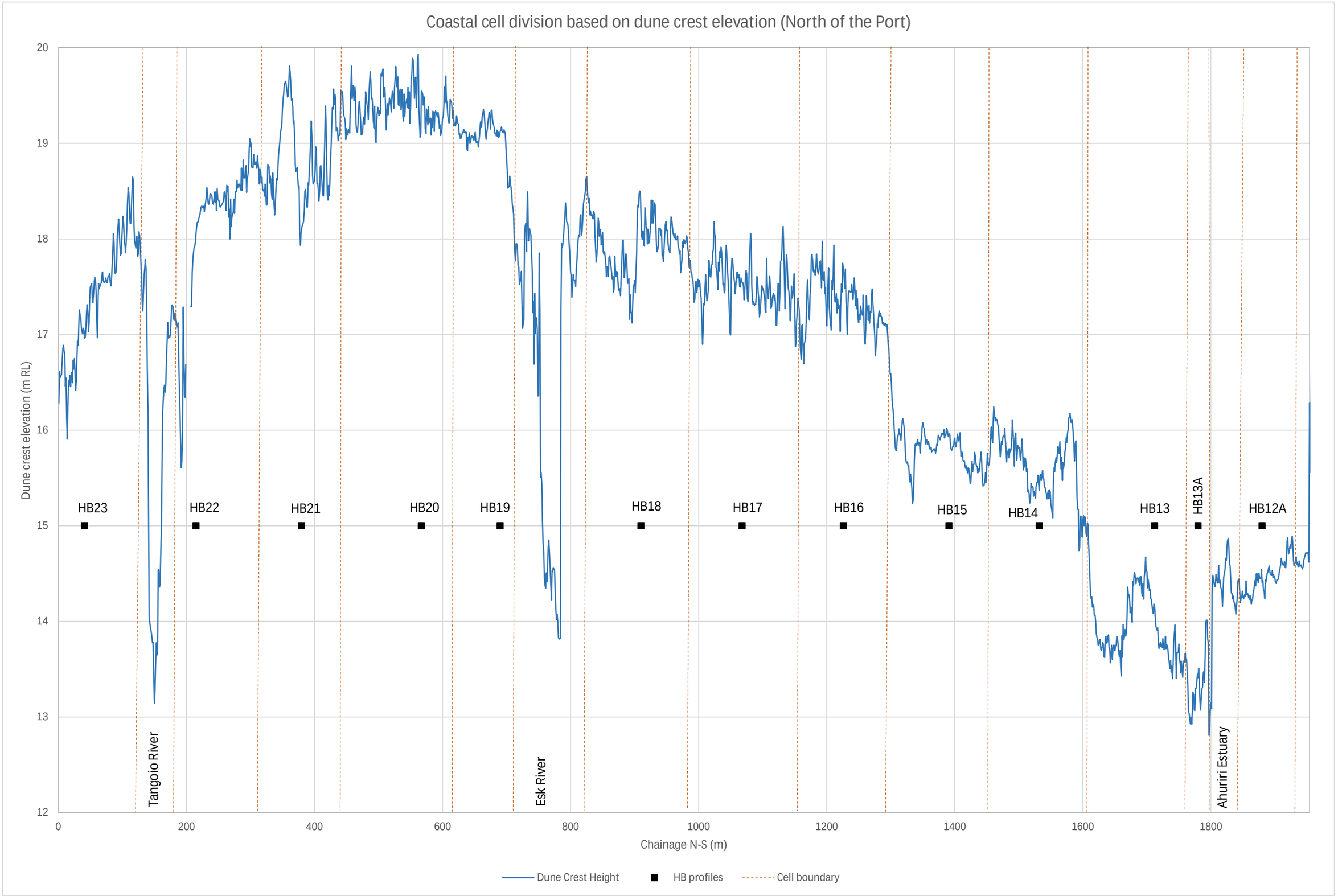
Coastal cell division based on dune crest elevation (North of the Port)
Dune crest elevation (m RL)
20
19
18
17
16
15
14
13
12
HB23
HB22
HB21
HB20
HB19
HB18
HB17
HB16
HB15
HB14
HB13
HB13A
HB12A
Tangoio River
Esk River
Ahuriri Estuary
0
200
400
600
800
1000
1200
1400
1600
1800
Chainage N-S (m)
Dune Crest Height
HB profiles
Cell boundary

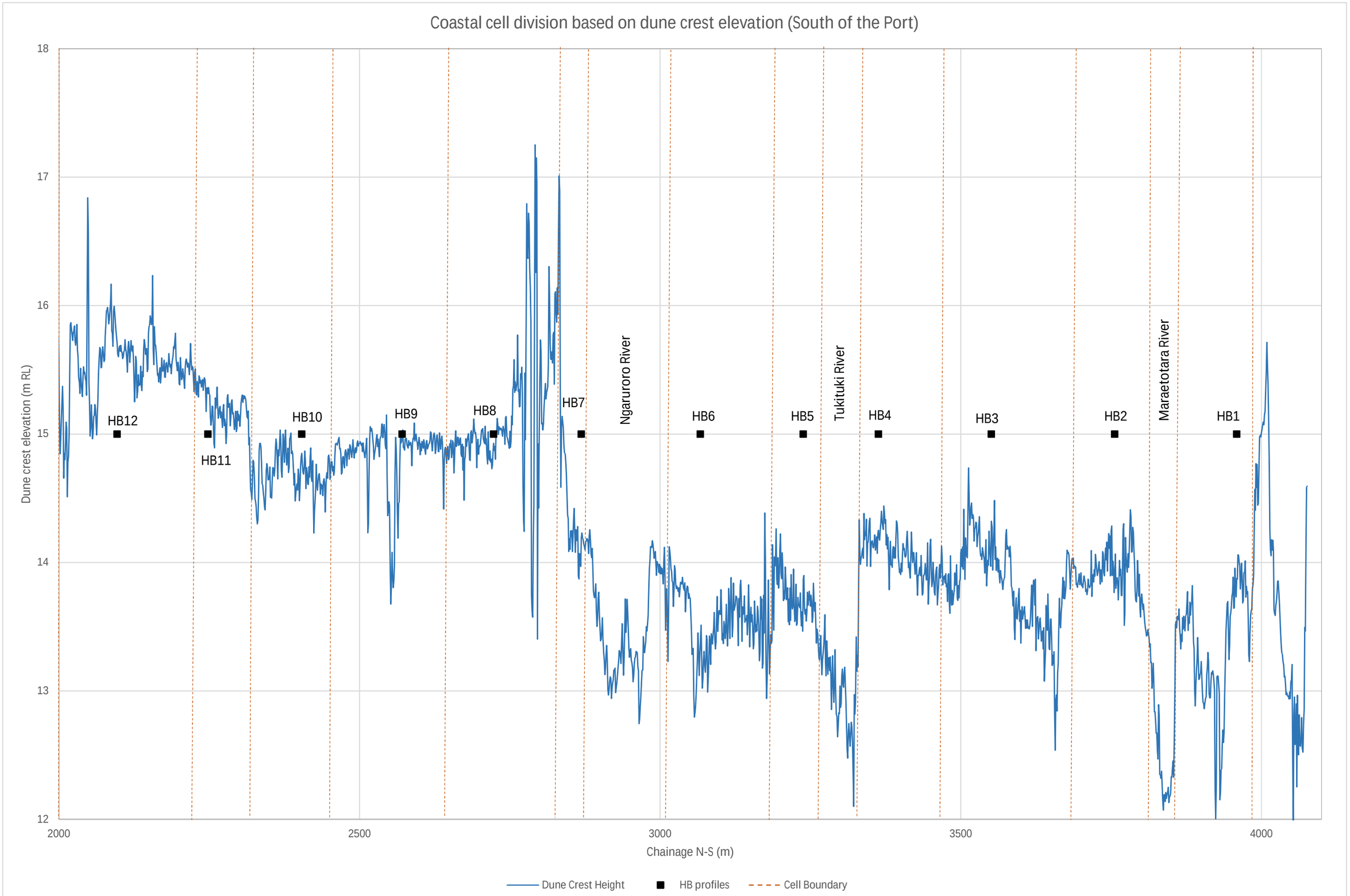
Coastal cell division based on dune crest elevation (South of the Port)
Dune crest elevation (m RL)
18
17
16
15
14
13
12
2000
2500
3000
3500
4000
Chainage N-S (m)
HB12
HB11
HB10
HB9
HB8
HB7
Ngaruroro River
HB6
HB5
Tukituki River
HB4
HB3
HB2
Maraetotara River
HB1
Dune Crest Height
HB profiles
Cell Boundary

www.tonkintaylor.co.nz